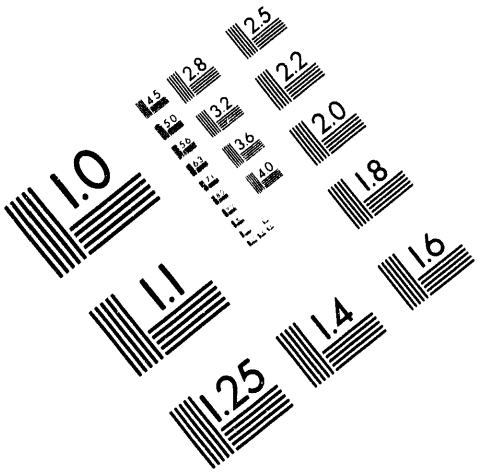

AIIM

**Association for Information and Image Management**
1100 Wayne Avenue, Suite 1100
Silver Spring, Maryland 20910
301/587-8202

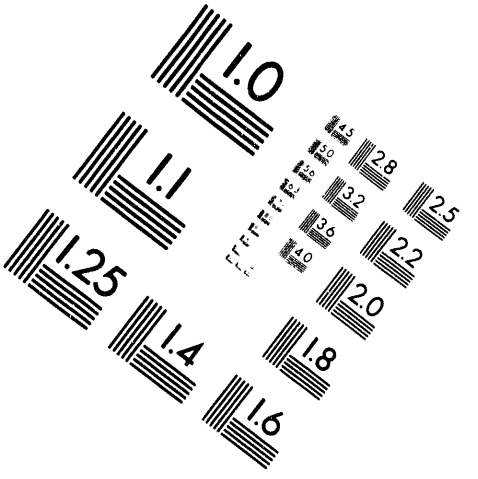

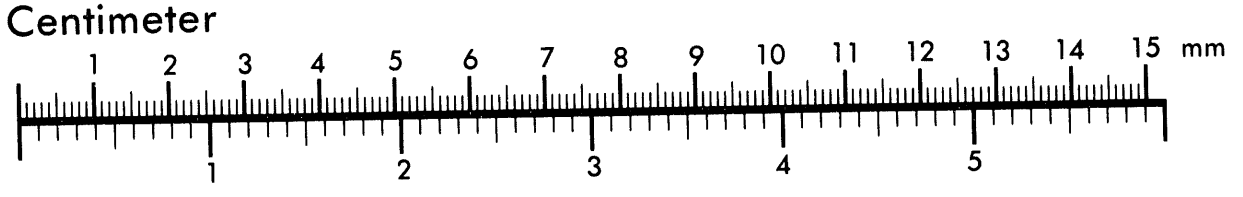


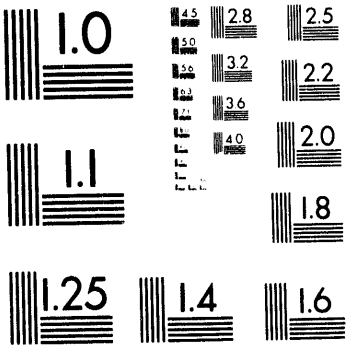

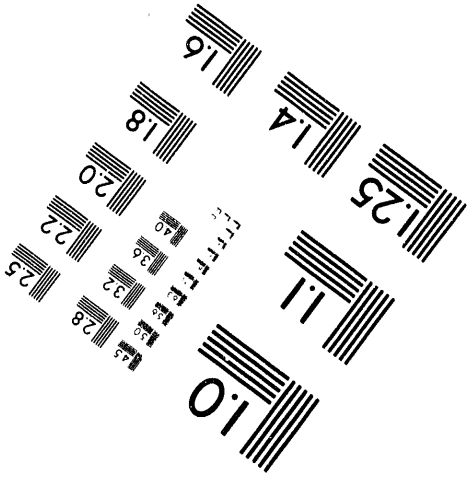

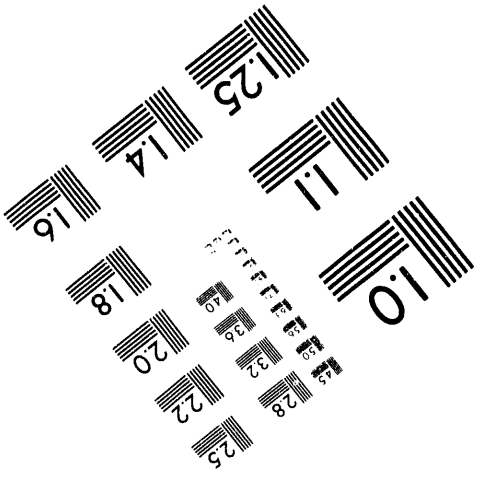

1 of 1

NUREG/CR–6213
BNL–NUREG–52414

# High-Temperature Hydrogen-Air-Steam Detonation Experiments in the BNL Small-Scale Development Apparatus

Manuscript Completed: July 1994
Date Published: August 1994

Prepared by
G. Ciccarelli, T. Ginsburg, J. Boccio, C. Economos, C. Finfrock, L. Gerlach, Brookhaven National Laboratory
K. Sato, M. Kinoshita, Nuclear Power Engineering Corporation

Brookhaven National Laboratory
Upton, NY 11973–5000

**Prepared for**
**Division of Systems Research**
**Office of Nuclear Regulatory Research**
**U.S. Nuclear Regulatory Commission**
**Washington, DC 20555–0001**
**NRC FIN L1924/A3991**

**and**

**Nuclear Power Engineering Corporation**
**Fujitakanko Building**
**17–1, 3–chome, Toranomon, Minato–ku**
**Tokyo 105, Japan**

# ABSTRACT

The Small-Scale Development Apparatus (SSDA) was constructed to provide a preliminary set of experimental data to characterize the effect of temperature on the ability of hydrogen-air-steam mixtures to undergo detonations and, equally important, to support design of the larger scale High-Temperature Combustion Facility (HTCF) by providing a test bed for solution of a number of high-temperature design and operational problems. The SSDA, the central element of which is a 10-cm inside diameter, 6.1-m long tubular test vessel designed to permit detonation experiments at temperatures up to 700K, was employed to study self-sustained detonations in gaseous mixtures of hydrogen, air, and steam at temperatures between 300K and 650K at a fixed initial pressure of 0.1 MPa. Hydrogen-air mixtures with hydrogen composition from 9 to 60 percent by volume and steam fractions up to 35 percent by volume were studied for stoichiometric hydrogen-air-steam mixtures.

Detonation cell size measurements provide clear evidence that the effect of hydrogen-air gas mixture temperature, in the range 300K-650K, is to decrease cell size and, hence, to increase the sensitivity of the mixture to undergo detonations. The effect of steam content, at any given temperature, is to increase the cell size and, thereby, to decrease the sensitivity of stoichiometric hydrogen-air mixtures. The hydrogen-air detonability limits for the 10-cm inside diameter SSDA test vessel, based upon the onset of single-head spin, decreased from 15 percent hydrogen at 300K down to between 9 and 10 percent hydrogen at 650K. The one-dimensional ZND model does a very good job at predicting the overall trends in the cell size data over the range of hydrogen-air-steam mixture compositions and temperature studied in the experiments. The experimentally measured detonation velocity generally agrees within 2 to 3 percent with predictions based upon Chapman-Jouget theory over the temperature range considered, and measured peak detonation pressure agrees within 10 percent of the calculated Chapman-Jouget pressure. In these fixed initial pressure experiments, the peak pressure is found, both experimentally and according to the theory, to decrease with increasing temperature.

Preliminary experiments indicated that the maximum temperature for which it was found possible to load combustible gases into the test vessel without an immediate burn was 650K. Experiments were conducted to measure the rate of hydrogen oxidation in the absence of ignition sources at temperatures of 500K and 650K, for hydrogen-air mixtures of 15 percent and 50 percent, and for a mixture of equimolar hydrogen-air and 30 percent steam at 650K. The rate of hydrogen oxidation was found to be significant at 650K. Reduction of hydrogen concentration by chemical reaction from 50 to 44 percent hydrogen, and from 15 to 11 percent hydrogen, were observed on a time frame of minutes. The DeSoete rate equation predicts the 50 percent experiment very well, but greatly underestimates the reaction rate of the lean mixtures.

# TABLE OF CONTENTS

# TABLE OF CONTENTS
(Continued)

# LIST OF FIGURES

# LIST OF FIGURES
(Continued)

# EXECUTIVE SUMMARY

The High-Temperature Hydrogen Combustion Research Program, jointly funded by the U.S. Nuclear Regulatory Commission and the Japanese Nuclear Power Engineering Corporation (NUPEC), is underway at Brookhaven National Laboratory (BNL) with the objective of development of the methods required to assess hydrogen combustion phenomena in mixtures of hydrogen, air, and steam at high temperature. The High-Temperature Combustion Facility (HTCF) is under construction to provide a unique vehicle for the experimental study of high-temperature detonation phenomena. The Small-Scale Development Apparatus (SSDA), described in this document, was constructed to provide a preliminary set of experimental data to characterize the effect of temperature on the ability of hydrogen-air-steam mixtures to undergo detonations and, equally importantly, to support design of the HTCF by providing a test bed for solution of a number of high-temperature design and operational problems.

The SSDA was designed to study self-sustained detonations in gaseous mixtures of hydrogen, air, and steam at temperatures up to 700K. The central element of the SSDA is a 10-cm inside diameter, 6.1-m long tubular test vessel, designed to accommodate a maximum allowable working pressure of 12.2 MPa at 700K. The test vessel is heated by ceramic heating blankets which are fastened to the test vessel and constructed of ceramic beads through which nichrome resistance wire is threaded. Heating uniformity tests demonstrated that the temperatures along the vessel are uniform within $\pm$ 14K. The system is remotely operated behind secure boundaries in an adjacent control room and is controlled by a personal computer equipped with commercially available data acquisition and control hardware and software. Instrumentation is provided to measure properties of the detonation wave, including detonation cell width, detonation propagation speed, and pressure.

A typical experiment is conducted by first evacuating the vessel and preheating the vessel to the desired temperature. The test gas mixture of hydrogen, air, and steam is premixed by partial pressures in a separate mixing chamber. The mixture is downloaded into the test vessel to a fill pressure of slightly less than 0.1 MPa. Detonations are initiated in the test vessel using a "gas driver" initiation system. Just prior to a run, a small quantity of acetylene-oxygen gas driver mixture is forced into the driver end of the test vessel, raising the vessel pressure to 0.1 MPa. A detonation is initiated in the acetylene-oxygen by discharge of a capacitor through a pair of electrodes connected by an exploding wire, which vaporizes when a large current is passed through it. The detonation is transmitted from the acetylene-oxygen slug to the test mixture within the test vessel. This method of detonation initiation obviates the need for high explosives required to initiate a detonation directly in hydrogen-air-steam systems.

The detonation cell size, the experimental measure of the sensitivity of the mixture to undergo self-sustained detonations, was measured using the smoked-foil technique, adapted and modified for the high-temperature experiments. Ion probes were used to measure the time-of-arrival of the detonation front at various positions along the tube, from which the detonation wave speed was computed. Water-cooled piezoelectric pressure transducers were employed to measure the transient detonation pressure. The ion probe and pressure transducer signals were monitored on a digital oscilloscope with a sampling rate of 100 MHz.

Preliminary experiments were performed to determine the maximum temperature for which hydrogen oxidation occurs at a sufficiently low rate so as to allow introduction of the test gases to the heated test vessel and firing of the detonation initiation system. These experiments showed that while the test vessel design temperature was 700K, the maximum temperature for which experiments could be practically run was 650K. At higher temperatures, the mixtures would immediately burn off upon introduction into the test vessel. Additionally, experiments were conducted to measure the rate of hydrogen oxidation at temperatures of 500K and 650K, for hydrogen-air mixtures of 15 percent and 50 percent, and for a mixture of equimolar hydrogen-air and 30 percent steam at 650K.

Experimental data for detonation cell size, detonation pressure, and velocity are presented for detonations in gaseous mixtures of hydrogen, air, and steam with hydrogen concentration in the range of 9 percent to 60 percent by volume, with steam fractions to 35 percent, and temperature in the range 300K to 650K. Initial pressure in all experiments was 0.1 MPa. The detonation cell width data are compared with predictions based on the one-dimensional ZND detonation model. The pressure and velocity data are compared with Chapman-Jouguet theory. The detonation limits for the SSDA test vessel were determined experimentally and compared with a criteria based on low-temperature data.

Detonation cell size measurements provide clear evidence that the effect of hydrogen-air gas mixture temperature, in the range 300K-650K, is to decrease cell size and, hence, to increase the sensitivity of the mixture to undergo detonations. The effect

of steam content, at any given temperature, is to increase the cell size and, thereby, to decrease the sensitivity of stoichiometric hydrogen-air mixtures. The hydrogen-air detonability limits for the 10-cm inside diameter SSDA test vessel, based upon the onset of single-head spin, decreased from 15 percent hydrogen at 300K down to about 9 percent hydrogen at 650K. The one-dimensional ZND model does a very good job at predicting the overall trends in the cell size data over the range of hydrogen-air-steam mixture compositions and temperature studied in the experiments. The experimentally measured detonation velocity generally agrees within 2 to 3 percent with predictions based upon Chapman-Jouget theory over the temperature range considered, and measured peak detonation pressure agrees within 10 percent of the calculated Chapman-Jouget pressure. The peak pressure is found, both experimentally and according to the theory, to decrease with increasing temperature.

The maximum temperature which it was found possible to load combustible gases into the test vessel without significant chemical reaction during the 30 to 60 second injection time period was 650K. At 700K, stoichiometric mixtures of hydrogen and air reacted during the gas injection time period, and detonation experiments could not be carried out. A hydrogen-air mixture of 50 percent hydrogen was reduced to 44 percent, and a hydrogen-air mixture of 15 percent hydrogen was reduced to 11 percent, in five minutes at 650K. The hydrogen oxidation rate for the 50 percent mixtures agreed quite well with the rate equation proposed by DeSoete. The measured rate of reaction was considerably greater than predicted by the DeSoete expresssion for the 15 percent mixtures.

A gas driver detonation initiation system was successfully implemented. This system replaces the more generally employed high-explosives initiation method. Tests demonstrated that the gas driver system initiates constant-velocity detonations at Chapman-Jouget wave speeds. This system will be used in the HTCF.

All instrumentation concepts were tested and evaluated in the SSDA. The smoked-foil technique for measurement of detonation cell width was successfully adapted to the high-temperature conditions of the SSDA experiments. The water-cooled pressure transducers operated successfully in the high-temperature environment of the SSDA. After some initial experimentation, ion probes were implemented to measure time-of-arrival and, hence, velocity of the detonation wave. These probes, and their associated circuitry, provided good quality signals for analysis under high-temperature conditions. All these techniques will be adopted for use in the HTCF.

Experiments planned for the High-Temperature Combustion Facility will provide additional data for the detonation cell size for leaner hydrogen mixtures, for larger steam fractions and larger pressure, and for temperatures in the range 300K-650K. Experiments will also address the effect of temperature on the conditions for deflagration-to-detonation and hot jet initiation mechanisms of detonation initiation. A more complete assessment of the effect of temperature on the likelihood of detonations in containment will be possible following availability of this data from the HTCF test program.

# ACKNOWLEDGEMENTS

The authors gratefully acknowledge the assistance of Dr. John Lee of McGill University and Dr. Joseph Shepherd of the California Institute of Technology for their technical guidance during the formative stages of the research reported here. As experts in detonation physics, they provided invaluable support to the program, both analytically and experimentally. They continue to provide technical assistance as the program advances.

The encouragement of Dr. Asimios Malliakos, Division of Systems Research, U.S. Nuclear Regulatory Commission, and Dr. Kenji Takumi of the Nuclear Power Engineering Corporation, Tokyo, Japan, through the various stages of this work is appreciated.

This work is performed within the Safety and Risk Evaluation Division of the Department of Advanced Technology (DAT), Brookhaven National Laboratory. Dr. W. T. Pratt, Division Head, has provided valued administrative and technical assistance during the course of this work. His help is acknowledged.

This project was initiated in April 1991 with the help of Dr. Walter Y. Kato, who was the Chairman of the Department of Nuclear Energy at that time.

A number of individuals have provided technical assistance to this project. Mr. Joseph Curtiss and Mr. Joseph Jahelka, project engineers for the High-Temperature Combustion Facility, provided their engineering advice and insights during the design of the Small-Scale Test Apparatus (SSDA). Mr. Curtiss provided the integration of the interlock system, previously used by the Neutral Beam Test Facility, into the safety system for the SSDA. As DAT Safety Coordinator, Mr. Walter Becker has provided access to his broad technical experience in safety as well as many other technical issues. Mr. Steven Hoey has served as an advisor representing the Safety and Environmental Protection (S&EP) Division, and Mr. Richard Lykins has served as S&EP Representative. They have both provided continual advice on safety-related issues.

The authors would especially like to thank Ms. Jean Frejka for her assistance in all administrative phases of this project. She is responsible for maintenance of all project records, for keeping our accounting of expenditures up to date and in reportable form, and is responsible for papers, presentations, and report manuscripts. We acknowledge her help in preparation of this manuscript for publication.

# 1 INTRODUCTION

The Three-Mile Island accident demonstrated that hydrogen combustion could occur in the containment atmosphere of a water-cooled nuclear reactor in the event of a severe accident involving extensive reactor core damage (Toth, 1986). As a result, intensive studies of combustion of mixtures of hydrogen, air and steam were carried out during the 1980s to characterize the potential modes of combustion and to develop methods to analyze the potential for associated mechanical and thermal loads on the containment building, internal structures and equipment. Deflagration, accelerated flame, detonation and diffusion flame modes of combustion were identified as possible under severe accident conditions, depending on gas mixture composition, initial pressure and temperature, and boundary conditions (Camp, 1983). The detonation mode of combustion was recognized as being of key importance when considering the potential for structural damage, since the pressures associated with this mode of combustion can be significantly greater than for the other modes of combustion. Experimental and analytical studies focussed on development of the ability to predict the combination of initial conditions for which detonations are possible, and to predict the loading on containment if a detonation should occur. This work led to development of an understanding of the detonation phenomena which allows judgements to be made of the conditions under which mixtures of hydrogen, air and steam are likely to undergo detonations.

It has been established that the "detonation cell size" is a key quantity which must be characterized in order to quantify the sensitivity of gaseous mixtures to undergo detonation and, additionally, to quantify other basic "dynamic detonation parameters" (Lee, 1984). The "critical energy," defined as the minimum energy required to directly initiate a detonation in a gas mixture, was shown to be proportional to the cube of the detonation cell size. A mixture which is sensitive to detonation has a small critical energy and, hence, small cell size. Much of the research in the past was directed towards providing experimental data and developing an analytical capability to predict the detonation cell size magnitude. The Zel'dovich (1940), von Neumann (1942), and Doring (1943) model, commonly referred to as the ZND model, was applied to describe the structure of a detonation (Westbrook, 1982; Shepherd, 1986). A calculated ZND chemical reaction length scale was found to be proportional to the detonation cell width (Lee, 1984), thereby providing a methodology for prediction of this cell size.

Since containment conditions during most severe accident sequences are characterized by atmospheres of hydrogen, air and steam at pressures between one and three atmospheres, and temperatures up to 400K, experimental data for detonation cell width were developed for this range of conditions (Lee, 1989; Tieszen, 1987). Accident sequence calculations suggested, however, that under some conditions, localized containment temperatures to 700K or greater (Yang, 1992) are possible. While there were no detonation cell size data available at such temperatures, application of the ZND model to elevated mixture temperatures suggested that the detonation cell size decreases with temperature for most mixture compositions and, therefore, that the mixture sensitivity to detonation increases with initial mixture temperature (Stamps, 1991). The experimental program reported here was initiated to provide experimental data to examine the effect of temperature on the sensitivity to detonation of mixtures of hydrogen, air and steam and, thereby, to provide an assessment of the ability of the ZND model to predict the influence of temperature on mixture sensitivity.

The High-Temperature Hydrogen Combustion Research Program, jointly funded by the U.S. Nuclear Regulatory Commission and the Japanese Nuclear Power Engineering Corporation (NUPEC), is underway at Brookhaven National Laboratory (BNL) with the objective of development of the methods required to assess hydrogen combustion phenomena in mixtures of hydrogen, air and steam at high-temperature.The High-Temperature Combustion Facility (HTCF) is under construction to provide a unique vehicle for the experimental study of high-temperature detonation phenomena. The Small-Scale Development Apparatus (SSDA), described in this document, was constructed to provide a preliminary set of experimental data to characterize the effect of temperature on the ability of hydrogen-air-steam mixtures to undergo detonations and, equally importantly, to support design of the HTCF by providing a test bed for solution of a number of high-temperature design and operational problems.

This report presents the results of the experimental program conducted in the Small-Scale Development Apparatus. The SSDA is described, experimental results for detonation cell size, detonation pressure and velocity, test vessel detonability limit, and preignition hydrogen oxidation rates are presented, and comparisons are made with theoretical predictions. Experimental conditions encompassed hydrogen-air mixtures with composition 9 percent to 60 percent hydrogen by volume, stoichiometric hydrogen-air-steam mixtures with steam fractions up to 35 percent by volume, pressure of one

atmosphere and gas mixture temperatures in the range 300K-650K. Experience gained relevant to design and performance of detonation experiments at high temperature is described.

## 1.1 Background

### 1.1.1 Detonation Phenomena and Detonation Cell Size

A self-sustained detonation wave is a combustion wave consisting of a leading supersonic front which propagates at a constant velocity, followed by a reaction front which provides the energy to sustain the leading shock wave. The first model describing the structure of a detonation wave was proposed independently by Zel'dovich (1940), von Neumann (1942), and Doring (1943). The model, commonly referred to as the ZND model, is based on the assumption that the detonation front consists of a planar shock wave followed by a reaction zone. The flow throughout the system is considered to be steady. The reaction zone is terminated by a sonic plane where the gas velocity is sonic relative to the leading shock wave. This condition, referred to as the Chapman-Jouget (CJ) state (Chapman, 1899; Jouget, 1917), is required to match the steady flow conditions which exist in the reaction zone to the unsteady flow which exists in the trailing expansion wave. Around this time, more was known of the detailed chemical kinetics involved in the reactions of common fuel-oxygen systems and thus intense theoretical studies into the detailed structure of the reaction zone was undertaken. One of the main outcomes from these studies was that energy is not instantaneously released after the adiabatic shock compression, as previously perceived; there exists an induction period during which chemical reaction rates are very low.

Up until the 1950s, it was generally believed that a detonation wave is one-dimensional and steady, since the CJ theory did such a good job at predicting the detonation velocity. However, during the 1940s, the ZND model came under close scrutiny, and it was shown analytically that the one-dimensional, steady-state detonation wave structure of a planar shock wave followed by a reaction zone was not stable. It wasn't until the later 1950s that White (1961), discovered experimentally using photographic interferometry, that a self-sustaining detonation is not one dimensional. From his photographs, he inferred that the true structure of a detonation is a nonplanar shock wave followed by a "turbulent reaction zone." It has since been well established that a detonation wave has a complex three-dimensional structure consisting of multiple shock waves and reaction zones (Lee, 1984). Not only is there a highly nonplanar shock wave which propagates in the direction of the front, but there are also finite amplitude compression waves which propagate in the transverse direction (i.e., normal to the direction of propagation).

The use of carbon "sooted foil," or "smoked foil," is currently widely used in the study of the structure of gaseous detonation waves. The smoked-foil technique was first used by Denisov et al. (1959). If such a foil is placed on the inner surface of a tube and a detonation wave is made to propagate over it, a characteristic "fish-scale" pattern is inscribed on the sooted foil. Such a foil is shown in Figure 1.1. The fish-scale pattern generated by the detonation wave and the detailed shock configuration is shown schematically in Figure 1.2a. The fish-scale pattern is comprised of individual cells, and for this reason a detonation is often referred to as having a cellular structure. The transverse width of the cell is referred to as the detonation cell size, and denoted by the symbol $\lambda$. In general, one speaks of average cell size since there is normally a variation in the cell size from cell to cell on a given foil.

The corrugated detonation shock front consists of three distinct waves which are defined as the incident, mach stem, and transverse wave, as shown in Figure 1.2b. The shock front in the cell which follows the collision of two transverse waves is defined as the mach stem, which is stronger than the incident wave in the adjacent cells.

It has been demonstrated that the inscription on the foil corresponds to the trajectory of triple points (i.e., the common point in a three shock wave interaction) which are present in all self-sustained detonation waves. It is believed that the scrubbing action of the strong shear layer, which is also present in a triple shock configuration, is responsible for etching of the fish-scaled pattern on the smoked foil. The apparent "turbulent reaction zone" observed by White (1961) was the result of the superposition of multiple shear layer across the detonation front.

With the availability of detailed chemical reaction mechanisms for mixtures of hydrogen, air and steam, the ZND model has become relatively simple to implement computationally, and attempts have been made to relate the chemical reaction zone length scale predicted by the ZND model to the measured cell size. The first attempt to relate the steady-state reaction zone length calculated using the ZND model with the experimentally measured cell size was by Schelkin and Troshin (1965). They proposed the linear correlation between the experimentally measured cell size and the calculated ZND reaction zone length, which is frequently used today. Since then, knowledge of the detailed chemical reaction mechanisms occurring for different mixtures has increased dramatically, especially for hydrogen-air mixtures. The availability of the reaction mechanisms led to detailed ZND analyses of hydrogen-air and hydrogen-air-diluent systems, where the diluents were steam, carbon dioxide, and nitrogen, by several authors (e.g., Westbrook et al., 1982; Shepherd, 1986).

Experimental data for the detonation cell size of hydrogen-air-steam mixtures were developed in the 1980s in considerable detail, for mixtures at initial temperatures in the range 300K to 400K, pressure of one atmosphere, and compositions covering the range of approximately 10 to 60 percent hydrogen by volume. These experiments were performed in detonation test vessels of diameter in the range of 5 cm to 43 cm. This data is largely summarized by Guirao, et al. (1989) and by Stamps (1991). Analyses of the available experimental data using ZND calculations indicated that, with suitable choice of the constant which relates the calculated chemical reaction length scale to the measured detonation cell size, the ZND model captures the effects of hydrogen concentration, diluent concentration and pressure (Stamps, 1991; Shepherd, 1986). The combined experimental evidence and analytical modeling clearly demonstrated that the effect of steam is to dramatically increase the reaction zone length or, equivalently, the detonation cell size. Thus, the sensitivity to detonation of hydrogen-air mixtures is dramatically reduced by the presence of quantities of steam of 10 percent by volume or greater.

Shepherd demonstrated that the constant of proportionality between the measured cell size and calculated chemical reaction length scale varies from a low of 5 to a high of 50 over the detonable range of hydrogen-air mixtures. The reaction zone length was defined, subjectively, by both Shepherd and Stamps by the location behind the leadinding shock wave where the local flow Mach number equals 0.75. Since that time, Shepherd has suggested that a better choice from a physical point of view is to base the reaction zone length on the location of peak heat release rate (Shepherd, 1993)[1]. This assumption was used in the work reported here, as is discussed in Section 3.2.

The effect of hydrogen-air mixture temperature on detonation cell size was apparently first discussed by Westbrook (1982). ZND model calculations suggested that, for stoichiometric mixtures at an initial pressure of one atmosphere, increasing the temperature from 200K to 500K results in increasing, although weakly, the induction length. No calculations were presented for off-stoichiometric mixtures. Westbrook attributed this behavior to a combination of the effects of initial temperature on reactant concentration and on the post-shock temperature. Shepherd (1986) examined the effect of temperature in the range 300K to 500K on reaction zone length in more detail. He found, with a result similar to that of Westbrook, that for stoichiometric mixtures of hydrogen-air at an initial pressure of one atmosphere, the effect of increasing temperature is to increase the reaction zone length. However, Shepherd also studied the combined effects of pressure and temperature on the calculated reaction zone length and found that the behavior with temperature of stoichiometric mixtures depends also on pressure. For pressures less than one atmosphere, the temperature dependence does not vary significantly. For pressures greater than one atmosphere, the trend is for the reaction zone length to first decrease somewhat with temperature, then to increase. Overall, the temperature dependence for stoichiometric hydrogen-air is predicted to be weak. Shepherd commented that additional calculations, not shown in the paper, demonstrated that for very lean or very rich mixtures, the reaction zone length decreases with temperature when the pressure is kept fixed. Shepherd attributed the trends of cell width with temperature to a combination of effects due to post-shock temperature, chemical reaction mechanism, and mixture density.

The combined effects of gas mixture temperature, hydrogen, and steam concentrations on detonation cell width was examined by Stamps (1991). ZND calculations, using the Shepherd version of the ZND model, were presented for

[1]Shepherd, J. E., personal communication, 1993.

temperatures in the range 200K to 1000K. The calculations demonstrated a strong dependence of cell width on temperature for off-stoichiometric mixtures, as discussed by Shepherd. This dependence on temperature is predicted to be strongest at the low end of the temperature range. The calculation results clearly demonstrate that temperature significantly decreases the cell wdith and, thereby, sensitizes off-stoichiometric mixtures to detonation. Stamps summarized the available data for cell width as a function of temperature. Data in the temperature r ~ge 300K to 440K were extracted from the literature and compared with the ZND predictions. No data were available fo~ temperatures above 440K. The available data provides some limited evidence to support the temperature dependence of predictions based upon the ZND model. However, the range of temperature for which data are available and the limited number of data points which are available, preclude the ability to reach firm conclusions regarding the variation of cell width with temperature over an extended temperature range.

The ZND calculations presented by Stamps, shown in Figure 1.3, demonstrates the strong effect of steam fraction on detonation cell width and, equally importantly, demonstrates that for a given steam fraction, increasing temperature has a pronounced effect in reducing the cell width. Thus, while steam clearly desensitizes mixture to detonations, increased temperature can override the steam effect by increasing the mixture sensitivity. At a temperature of 700K, the ZND model predicts that the inerting effect of steam is sharply reduced due to the effect of temperature. Data are presented for stoichiometric mixtures of hydrogen-air-steam for a temperature of 373K only. Thus, the data cannot be used to verify the strongly desensitizing effect of temperature on the cell width of steam-laden mixtures of hydrogen and air.

The limited availability of experimental data has precluded the ability to definitively assess the effect of temperature on the sensitivity of hydrogen, air, and steam to undergo self-sustaining detonations for temperatures in the range 400K-700K, of interest under some severe accident conditions. While the ZND model has been demonstrated to capture relevant aspects of the detonation phenomenon, data are required over a larger range of temperature than heretofore available, in order to provide a complete assessment of the effect of temperature. The experimental program reported here is directed towards providing the required data.

## 1.1.2 SSDA Test Vessel Detonability Limit

It has been found that the mixture "detonability limits" correlate with detonation cell size (Lee, 1984). These limits are the lean and rich fuel concentrations inside of which a self-sustained detonation is possible. In a circular tube of diameter "d," as one approaches either the lean or rich detonability limit, the structure of the detonations changes from the multi-cellular structure described earlier to a "single-head spin" (Moen et al., 1981). In a single-head spin, there exists only one transverse wave which rotates about the centerline of the tube. Smoked-foil records of a single-head spin show a helical etching on the tube wall which is the result of the combined tangential and axial motion of the single triple point. It has been shown experimentally by Dupre et al. (1985) that for a planar detonation propagating in a rigid circular tube, the lean and rich detonability limits correspond to the mixture whose cell size is equal to the tube circumference (i.e., $\lambda = \pi d$). The cell size at the detonability limit for a tube is generally taken to be the range $d < \lambda < \pi d$ (Guirao et al., 1987). No data are available to test this criterion at elevated temperature. The SSDA experiments reported here were designed, in part, to provide data for the detonability limits of the test vessel as a function of mixture temperature.

## 1.1.3 High-Temperature Experimental Design and Operational Questions

Design of the HTCF led to identification of a number of high-temperature design and operational problems which required experimental resolution. The SSDA program was designed to provide a test apparatus to obtain the design parameters and operational characteristics required to complete design of the HTCF. The three major technical issues were: (1) identification of maximum experimental operating temperature, (2) design and operation of the gas driver detonation initiation system, and (3) design and operation of high-temperature instrumentation.

### 1.1.3.1 Maximum Operating Temperature

The HTCF was designed to perform detonation experiments using hydrogen-air-steam mixtures at temperatures up to 700K. One of the reasons for the choice of this upper temperature specification was the recognition that at high

temperature, the reactants would chemically react in the absence of ignition sources. Experimental data suggested that slow chemical reaction between hydrogen and air occurred without ignition sources for temperatures of 773K (Hustad, 1988) and as low at 573K for mixtures rich in hydrogen (DeSoete, 1975). It was also understood that at sufficiently high temperature, the mixture would "autoignite" (Zabetakis, 1956) on a time frame so short that it would not be possible to initiate a detonation in an experimentally controlled manner. While the combustion literature contains much literature dealing with the autoignition temperature, it is at the same time recognized that the autoignition temperature is not very well defined, that several methods are used to determine its magnitude, that bounding metallic surface properties can influence the measured value, and the large variations exist in reported data (Sheldon, 1984). The most often quoted minimum autoignition temperature for hydrogen-air systems is approximately 793K (Zabetakis, 1956).

Experimental data were required in order to determine the maximum temperature at which gases can be loaded into the HTCF test apparatus and experiments carried out prior to mixture burnoff by slow chemical reaction in the absence of initiation sources. Additionally, it was desirable to obtain data for the rate of predetonation chemical reaction. The SSDA program was designed to obtain this information for guidance in specifying test conditions for both the HTCF and SSDA test programs.

#### 1.1.3.2 Gas Driver Detonation Initiation System

The hydrogen detonation program planned for the HTCF required design of a "driver system" to initiate detonations in hydrogen-air-steam test mixtures. Since such mixtures require a substantial quantity of energy for direct initiation of detonations, high explosives have been generally used as the source of energy. The use of "gas driver" initiation systems have also been reported (Moen et al., 1981). In order to avoid the need for high explosives, and thereby obviate the need for construction of explosives handling facilities and extensive explosives training, a decision was reached to adapt the concept of a gas driver initiation system to the needs of the high-temperature detonation experiments. A number of technical issues, including the effect of elevated temperature on the behavior of the system, needed to be resolved. The SSDA was designed to permit design and development of the gas driver detonation initiation system for application to the HTCF and for use in the SSDA detonation experiments.

#### 1.1.3.3 Instrumentation

The planned high-temperature detonation experiments required adaptation of experimental techniques which have previously been employed at room temperature, or somewhat above, to temperatures up to approximately 700K. It was conjectured that problems related to the high-temperature environment could arise with the smoked foil technique, dynamic pressure instrumentation and with probes for measurement of detonation velocity. The SSDA was designed to provide a vehicle for resolution of these high-temperature instrumentation problems.

## 1.2 Objectives

The BNL High-Temperature Combustion Facility (HTCF) is being constructed to investigate hydrogen combustion phenomena in gaseous mixtures of hydrogen, air, and steam at temperatures up to 700K, and steam fractions up to 40 percent steam. The major element of this facility is a 21.3-m long, 30-cm inner diameter heated detonation tube. The HTCF will be operational in the fall of 1993. The Small-Scale Development Apparatus, the central element of which is a 6.1-m long, 10-cm inside diameter detonation tube, was constructed to provide preliminary experimental data on the effect of temperature on the sensitivity of gas mixtures as measured by the detonation cell size and to resolve a number of high-temperature problems associated with the design and operation of the HTCF.

This report presents the results of the experiments performed in the SSDA. The specific objectives of the SSDA program were:

(1) Provide experimental data for the detonation cell size of mixtures of hydrogen, air and steam as a function of gas temperature, in order to determine the effect of temperature in the range 300K-650K on

the sensitivity of the mixtures to undergo self-sustained detonations. The same experiments also provide measurements of the detonation velocity and pressure, and the SSDA detonability limit.

(2) Assess the ability of the ZND model to predict the effect of temperature on the detonation cell size of mixtures of hydrgen, air and steam. Additionally, the data for test vessel detonation limit are compared with criteria for tube detonation limits, and detonation pressure and velocity are compared with predictions based upon Chapman-Jouget theory.

(3) Provide experimental data required to address a number of high-temperature experimental design problems which arose during the design of the High-Temperature Combustion Facility. This includes a determination of the maximum temperature for which spontaneous hydrogen oxidation occurs at a sufficiently low rate so as to allow sufficient time for introduction of the test gases into the detonation test vessel and initiation of the detonation prior to depletion of thereactive constituents. Data are also provided for the rate of preignition hydrogen oxidation at temperatures up to 650K.

The report describes the accomplishments of the experimental program in the SSDA. Section 2 describes the experimental apparatus and the experimental test procedures. Section 3 presents the results of the experimental program, focussing on the high-temperature detonation experiments. Section 4 discusses the implications of the experimental results from the standpoint of reactor safety. The results of the SSDA program are summarized and conclusions are presented in Section 5. Plans for future experiments are discussed in Section 6.

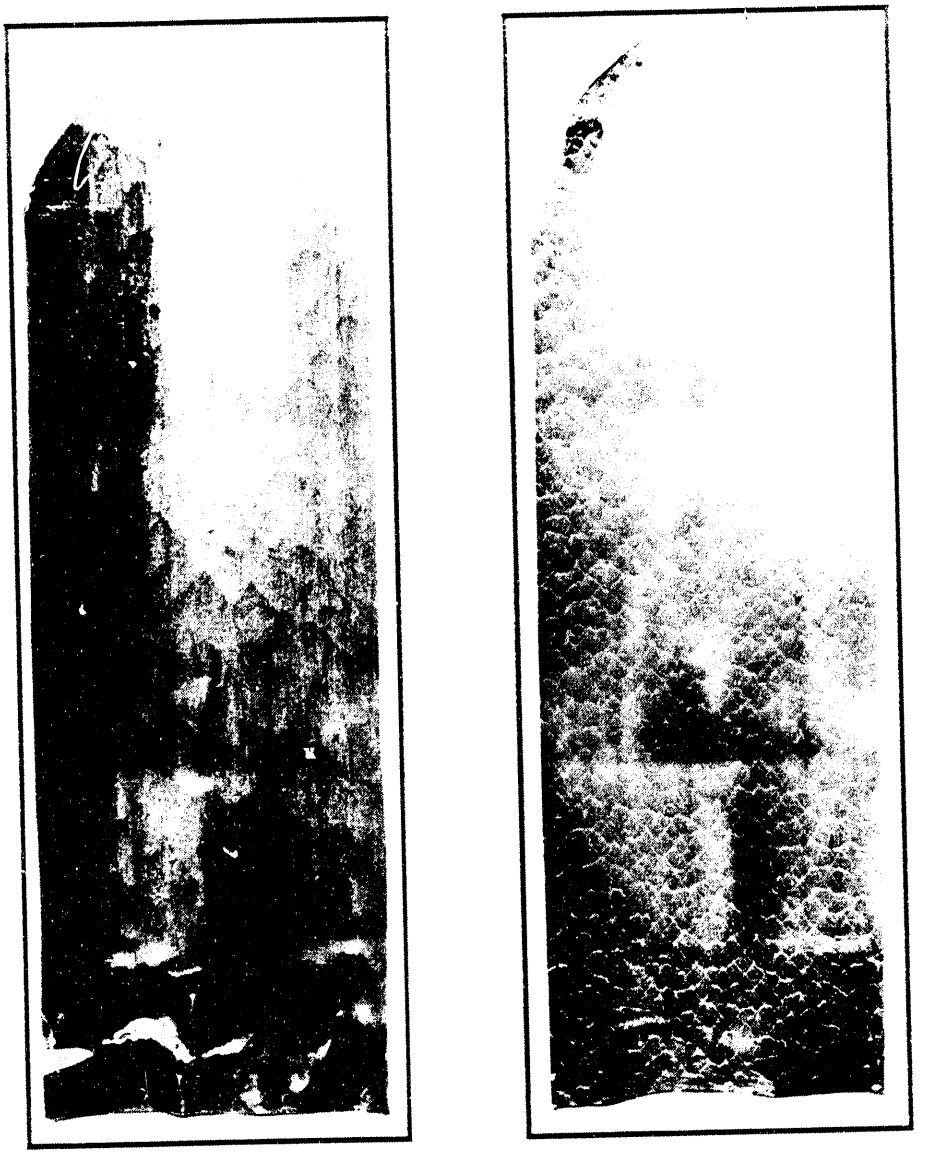


Figure 1.1: Smoked foil records obtained from the SSDA for detonations in hydrogen-air mixtures at 0.1 MPa

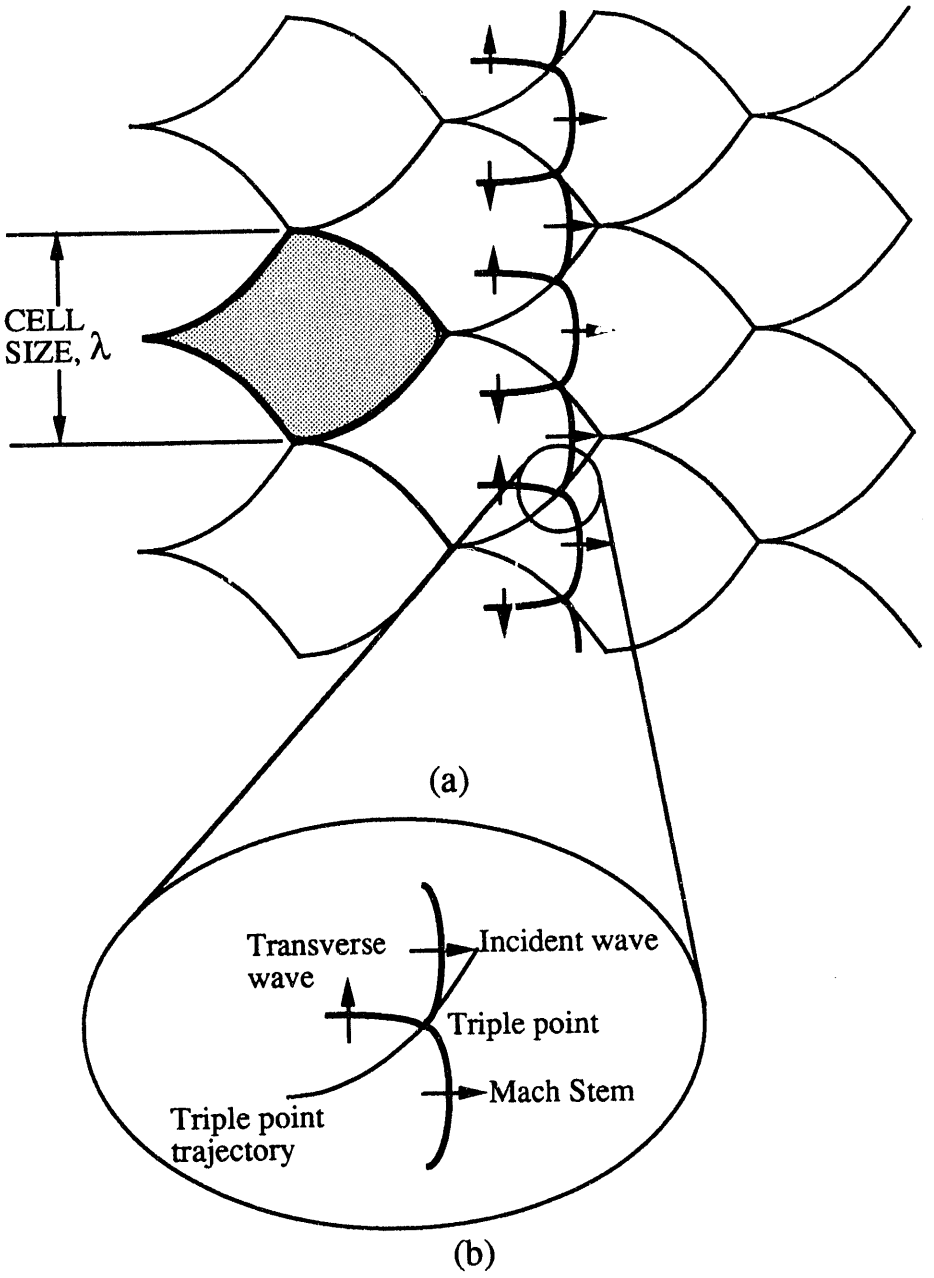


Figure 1.2: (a) Cellular structure of a detonation front and the "fish scale" pattern produced by the triple point trajectories; (b) inset from (a), showing the labelling convention for a three wave interaction

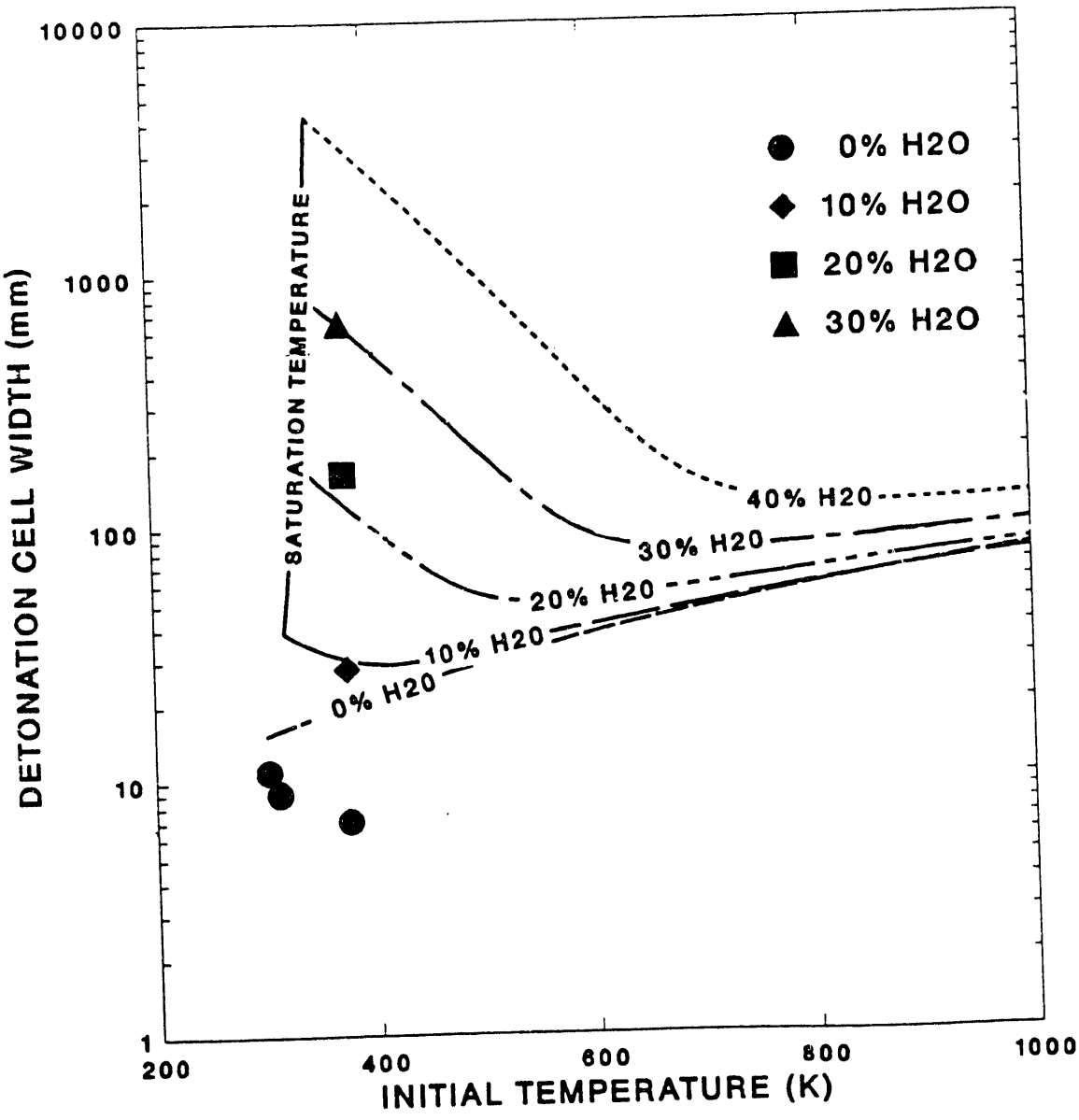


Figure 1.3: The effect of initial temperature on the detonation cell width as a function of steam dilution for stoichiometric hydrogen-air-steam mixture at 1 atm initial pressure (Stamps et al., 1991).

# 2 EXPERIMENTAL DETAILS

## 2.1 Experimental Apparatus

### 2.1.1 Overview of the Small-Scale Developmental Apparatus

The SSDA consists of the heated detonation test vessel and supporting systems, as shown schematically in Figure 2.1. The sections of this report which describe specific systems are identified in the figure. The data acquisition and control system provides monitoring and control functions for the test gas mixing process in the mixing vessel, for the delivery of the test gas to the test vessel, and for initiation of the experiment using the gas driver detonation initiation system. Additionally, the data acquisition system monitors and stores the initial conditions of each experiment.

A photograph of the major elements of the SSDA is shown in Figure 2.2, highlighting the test vessel, mixing chamber, and associated gas flow system. The test vessel is shown mounted on a stand constructed of welded 1.91-cm angle iron. The photograph shows the test vessel and mixing chamber assembled and wrapped with insulation. Cable trays carrying instrumentation, control and heating cables are located directly above the test vessel. Experiments are executed remotely from an adjacent control room.

The test vessel and supporting systems are described in the section which follow, as identified in Figure 2.1. Figure 2.3 is a schematic diagram of the test vessel, mixing vessel, and associated gas flow system.

### 2.1.2 Test Vessel and Mixing Chamber

Figure 2.4 is a photograph taken of the test vessel and mixing chamber prior to installation of any heaters or insulation. The vessel was constructed and tested by Fluitron Inc., of Ivyland, Pennsylvania, in compliance with provisions of the ASME Boiler and Pressure Vessel Code Section VIII, Division 1. Mechanical drawings for the test vessel are provided in Appendix A. The test vessel consists of two mated 3.05-meter long 316 stainless steel tubes with an inner diameter of 10 cm and a wall thickness of 1.91 cm. For the remainder of this report, the end of the test vessel where the detonation is initiated will be referred to as the "driver end" and the opposite end will be referred to as the "driven end". Standard ANSI flanges are used throughout. The middle and end pair of flanges are 1500 CLASS, and the driver pair are 2500 CLASS. The test vessel is ASME certified for a maximum allowable working pressure of 12.2 MPa at 700K. In order to comply with the Boiler and Pressure Vessel code, a rupture disc rated at 13.6 MPa at 700K was installed at an axial distance of 2.13 meters from the driven endcover. Each pipe section is supported on two steel "V" block supports whose height is adjustable. Eighteen equally spaced (i.e., 30.5-cm spacing) 1/2-20 threaded holes are drilled into one side of the vessel to be used as instrumentation ports. Two additional ports are located on the opposite side of the vessel at axial distances of 0.914 and 1.219 meters from the driven endcover.

The mixing chamber is a 30-liter pressure vessel which is ASME certified for a maximum allowable working pressure of 3.4 MPa at 425K. The main body of the mixing chamber consists of a vertically mounted 0.5-meter long, 25-cm diameter cylinder capped off with two elliptical heads. The top elliptical head is bored through and connected to a 15-cm long, 15-cm diameter tube which is capped with a standard 300 CLASS ANSI flange and endcover. The mixing chamber is equipped with a rupture disc rated at 3.74 MPa at 425K. The test mixture is prepared inside the mixing chamber and is mixed using an impeller. The impeller is rotated by an air-driven motor located just above the mixing chamber. A Parr Instruments rotating sealing gland is used to feed the impeller axle through the mixing chamber cover plate. A 150 ml gas sample bottle which is used as a water reservoir is connected to the mixing chamber. The bottle is isolated from the mixing chamber by a pneumatically-controlled ball valve.

### 2.1.3 Gas Handling System

A schematic showing the details of all the secondary gas lines is shown in Figure 2.3. All the gases (i.e., hydrogen, air, acetylene, nitrogen, and oxygen) are commercial grade and are supplied in standard gas cylinders. A gas panel is used for gas distribution from the various gas bottles to the test vessel, mixing chamber, and vent line. All gas lines are made up

from 0.635-cm (0.25 in.) and 1.27-cm (0.5 in.) seamless stainless steel tubing with wall thicknesses of 0.71 mm (0.028 in.) and 1.24 mm (0.049 in.), respectively. Stainless steel Swagelok pressure fittings are used throughout. The valves are pneumatically actuated sealed bellows type which are actuated by 24 VDC solenoid valves. All valves which are directly connected to the test vessel are rated for 17.0 MPa up to 644K and 9.25 MPa at 700K. A mechanical roughing pump is used to evacuate the test vessel and mixing chamber.

After each experiment, combustion products from the test vessel and remaining fresh test mixture from the mixing chamber are purged from the system using nitrogen. The purged gases are diluted with nitrogen in the vent mixing chamber to below flammability limit concentration before exhausting into the vent line.

### 2.1.4 Gas Driver System

In general, fuel-air mixtures require a substantial amount of energy for direct initiation of a detonation. As a result, high explosives have been typically used as the source of energy. In order to avoid the need of high explosives, and thereby obviate the need for extensive and costly explosives handling facilities and training, a decision was made to adapt the concept of a gas driver detonation initiation system to the needs of the high-temperature detonation experiments. Typically, in such a system, a plastic or metal diaphragm is used to separate a sensitive driver gas, usually a fuel-oxygen mixture, from the test gas. A detonation is directly initiated in the driver gas by a relatively weak electrical spark and the resulting detonation ruptures the diaphragm and initiates a detonation in the test gas. One of the unique features of the SSDA gas driver concept is that it uses no diaphragm. Instead, the driver gases are impulsively injected into the driver end of the test vessel in a very short time. The injection time is minimized so as to limit the amount of mixing between the driver gas and the test gas. Also, because of the relative high sensitivity of the driver gas mixture, one wants to minimize its residence time to avoid autoignition. To further reduce the possibility of autoignition, the driver flange is not heated. There are several reasons why a diaphragm is not desirable. When using a diaphragm system, the diaphragm must be replaced after each experiment. This process adds considerable time to run an experiment, especially at elevated temperatures. Also, the rupturing of the diaphragm disrupts and reduces the effectiveness of the transmission of the driver gas detonation and subsequent initiation of the detonation in the test gas.

A schematic representation of the driver system is shown in Figure 2.5. The driver gas used in the SSDA experiment is a mixture of acetylene and oxygen. The acetylene and oxygen gases are mixed by annular flow in two 12.5-mm diameter tubes. The acetylene is introduced via a central 6-mm tube, and the oxygen is introduced through the annular space between the 6-mm and 12.5-mm tubes. There is a redundant valve on both the oxygen and acetylene lines and flame arresters to prevent any flashback to the respective gas cylinders. The premixed oxygen-acetylene mixture is injected through two ports into an 8.6-cm diameter by 10-cm long cylindrical initiation chamber which is welded to the driver endcover. Photographs of the initiation chamber are shown in Figure 2.6. Figure 2.6a shows the side-view of the chamber with the endcover bolted in place. The stainless steel hex nut visible on the side of the chamber is a feedthru for a GM AC 7 glow plug used to burn the test mixture in the event of a test abort. The two ports where the driver gas is injected into the ignition chamber are located on the side of the chamber directly opposite the glow plug, as seen in Figure 2.6b. This chamber is connected to the main test vessel through a 5-cm diameter orifice in the flange. The pre-chamber was required because of space limitations for installing the initiation electrodes and injection ports for the driver gas.

A detonation is initiated in the initiation chamber by an "exploding wire" which is fastened between the two electrodes mounted on the initiation chamber endcover as can be seen in Figure 2.6b. An exploding wire is a fine gage wire that vaporizes instantaneously when a very large current is made to pass through it. The rapid expansion of the vapor generates a blast wave which, in turn, initiates the detonation in the driver gas mixture. The large current required to vaporize the wire is derived from the shorting a charged high-voltage capacitor across the wire. The high-voltage discharge system is shown in Figure 2.7. The main circuit consists of a Maxwell 20 $\mu$f, 7.5 kV capacitor in series with an EG&G GP-85-10 spark gap. The spark gap is triggered using an EG&G TM11A trigger module. A 30kV Hipotroncs power supply is used to charge the capacitor. The wire leads from the high voltage circuit are fastened to the external portion of the electrodes seen in Figure 2.6a.

Using this system, acetylene-oxygen gas driver slugs of any strength and length can be produced by adjustment of the relative constituent flow rates and mixture fill time. After many shakedown tests, it was found that the most effective driver mixture composition was 20 volume percent acetylene and 80 percent oxygen. Typically, driver lengths of up to 40 cm were used which corresponds to a maximum driver gas injection time of about 3 seconds.

### 2.1.5 Heating System

The heating system was designed, manufactured, and installed by Cooperheat Inc., of Piscataway, New Jersey. The system is capable of heating the test vessel to 700K in 3 hours with $\pm$ 14K spatial uniformity. This spatial temperature specification was arrived at by considering the sensitivity of the calculated cell size to temperature. A considerable amount of time and effort was spent on achieving this spatial temperature uniformity. Several heater pad and insulation configurations were investigated. The BNL group was actively involved in the design and acceptance testing of the heating system.

The heating system for the test vessel consists of the master control unit, a slave unit, heater elements, and insulation. A system configuration diagram is given in Figure 2.8. The master control unit is located in the control room, and the slave unit is located about 2 meters from the driver end of the test vessel. The master control enclosure contains Honeywell UDC 2000 Mini-Pro digital temperature controllers, one for each heating zone, and control and monitoring indicators. The system is equipped with ground fault protection whereby the main power is cut if a heater element comes in contact with the test vessel. The slave enclosure contains the main power transformer as well as all zone conductors, current switches, and ground fault interrupter modules. All interface signals between the master control and the slave unit are 24 VDC. The cable length is approximately 38 meters. There are two heater junction boxes secured to the test vessel support frame where the power from the slave unit for each zone terminates at a power distribution block. The heater pad leads are routed through a small cable tray, located adjacent to the test vessel, into the junction box and fastened to the appropriate distribution block.

One pipe section of the test vessel equipped with heater elements is shown in Figure 2.9. In the figure, the middle and end flange pair are covered with the first of two 5-cm thick Kaowool insulation blankets which cover the entire vessel. There are five independent heating zones, one for each pipe section and one per flange pair. A typical heater pad is shown in Figure 2.10. The resistance wire heating element is woven into a flexible ceramic pad which is fastened to the vessel using stainless steel pipe clamps. The heater circuit for the two pipe sections are identical, each having sixteen 60V ceramic heater pads. There are eight parallel circuits with two heater pads, typically at the three and nine o'clock positions of the tube, connected in series. The current draw for each heater pad pair is nominally 30A and 240A per zone. A "snake-type" heater is used to apply heat at the flange hubs where it is difficult to fit heater pads. In order to minimize heat losses to the supports through the "V" blocks, two measures were taken. First, the contact area between the vessel and the blocks were minimized to a line contact of 2.54 cm in length. Secondly, a "snake" heater was used to concentrate heat around the "V" blocks. The heaters for the three flange pair zones are identical. Each zone has two 80V ceramic heater pads connected in parallel, also located in the three and nine o'clock positions. The current draw for each heater pad is approximately 45A and 90A per zone.

Each zone has a K-type sheathed thermocouple placed under a centrally located heating pad which is used by the temperature controller to monitor the zone temperature. Additional monitoring thermocouples are positioned in several strategic locations on the test vessel. Due to the large mass of the flanges, a potential cold spot would be the flange hubs. For this reason, a thermocouple is placed on each of the flange hubs. Typically, every other port in the driven end pipe section is taken up by an exposed junction probe-type thermocouple monitoring the gas temperature just inside the tube wall. An experiment does not proceed until all these temperatures converge within the $\pm$ 14K specification.

Extra thermocouples were added to the test vessel for the purpose of testing the heating system to ensure that it met the temperature uniformity specification. The philosophy adopted in the testing the pipe section of the test vessel was to use a high density of thermocouples around a pair of heater pads and consider the results to be typical for the entire pipe section. This is possible since the heater pad layout on the pipe section is symmetric. Figure 2.11 is a schematic of a section of the pipe, slit axially and flattened, showing the thermocouple positions relative to the heater pads and the final steady state-

temperatures. Recall the heaters are in the 3 and 9 o'clock positions looking axially down the pipe. The 6 mm sheathed ungrounded thermocouples are strapped to the vessel using stainless steel pipe clamps. The temperature set point in this run is 650K. The average temperature measured is 649K with a maximum of 655K and a minimum of 641K yielding a spread of 14K.

Heating systems for the mixing chamber and secondary piping were assembled by BNL staff. The mixing chamber body and flange pair are heated independently using 240 V heating tape. Omega CN320K temperature controllers in conjunction with a solid state relay are used for power control to the heating tape. A 5-cm thick layer of Kaowool is wrapped around the entire mixing chamber. Heating tape was also used for trace heating the water reservoir and select tubing, including the run between the mixing chamber and the test vessel. The power source for the trace heating tape is a standard 120V variac. As shown in Figure 2.3, in the downloading process from the mixing chamber to the test vessel, the gas goes through a 2-meter long coiled section of tubing which is heated inside of a 240V 2.3 kW cylindrical ceramic heater. The purpose of this heater is to pre-heat the test mixture to the test temperature before being injected into the test vessel. This minimizes the residence time in the test vessel prior to initiation. The cylindrical heater is controlled using an Omega CN320 temperature controller.

## 2.1.6 Instrumentation

Test parameters to be measured in an experiment include the initial mixture conditions, such as temperature, pressure and hydrogen concentration, and detonation parameters, such as pressure, time of arrival, and cell size. This section describes the instruments used to measure each of the above mentioned parameters.

### 2.1.6.1 Test Vessel Pressure

All the detonation experiments performed on the SSDA are at an initial pressure of 0.1 MPa. The pressure transducer used for monitoring the test vessel pressure during the filling process is a strain gage type Sensotec Model TJE absolute pressure transducer with a range of 0 to 0.34 MPa with an accuracy of 0.1 percent of full-scale. The pressure transducer is isolated from the test vessel by a valve at the time of detonation initiation

### 2.1.6.2 Test Vessel Gas Temperature

Gas temperature measurement is made with K-type exposed junction sheathed thermocouple probes inserted into instrumentation ports using standard bored through Swagelok pressure fittings. The thermocouple output is processed on a A/D board installed on a personal computer, as described in Section 2.1.7. The thermocouple leads are connected to an external terminal panel equipped with an isothermal plate specifically designed for thermcouples. The driver software performs the cold junction compensation and linearization. As quoted from the vendors catalog the accuracy of the reading from this sytem for a K-type thermocouple is 1.2K. During each experiment there are typically five of such thermocouples whose signals are logged during the test vessel fill. The temperature readings for these thermocouples at the time of ignition are given in Appendix B for each run.

### 2.1.6.3 Mixture Composition

The test mixture is prepared in the mixing chamber by the method of partial pressures. That is, the fraction of the total number of moles in the final mixture for each gas constituent is equal to the ratio of its partial pressure over the final mixture pressure. Therefore, the accuracy of the mixture composition is soley dependent on the accuracy of the pressure transducer used to monitor the mixing chamber fill process. The pressure transducer used to monitor the mixing chamber pressure is identical to the pressure transducer used in the test vessel, described in Section 2.1.6.1, which has an accuracy of $\pm$ 340 Pa. Therefore, the uncertainty in the hydrogen concentration in a 10 percent nominal hydrogen mixture is $\pm$ 0.124 percent hydrogen.

For the slow oxidation experiments hydrogen concentration is measured directly using a Carle Analytic Gas Chromatograph model 311H. Gas samples are taken from the test vessel using a pre-evacuated 150 ml gas sample bottles

valved off from the test vessel using pneumatically controlled ball valves. The gas chromatograph is calibrated using three external gas standards; 10.2 percent, 25.2 percent, and 49 percent hydrogen in nitrogen. The gas chromatograph uses nitrogen as the carrier gas at a flow rate of 27 cc/min. A 2.1-meter long, 3.175-mm diameter column filled with CARBO S 100-120 mesh is used in conjunction with a thermal conductivity detector. At least five measurements are taken from each sample bottle using a small volume "sampling loop." The signal from the gas chromatograph is processed using a Spectra Physics 4270 Integrator.

The gas chromatograph is calibrated using the standards on the same day that gas samples are to be analyzed. This is to avoid any uncertainty in the measurement due to change in the atmospheric pressure from the time of calibration to the time of the actual gas analysis. The atmospheric pressure determines the amount of gas which is actuall, sampled in the gas chromatograph loop. Clearly the accuracy of any measurements taken using a gas chromatograph cannot be any more accurate than the certified accuracy of the gas standards used to calibrate it. The accuracy of the standards which were used routinely are: $\pm 1$ percent of reading for the 25.2 percent and 49 percent hydrogen standards and $\pm 2$ percent for the 10.2 percent hydrogen standard. In calibrating the gas chromatograph five samples are taken from each standard. Typically, the repeatability for these five measurements are between $\pm 0.1$ percent and $\pm 0.2$ percent of reading.

A series of tests were performed where hydrogen-air mixtures were prepared in the mixing chamber and then downloaded into the test vessel at room temperature. Gas samples were taken from the test vessel and analyzed using the gas chromatograph. The hydrogen content of the mixture, as determined by the method of partial pressures, was then compared to that measured by the gas chromatograph. Five mixtures were tested with nominal hydrogen mole fractions of 10, 20, 30, 40 and 48 percent. The difference in the partial-pressures hydrogen content and that measured using the gas chromatograph varied from a low of 0.48 percent of reading for the 48 percent hydrogen sample and a high of 2.35 percent of reading for the 10 percent hydrogen sample.

### 2.1.6.4 Detonation Pressure

Fast response PCB 113A24 quartz piezoelectric pressure transducers are used for measuring detonation pressure. These transducers have a maximum pressure range of 6.8 MPa with a risetime of 1 $\mu$s. The accuracy of the transducer is quoted by the vendor to be less than 1 percent of full scale. The maximum operating temperature for the transducer is 408K. The majority of the experiments are performed at temperatures well above the transducers maximum operating temperature, so a special PCB water-cooled adapter is used. Experience demonstrated that the transducers functioned properly as long as water supply was maintained to the adapter.

### 2.1.6.5 Detonation Velocity

Detonation time-of-arrival is measured almost exclusively using homemade "ionization probes." An ionization probe consists of two electrically isolated electrodes, about 2 mm in diameter and 1 cm apart, which are connected to an electrical circuit shown in Figure 2.12. The electrodes are inserted about 2 cm into the test vessel through an instrumentation port. The principal of operation of these probes is that the detonation reaction zone, which is rich in ions, shorts out the ionization probe electrodes as it passes the probe. The electrical circuit converts the shorting of the two electrodes into a rapid voltage drop measured across an output resistor. For a sensitive mixture, the reaction zone is very close to the leading shock wave so both the ionization probe and the pressure transducer should record a rapid transient at precisely the same time as the detonation passes. This principle was used to check the performance of the ionization probe by comparing its signal with that of a piezoelectric pressure transducer placed in a instrumentation port directly opposite the ionization probe (i.e., the same axial location). The time difference between the sharp drop in voltage characteristic of the ionization probe and the steep pressure rise recorded by the pressure transducer was within the 1 $\mu$s rise time of the pressure transducer.

The detonation velocity is calculated based on the distance and the detonation time-of-flight between consecutive ionization probes. This gives an average velocity over the axial distance between probes. Typically, this distance is $60.96 \pm 0.30$ cm. The ionization probe layout for a typical detonation experiment is given in Figure 2.13 with a characteristic output signal. There are a total of eight probes monitored on two oscilloscope channels. As dicussed above, response time of the

ionization probes is similar to that of a piezoelectric pressure transducer which is 1 $\mu$s. Typically, the oscilloscope is run at a sample every 0.5 $\mu$s, therefore, any uncertainty in the calculated velocity must be attributed to the 1 $\mu$s response time of the ionization probe. Considering a $\pm$0.30 cm uncertainty in the distance between ionization probes, for a typical detonation velocity of 2000 m/s, the uncertainty is $\pm$ 7.6 m/s.

#### 2.1.6.6 Measurement of Detonation Cell Size

The measurement of cell size from smoked foils is considered to be one of the most important aspects of the experimental program. The smoked-foil technique has been successfully used in the past with mixture temperatures below 400K. Since the majority of the experiments in this program are at temperatures above 400K, there were many uncertainties concerning the effect of temperature and steam on smoked-foil performance.

The first stage in developing the smoked-foil technique was to obtain foils which performed satisfactorily at room temperature. Aluminum sheet metal 0.5-mm thick was chosen as the material for the foil because of its flexibility. The sheet could easily be rolled into a 10-cm diameter cylinder to be inserted into the test vessel and could easily be unrolled for post test analysis. Typically, the foil is 30.5-cm wide x 91.5-cm long. However, in some cases where longer tracks are desired, foils as long as 1.5 m are used. When the foil is inserted into the tube, it does not cover the entire circumference, a 1.27-cm gap is left at the top for instrumentation purposes.

For weak mixtures, the flow associated with the detonation causes the two corners of the leading edge of the foil to fold, and in the case of very weak mixtures approaching single-head spin, the entire foil is crumpled beyond recognition. In the past, this was prevented by using some sort of stiffening ring at the leading edge of the foil. This ring is undesirable since it introduces a perturbation to the detonation right at the point where the cell size measurement is taken. A different approach was adopted where the corners of the leading edge of the foil are rounded off, as can be seen in Figure 1.1.

After the foil is cut, it is rolled into an 11.4-cm diameter cylinder. It is then inserted into a 10-cm diameter, 91.5-cm long aluminum tube which is held vertically. The top of the cylinder is blocked off with a metal plate. A burning kerosene lamp is placed beneath the bottom opening of the cylinder so that the soot generated from the lamp rises and accumulates inside the cylinder. In this way, the soot adheres evenly to the aluminum foil inside the tube. This is done for 90 seconds on each end of the foil. The foil is then removed from the tube and inserted into the driven end of the test vessel, as shown in Figure 2.1. After an experiment is completed, the foil is removed, unfolded, and the smoked side of the foil is sprayed with a clear lacquer to preserve the inscribed cellular pattern.

It was found during shakedown experiments at elevated temperatures that the soot did not adhere to the foil. Post-test foils were predominantly clear of soot except for some isolated patches. We then began experimenting with coating the foil with different liquids before sooting. The best result was obtained by spreading approximately 1 ml of Dow Corning DC200 silicone fluid with a 10 centistoke viscosity over the entire foil with a paper tissue. The flash point for this fluid is 436K using the closed cup technique. For high temperature experiments, when foils are prepared in this fashion, the foil is inserted while the tube is cold. The tube is then heated with air remaining inside so that the silicone fluid reacts with the air to form $SiO_2$ particulate. If the foil is inserted while the tube is at temperature, fumes instantly start to come off the foil for about 20 seconds. In most cases, foils used in high-temperature experiments prepared in this manner are of better quality than the room-temperature foils prepared in the standard way. Photographs of two foils obtained from experiments at room temperature and 650K are shown in Figure 1.1. The reason why this sublayer of $SiO_2$ produces better foils is not known. Interpretation of the cell patterns recorded on the foils is discussed in Section 3.2.1.

### 2.1.7 Control and Data Acquisition

All data acquisition and control equipment is located in the control room, requiring a maximum cable length of 15 meters to reach the furthest point on the test vessel. Figure 2.14 is a photograph taken of the instrument layout in the control room. The unit on the far right is the heating system master control console. The rack on the left contains oxygen and hydrogen detector readouts, three temperature controllers, pressure transducer conditioner and readout, interlock status indicators, and power supplies for the ionization probes and high voltage firing circuit.

The low-speed control and monitoring of the experiment is done from a 486 Gateway personal computer equipped with commercially available data acquisition and control hardware from Strawberry Tree. The hardware includes two ACPC-12 cards which have 12-bit resolution and a 10kHz sampling rate. This card has 16 digital input/output channels and 16 differential analog inputs with thermocouple cold junction compensation. A second ACPC-I/O card with 160 digital input/output channels is used mainly for valve actuation and verification. A Personal 488 card adds GPIB (General Purpose Interface Bus) capabilities to the computer. The hardware is driven by an icon based program from Strawberry Tree called Workbench.

Typically, hydrogen-air detonations propagate at velocities between 1500 and 2000 m/s. In order to track the detonation front position and pressure as it propagates down the length of the test vessel, a high-speed data acquisition capability is required. A four channel LeCroy 314L digital oscilloscope with a sampling rate of 100 MHz and 1 Mbyte storage per channel is used to capture the signal from the ionization probes and the piezoelectric pressure transducers. The oscilloscope is equipped with a floppy disk for data storage, or the GPIB interface can be used to download the data from the oscilloscope to the computer for permanent storage.

## 2.2 Experimental Procedures

The following is a brief description of the operating procedures used for the various types of experiments. Since the interlock system is an integral feature of all experiments, it is discussed first in Section 2.2.1.

### 2.2.1 Interlock System

The test vessel is located in a large experimental hall. The data acquisition and control equipment is located in an adjacent control room which is isolated from the hall by a large plug door. An interlock system in place requires the operator to perform certain tasks before any experiment can be started and which determines when he can re-enter the experimental hall after an experiment. No personnel are allowed in the experimental hall while an experiment is underway. It is required that the experimental hall be cleared of all personnel before either the fuel (i.e., hydrogen or acetylene) or oxygen valves can be actuated. There is a set of buttons located at various positions around the experimental hall that must be depressed in a prescribed time and sequence. During this procedure, the operator searches for personnel who might inadvertently otherwise remain in the experimental hall during an experiment. Once the hall is cleared, the plug door is closed and the plug door key is removed. The key is then inserted into a keyhole located on the equipment rack in the control room. If the clearing process is properly performed, turning the key sets off a tone for 15 seconds, which is heard throughout the experimental hall and the control room. This clearing process is also required in order to operate the power supply for the high-voltage circuit. After the experiment is performed, it is required to purge the test vessel and mixing chamber with nitrogen in order to re-enter the experimental hall. The interlock system searches for a sequence of valve openings which ensures that purging is taking place. Only after this valve sequence is observed for a prescribed period of time is power returned to the plug door, thereby enabling re-entry into the experimental hall.

### 2.2.2 Detonation Experiments

The first step in preparing for a detonation experiment is to prepare a smoked foil as described in Section 2.1.6. The foil is inserted into the driven end of the test vessel and the endcover is bolted onto the vessel. Next, an "exploding wire" is placed between the ignition electrodes and the initiation chamber cover is bolted in place. Once the entire vessel is secured, the appropriate temperature set points are entered into the temperature controllers and the heating of the test vessel, mixing chamber, and secondary piping is started. At the same time that the test vessel and mixing chamber are being heated they are also evacuated using the roughing pump.

Once the test vessel has reached the desired temperature the experimental hall is cleared and the plug door is closed. Upon closure of the plug door the combustible gas mixture is prepared in the mixing chamber by the method of partial pressures to a final mixture pressure of 0.3 MPa . For experiments where steam is one of the mixture constituents, a predetermined amount of water is added into the water reservoir and then injected into the mixing chamber. The mixture is stirred for five minutes using the mixing chamber impeller in order to ensure proper mixing of the gas constituents.

After the five-minute mixing period, the test mixture is downloaded into the test vessel to a pressure just below 0.1 MPa. This downloading of the gas takes about 30 seconds. The mixture is allowed to sit in the test vessel for an additional 30 seconds in order to achieve a uniform gas temperature. Before the mixture downloading is started, all heaters are shut off to minimize any electrical noise which may be picked up by the instrumentation. At this point, the oxygen-acetylene mixture is injected into the driver end of the test vessel. When the test vessel pressure reaches 0.1 MPa, the ignition system is activated and the detonation is initiated. The downloading and ignition sequence described above is completely performed by computer control. The raw data is then saved and the test vessel and mixing chamber are purged. After the purge, the operator re-enters the experimental hall and recovers the smoked foil.

### 2.2.3 Volumetric Oxidation Experiments

The procedure is identical to that just described in Section 2.2.2 except for the following: In the oxidation experiments, a detonation is not initiated and, therefore, no exploding wire or smoked foil are used. The experimental hall is cleared, the test vessel is heated, and the test mixture is prepared in the mixing chamber in the same manner described in Section 2.2.2. The main difference in the procedure is that once the test mixture is downloaded into the test vessel, it is not deliberately ignited. During and after the test mixture has been loaded into the test vessel, the vessel pressure and gas temperature at several locations are monitored. For test where gas samples are taken, the sample bottles are mounted on the vessel before the Experimental Hall is cleared. The sample bottles are evacuated at the same time as the test vessel by opening the isolation valves. As in the detonation experiments, the vessels are purged and the plug door is opened, at the termination of an experiment.

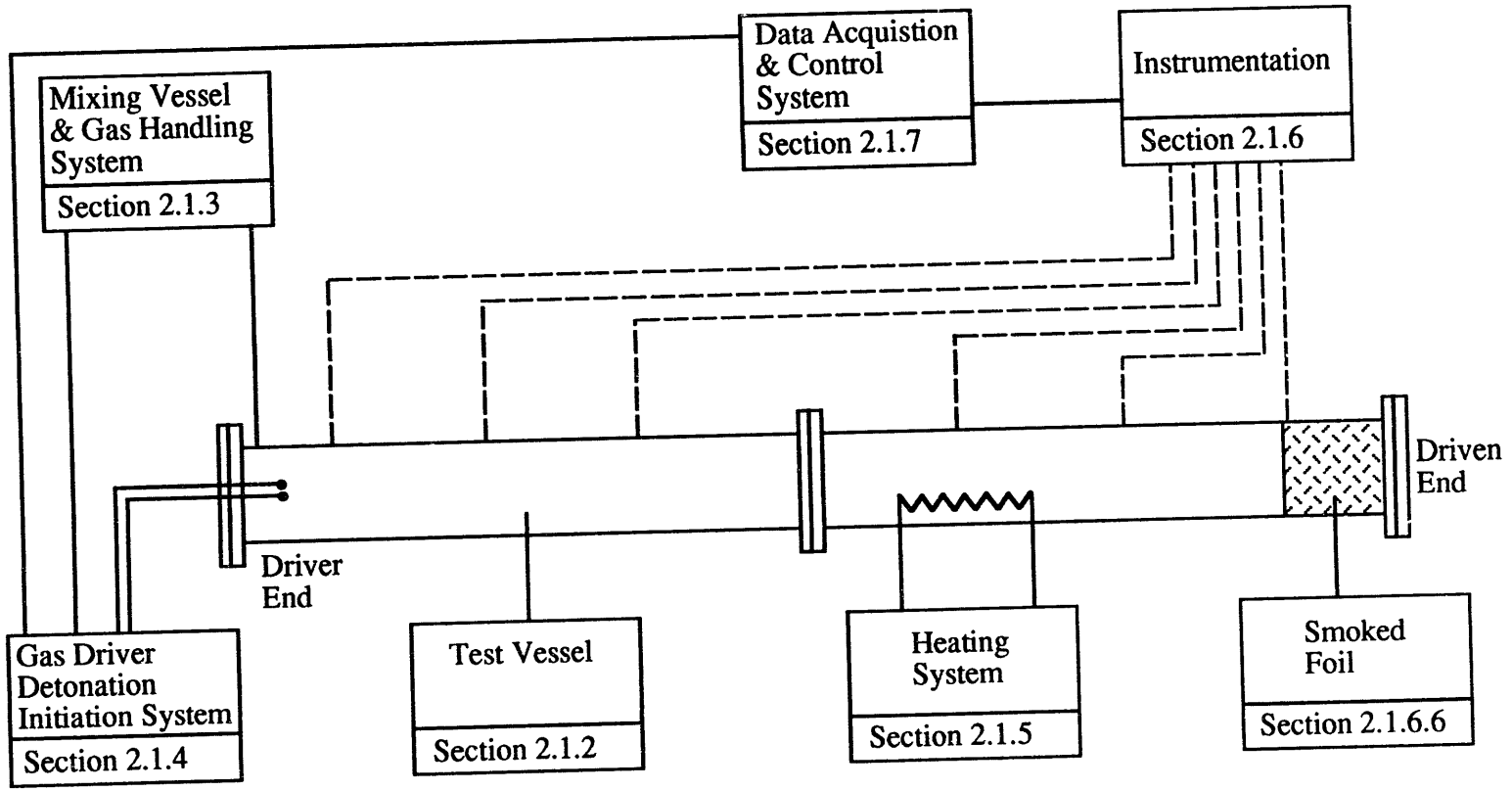


Figure 2.1 Schematic overview of test vessel and operating system

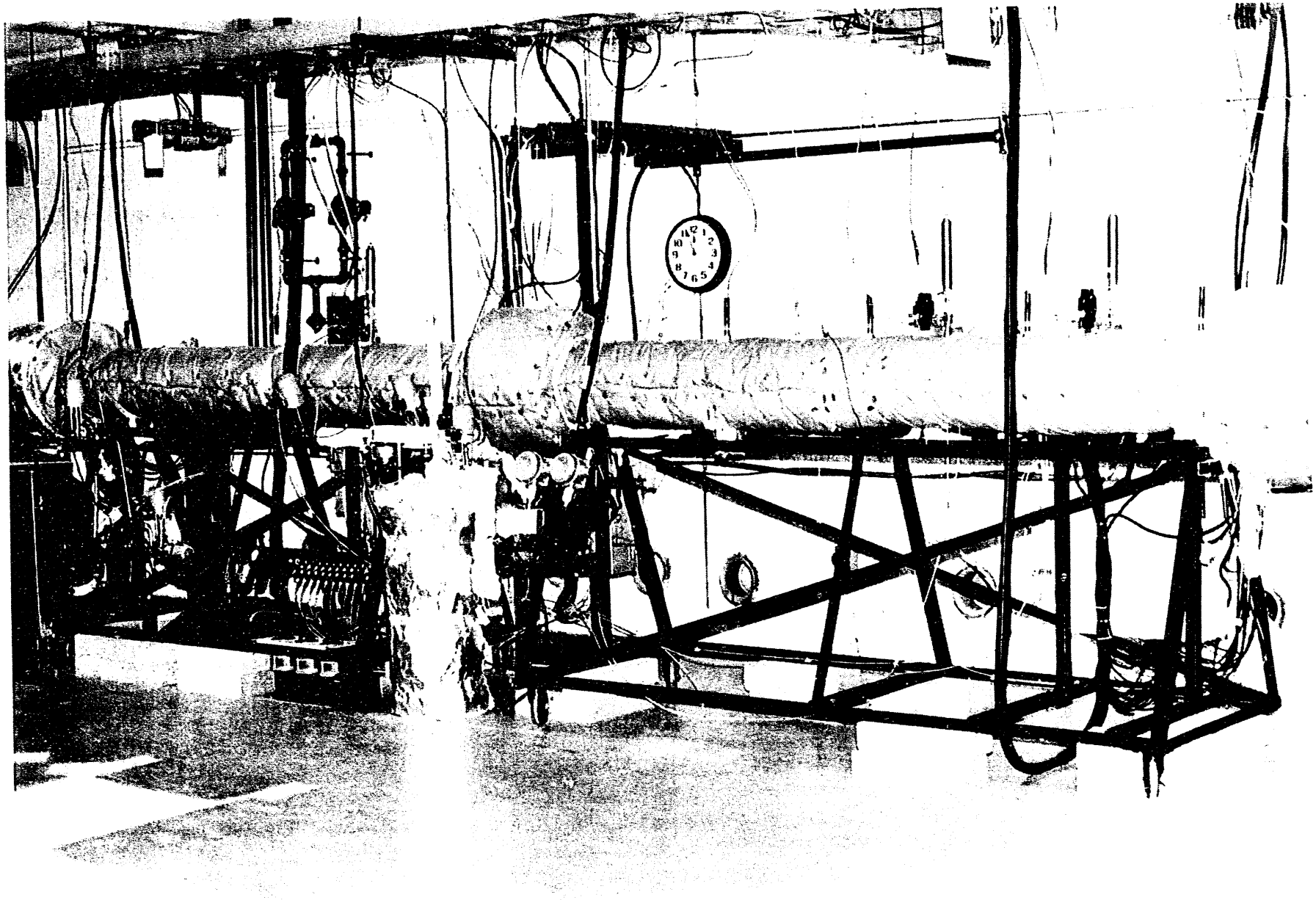

Figure 2.2: Photograph of Small-Scale Development Apparatus (SSDA)

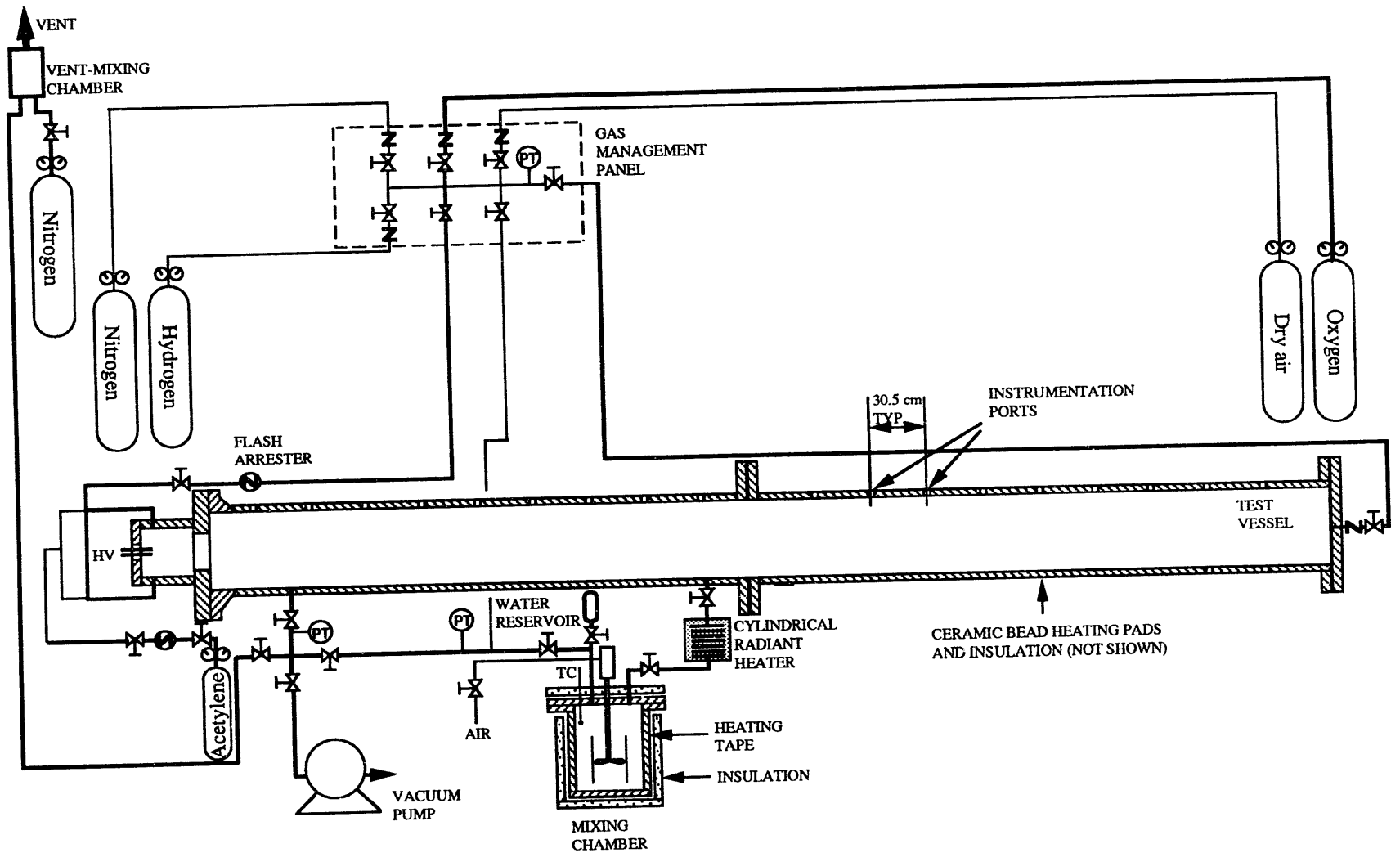


Figure 2.3: Schematic of SSDA showing the test vessel, mixing chamber and secondary piping

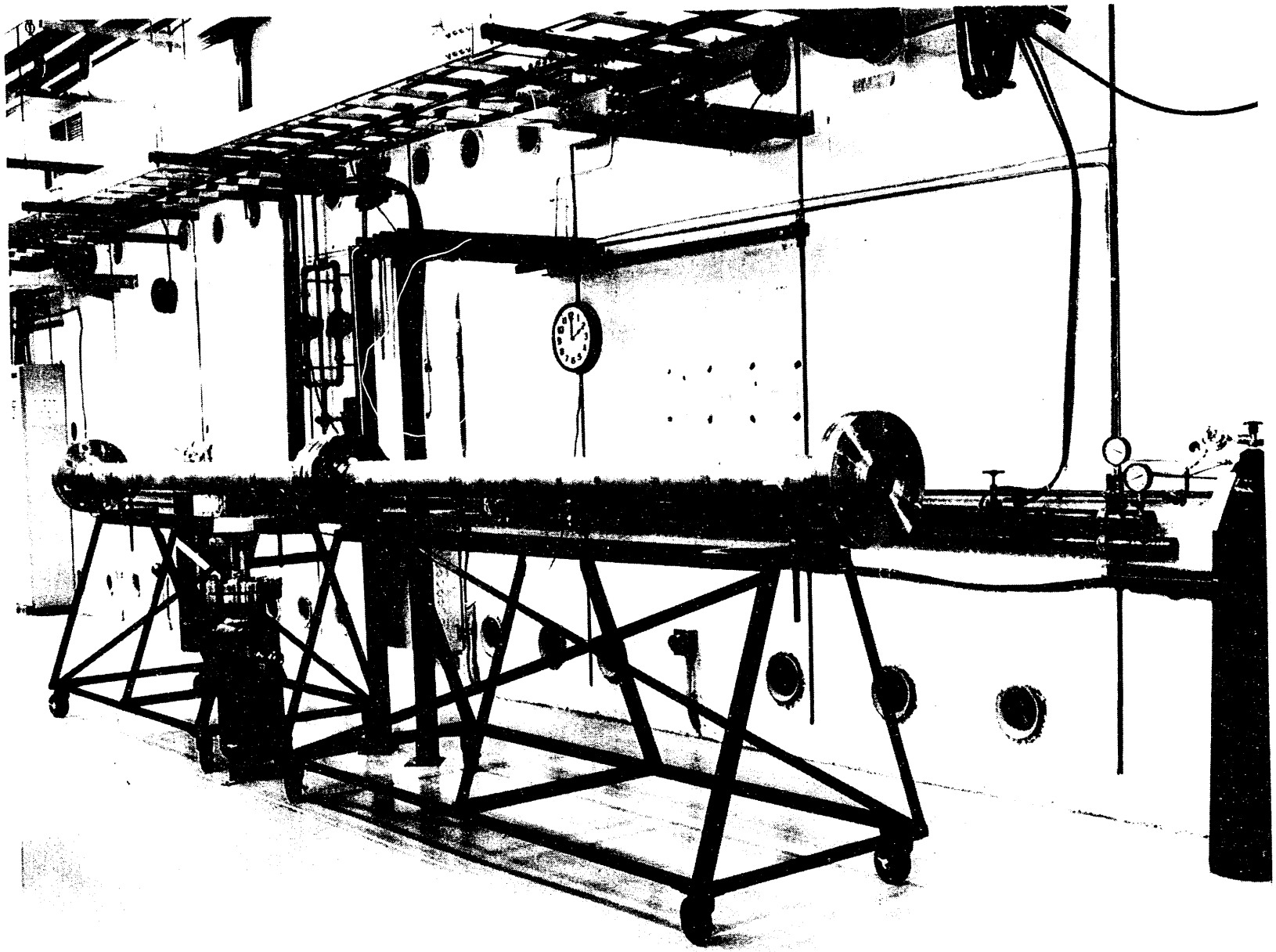

Figure 2.4: Photograph of the SSDA test vessel and mixing chamber prior to installation of heaters or insulation

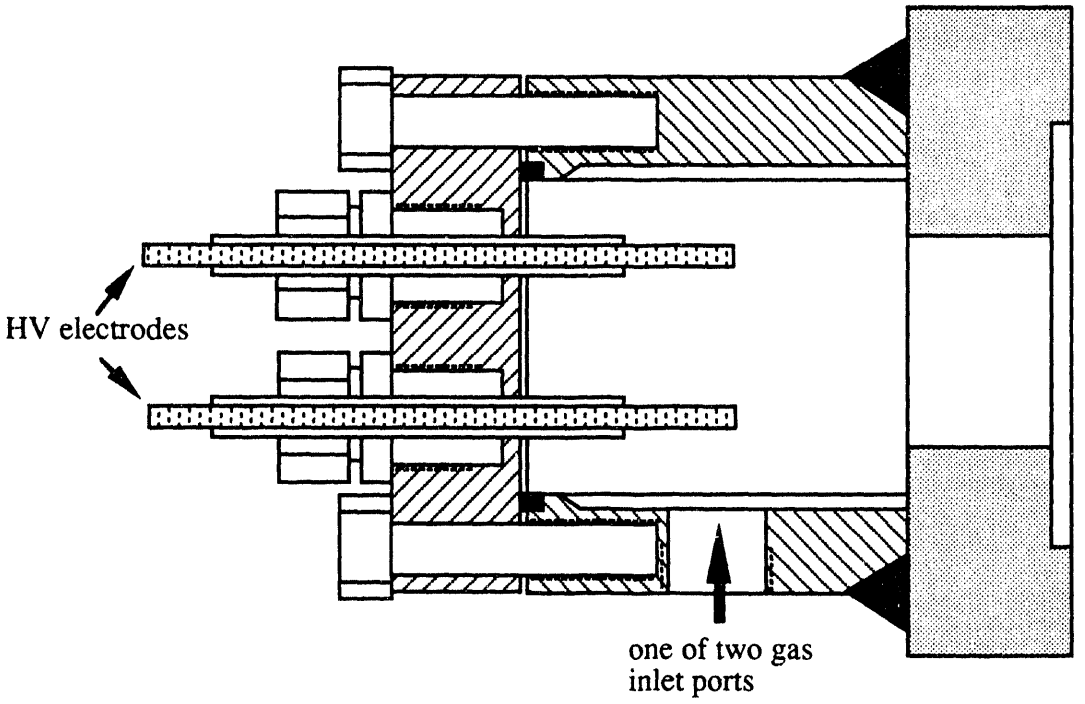


(a) Side-view of Initiation Chamber

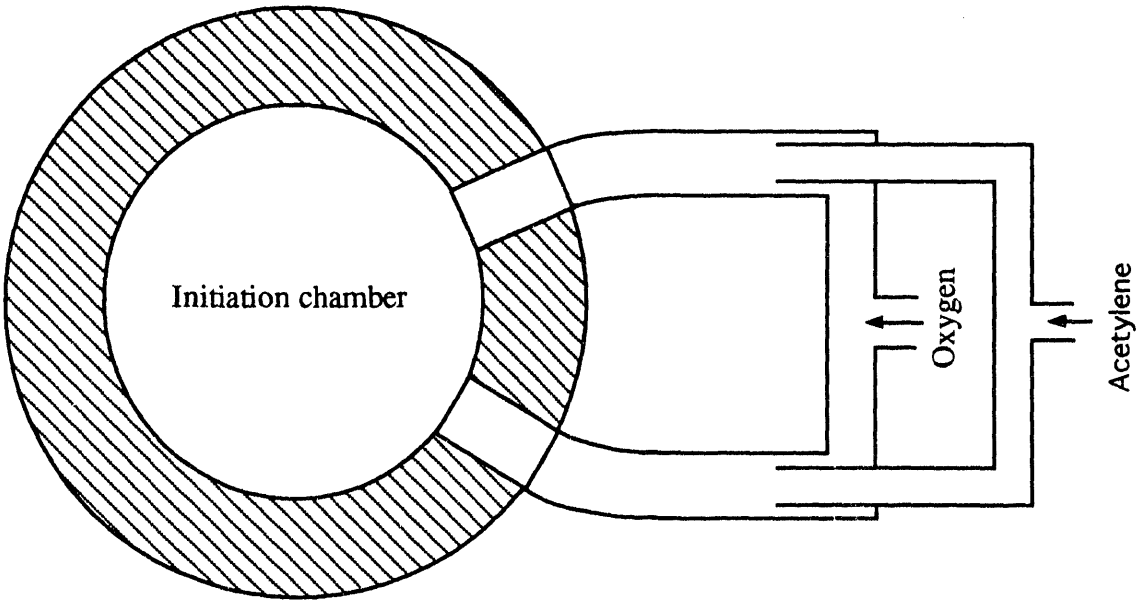


(b) Oxygen and acetylene gas lines

Figure 2.5: Schematic of the Gas Driver System

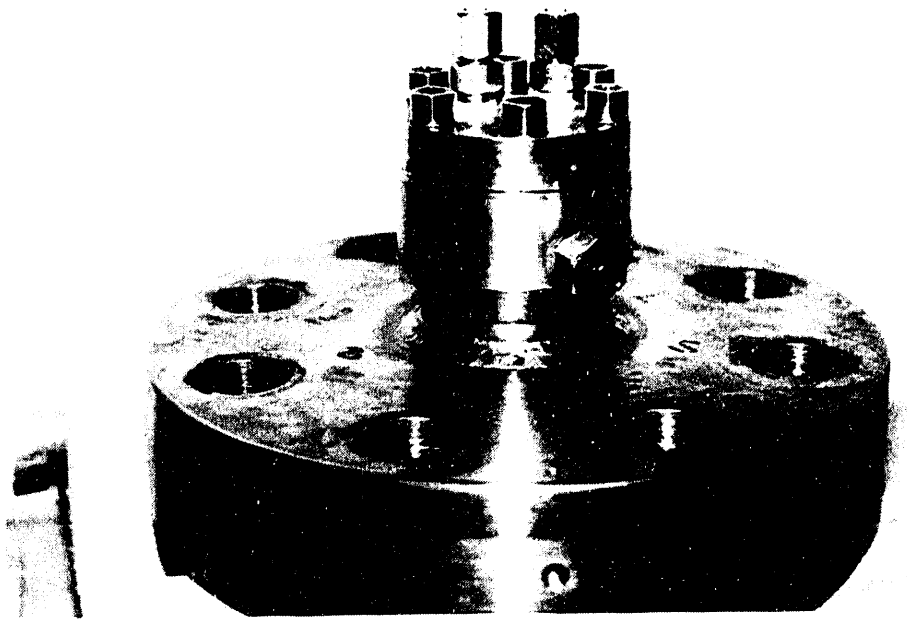

(a) Side-view

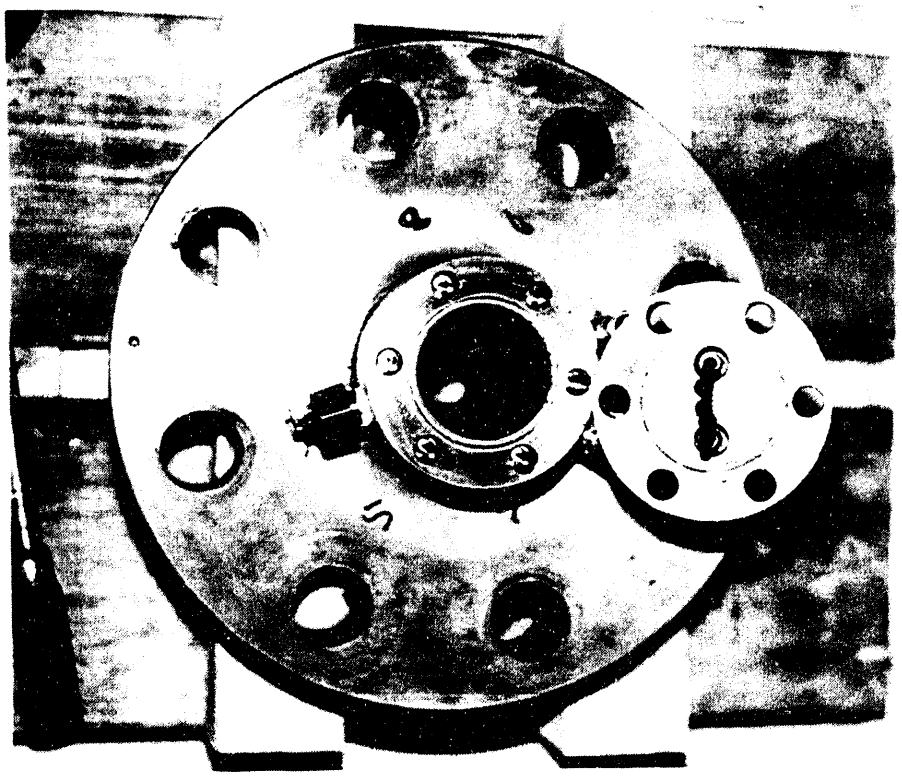

(b) Axial-view

Figure 2.6: Photographs of the gas driver "initiation chamber"

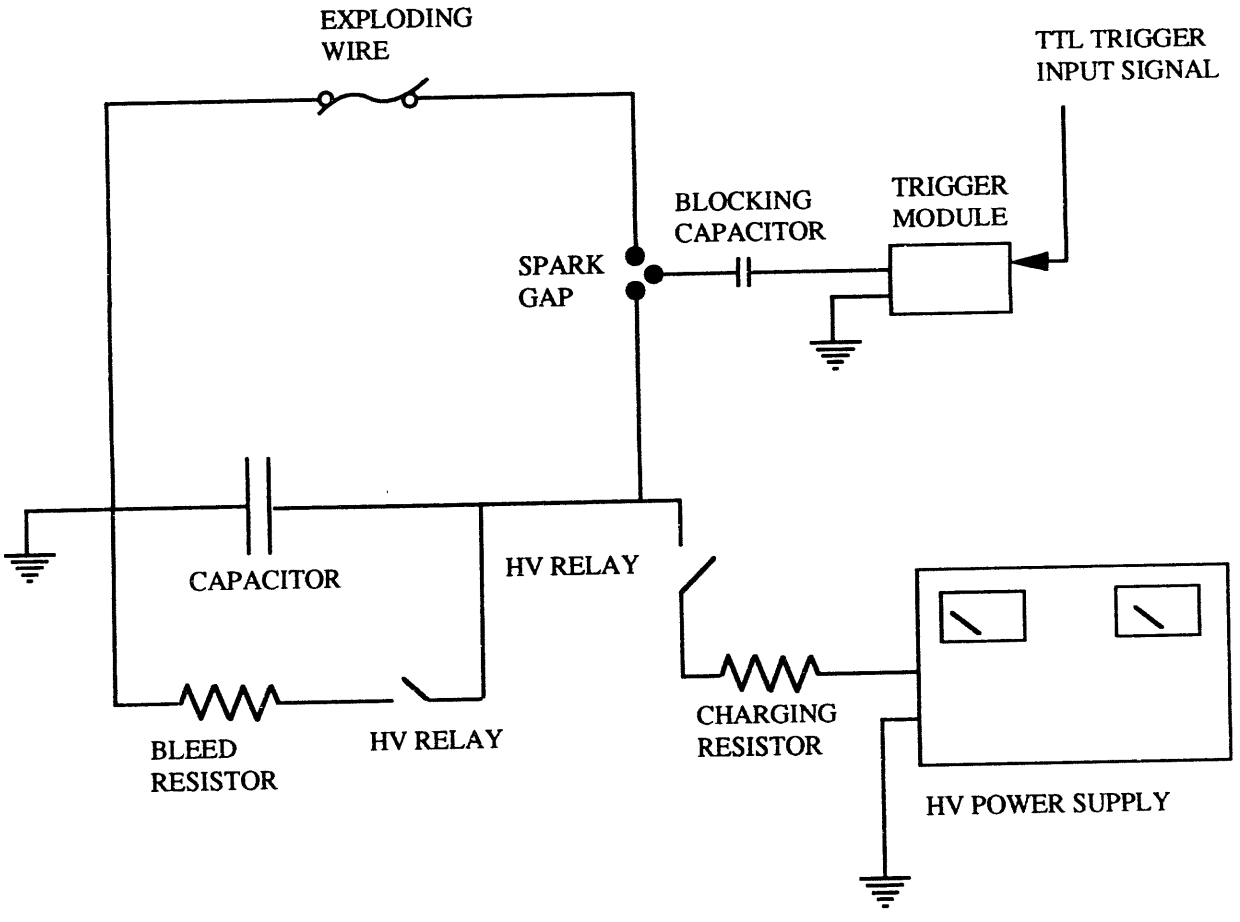


Figure 2.7: High voltage discharge circuit used for initiation in the driver ststem

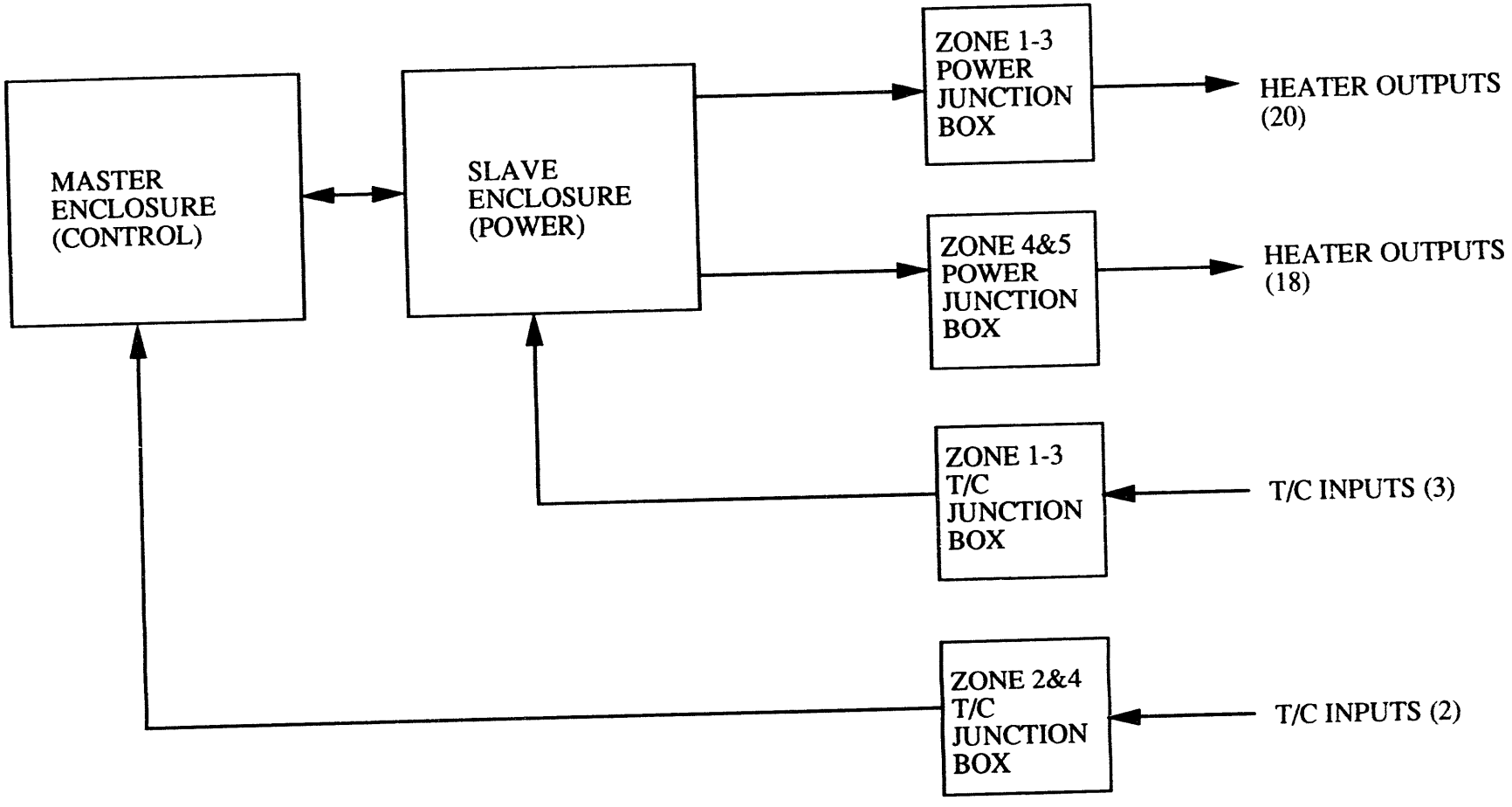


Figure 2.8: Heating system configuration diagram

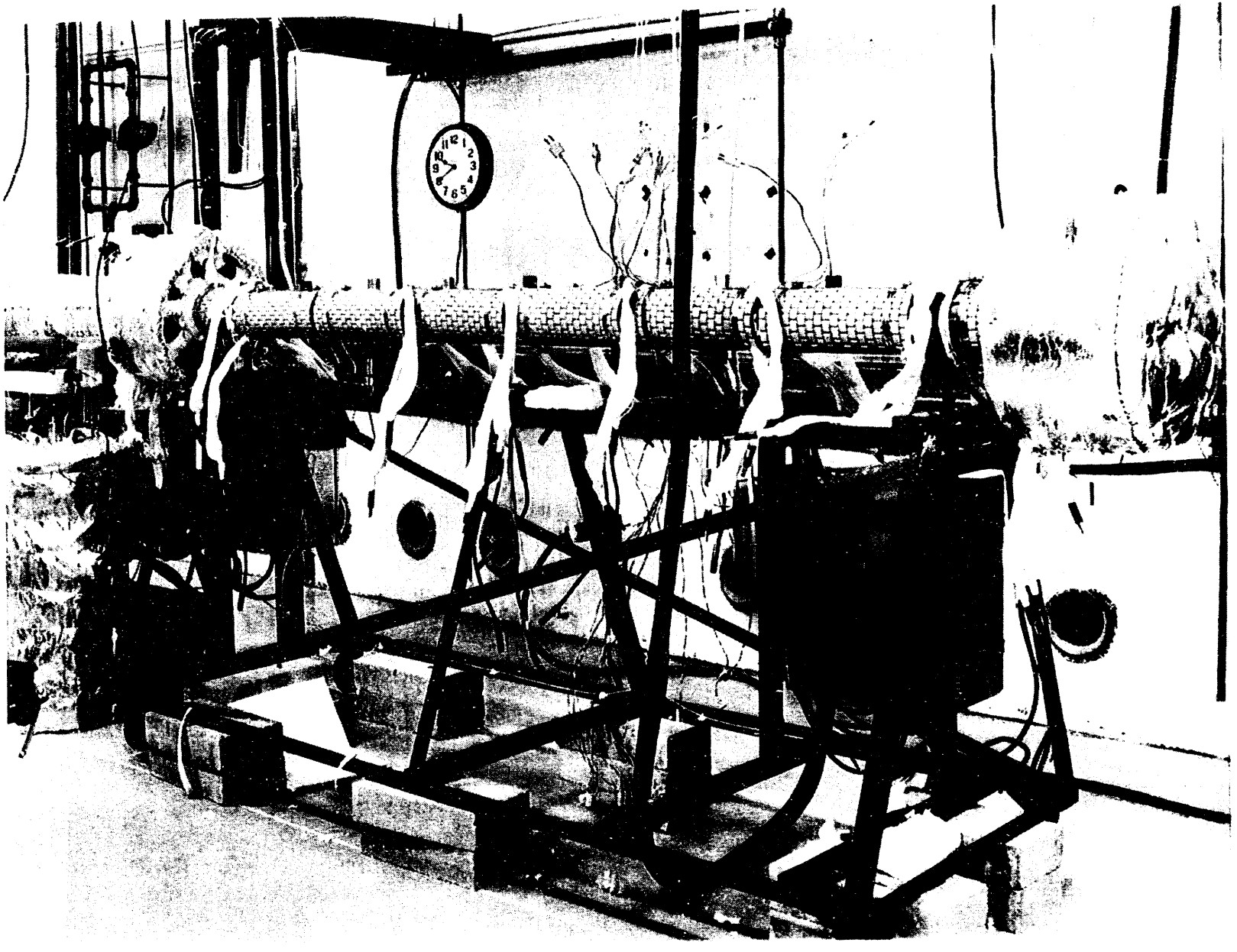

Figure 2.9: Photograph of one pipe section of the test vessel equipped with heaters

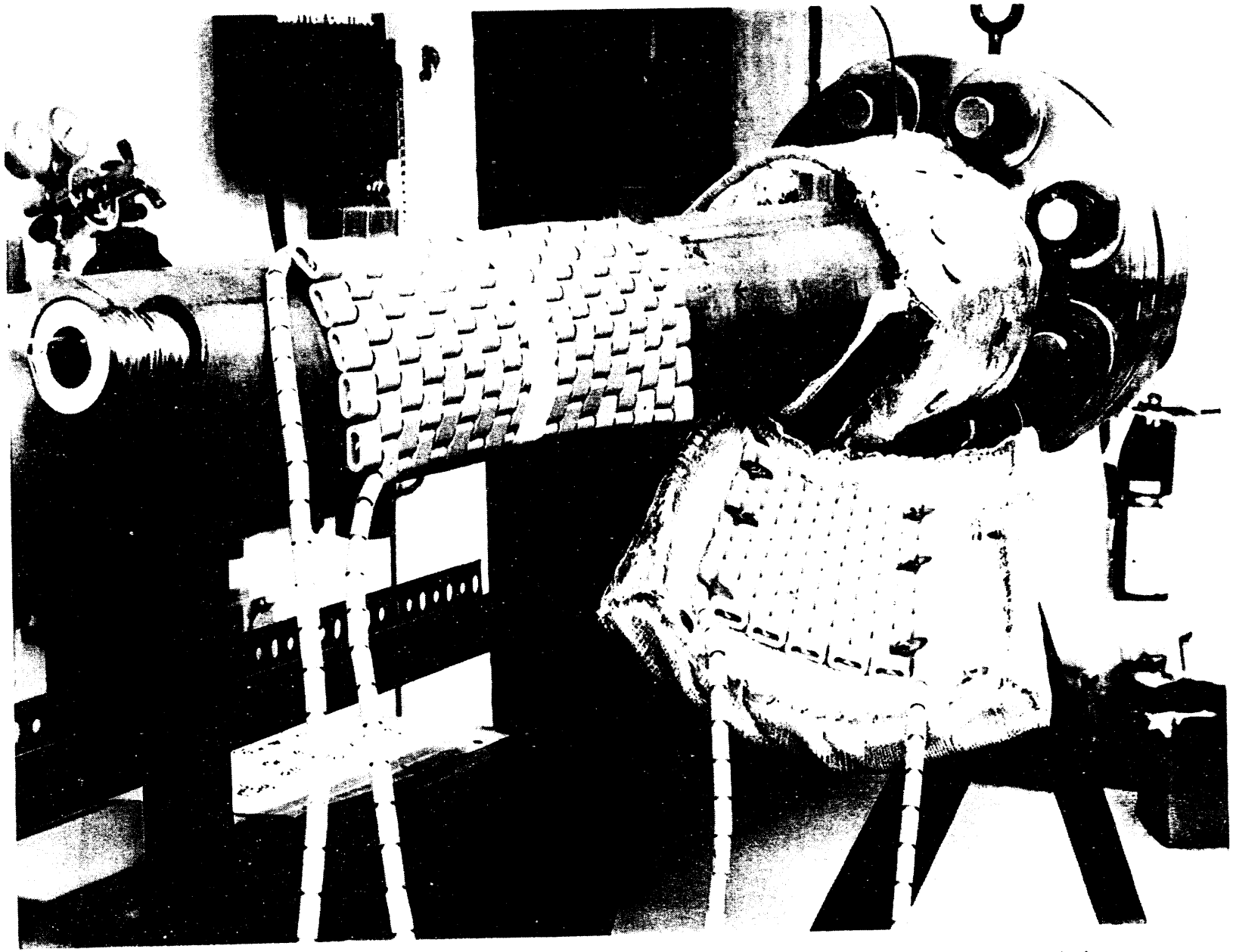

Figure 2.10: Photograph of two ceramic bead heater pads and a section of the inner layer of insulation

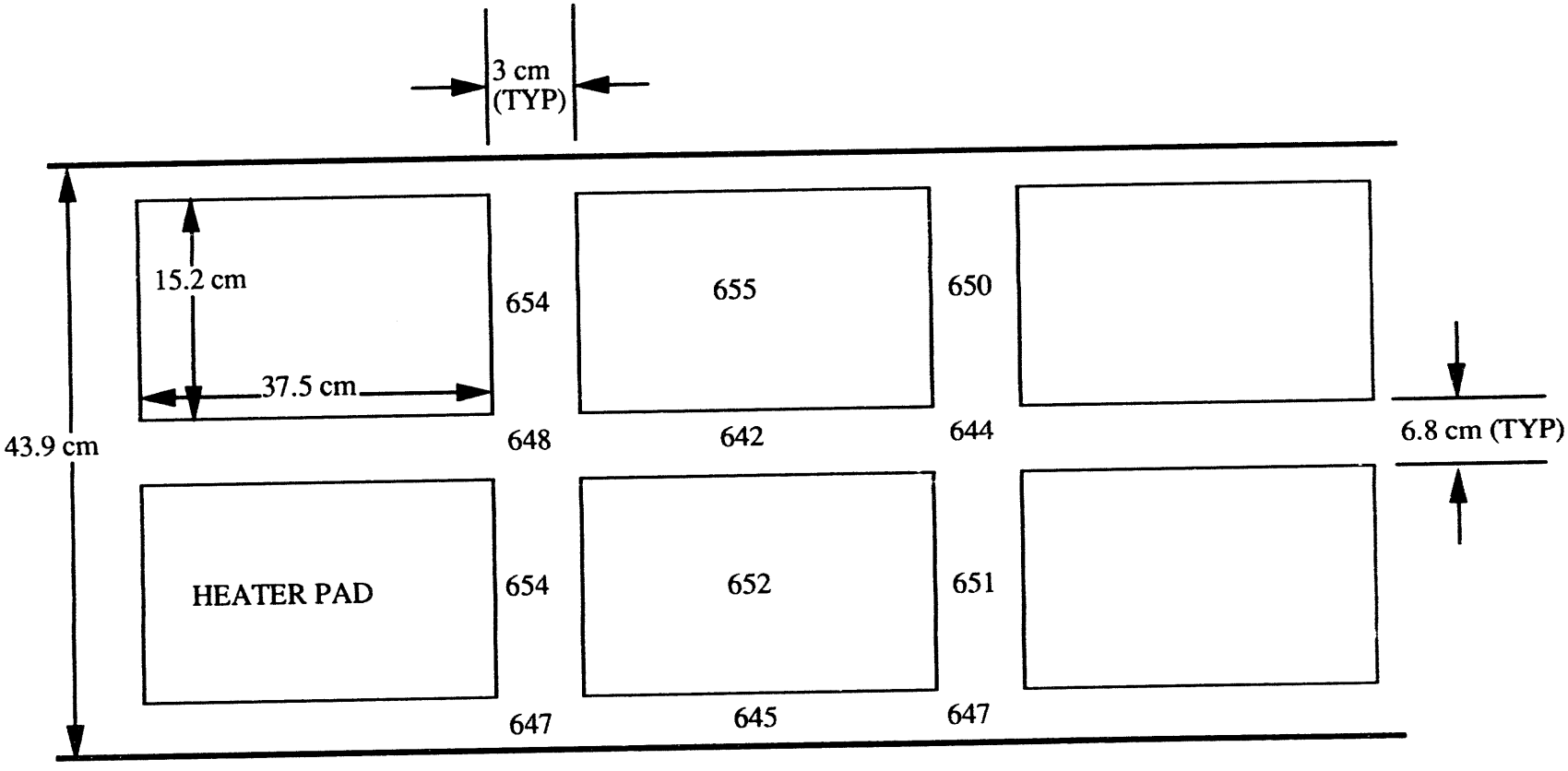


Figure 2.11: Temperature distribution on outer surface of test vessel at 650K (all temperatures in degrees K)

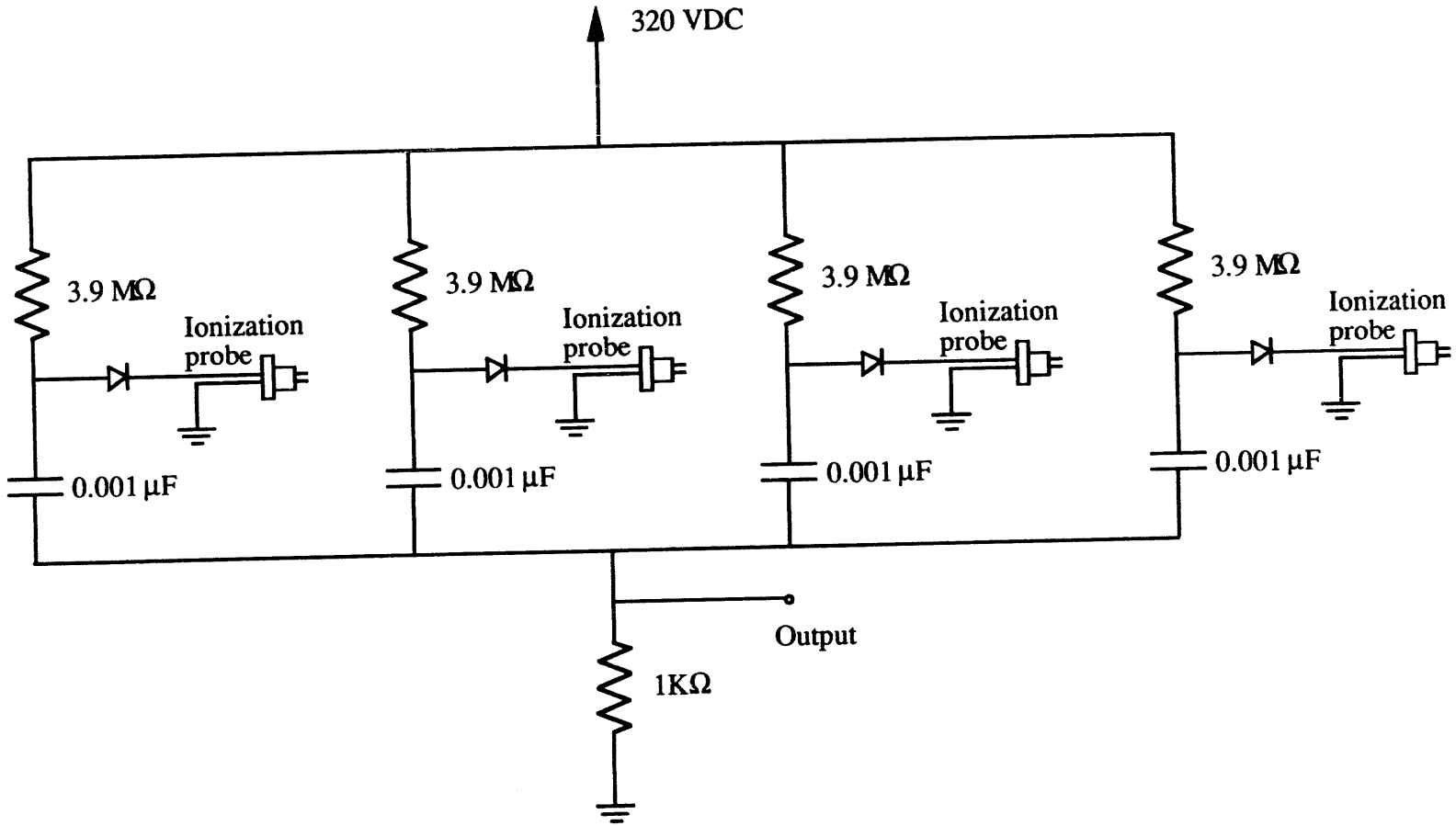


Figure 2.12: Schematic of ionization probe circuit

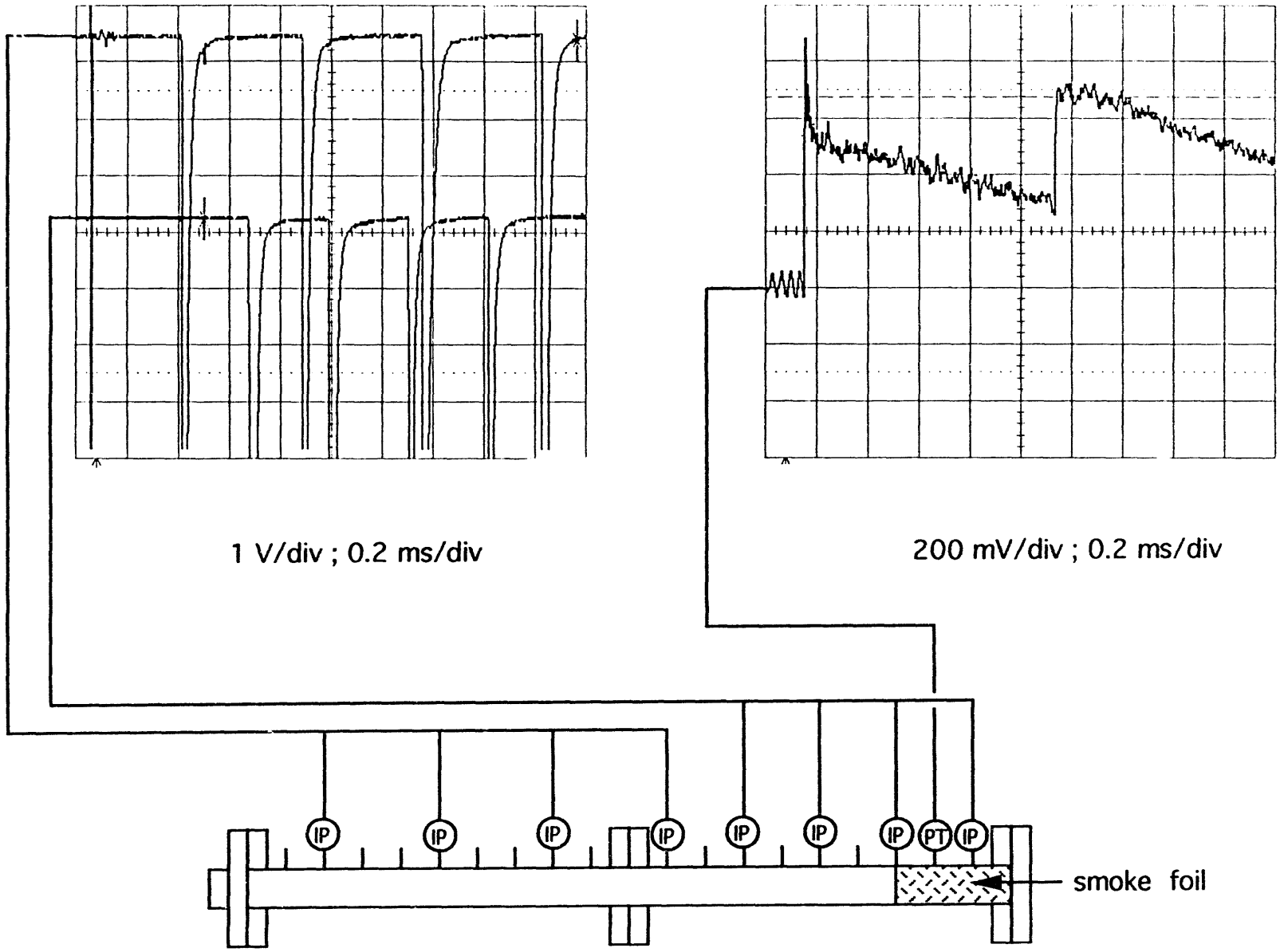


Figure 2.13: Schematic showing typical ionization probe and pressure transducer locations on the test vessel and output signals as recorded on the oscilloscope

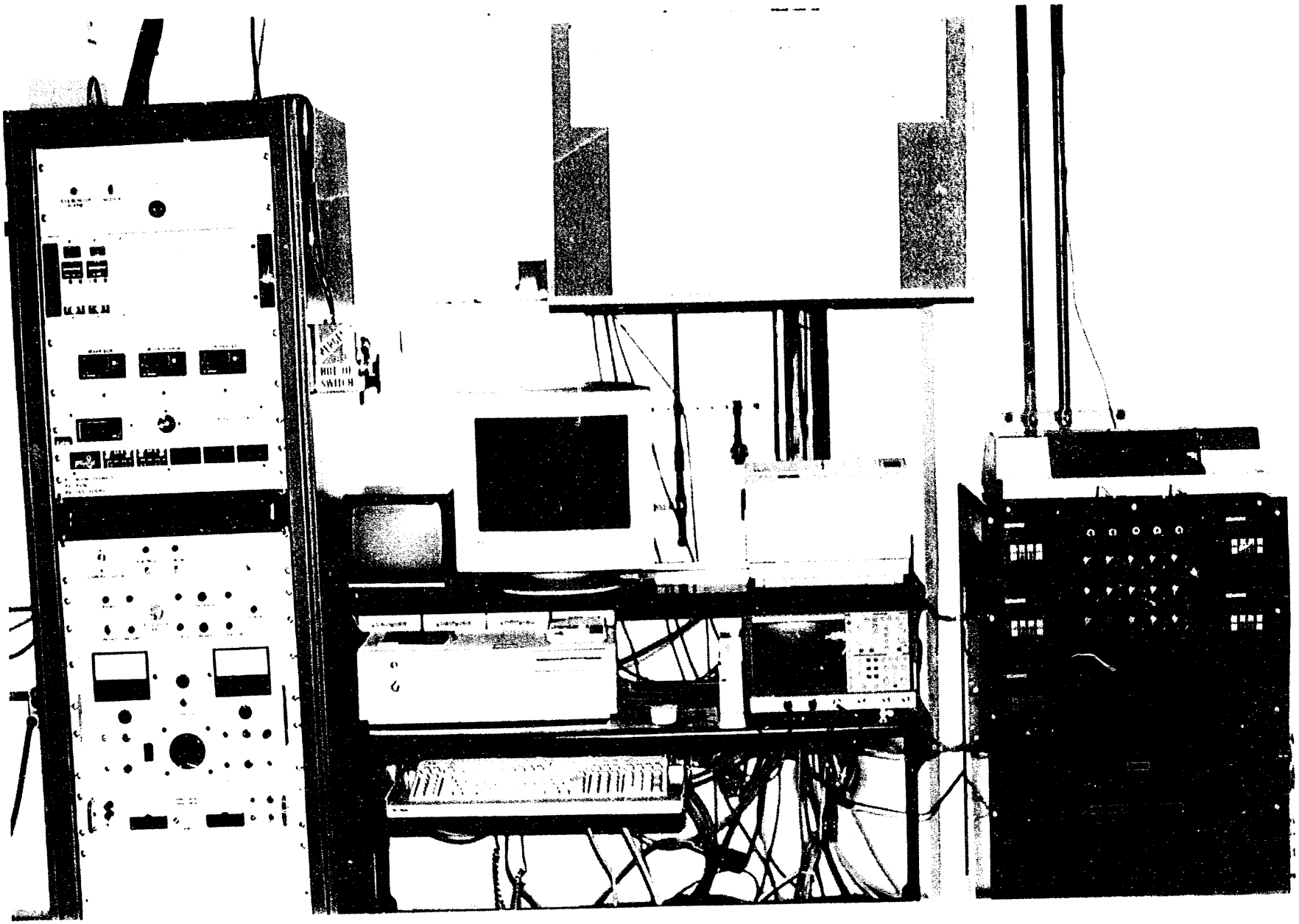

Figure 2.14: Photograph of the SSDA control room

# 3 EXPERIMENTAL RESULTS

## 3.1 Volumetric Oxidation Experiments

All combustible mixtures undergo chemical reaction at any temperature. The rate at which these reactions proceed is highly dependent on the mixture temperature and tend to follow an Arrhenius law. If the mixture temperature is sufficiently high the mixture may ignite without an external ignition source. However, even at temperatures below the "auto-igntion temperature" chemical reactions occur which would tend to change the mixture composition with time. In this section two experiments are described which were performed to : (1) determine the maximum temperature below which the mixture does not burn upon injection into the test vessel, so as to set a maximum operating temperature and (2) characterize the slow oxidation process at the maximum operating temperature. Additionally, experiments were carried out to determine the effect of predetonation hydrogen oxidation on the deontations. These experiments are described in Section 3.5.

### 3.1.1 SSDA Operating Temperature Limit Experiments

Preliminary experiments were carried out to determine the maximum vessel temperature which results in the test mixture being injected into the heated test vessel without burning. During these tests the test vessel pressure and gas temperature at several locations are monitored during the test vessel fill period for temperature or pressure excursions from steady-state. Such an excursion would be an indication of chemical reaction. If no such excursions are observed an attempt is made to ignite the mixture using a glow plug located at the driver end of the test vessel. Stoichiometric hydrogen-air is used as the test mixture for these experiments since it is the most sensitive hydrogen-air mixture and thus would yield the lowest temperature limit. The initial mixture pressure, after downloading from the mixing chamber, in all cases is 0.1 MPa. Table 3.1 presents the initial conditions for these experiments and the test results.

Experimental results are shown in Figures 3.1 and 3.2. Figure 3.1 shows results for the downloading of the test mixture into the test vessel heated to a temperature of 588K. This experiment is typical of a test where the mixture does not burn upon injection into the test vessel. The test vessel (TV) and mixing chamber (MC) pressure histories are shown along with gas temperature histories, for thermocouple positions shown in the schematic of the test vessel at the bottom of Figure 3.1. The pressure profiles show the test vessel being loaded from a vacuum to a final pressure of 0.1 MPa (14.7 psia) and the corresponding mixing chamber depressurization. During the fill process the ratio of the mixing chamber to the test vessel pressure is at all times greater than two, so the jet is choked and no flame can backflash into the mixing chamber. Thermocouple T2, located opposite the mixture injection port from the mixing chamber, shows a rapid drop in temperature upon introduction of the test mixture, caused by the temperature drop of the gas as it expands into the evacuated test vessel. At the end of the fill, the test vessel pressure reaches a steady-state value. After 30 minutes, the mixture was ignited successfully using the glow plug.

Figure 3.2 presents results for a test vessel temperature of 700K. As in the no-burn case, thermocouple T2 initially measures a drop in temperature due to the expanding jet. This is followed by a rapid temperature increase resulting from the burning of the test mixture. Clearly the maximum temperature measured by T2 is above the operating range of the Type K thermocouple. Thermocouple T1 shows a mild temperature pulse and T3 shows no transient at all. This indicates that the mixture is burning only in the vicinity of thermocouple T2, perhaps as the jet impinges on the tube wall. It is believed that the combustion products cool down quickly to the test vessel temperature. There is evidence of a small spike in the test vessel pressure which occurs at the same time as the temperature pulse. Aside from this small spike the test vessel and mixing chamber pressure time history are identical to that of the no-burn case shown in Figure 3.1.

Table 3.1 summarizes the experimental results for this series of tests. The parameters which were varied are the vessel temperature and the vessel fill time. The results suggest that no "significant" chemical reaction occurred at 588K. At 700K, a burn was observed in all cases, independent of mixture fill time. At 650K, a burn was observed with a short fill time, and no burn was observed with a relatively long fill time. The experimental results are compared with the corresponding calculated "reaction time" using CHEMKIN (Kee, 1989), a chemical kinetics code. The CHEMKIN calculations are based on an adiabatic isobaric process. In these calculations the reaction time is arbitrarily chosen to be the time for the mixture temperature to increase by 10 percent.

**Table 3.1 Summary of maximum operating temperature experiments**

| Temperature K | Computed "Reaction Time" (Chemkin code)* | Gas Mixture Vessel Fill Time** | Results |
|---|---|---|---|
| 588 | > 3 hours | 5s | No burn observed |
| 650 | ~ 3 hours | 5s | Burn observed during fill time |
| 650 | ~ 3 hours | 25s | No burn observed |
| 700 | 1000s | 5s | Burn observed during fill time |
| 700 | 1000s | 25s | Burn observed during fill time |
| 700 | 1000s | 90s | Burn observed during fill time |

*Time for mixture temperature to increase by 10 percent (adiabatic system).
**Time to fill the test vessel from vacuum to 0.1 MPa.

From Table 3.1, it is evident that the measured time for ignition of the mixture upon injection, which is almost immediate, is significantly shorter than the reaction times predicted by the CHEMKIN code. This indicates that either (1) wall effects, which are not modeled in the CHEMKIN calculation play an important role in the ignition of the mixture or (2) the constants used in the chemical kinetics equations are not accurate at the temperature of these experiments. The experimental results at 650K indicate that the ignition phenomenon is related to the fill time, or jet velocity. The mechanism, however, is not known.

The experimental results obtained indicate that 650K is the maximum temperature at which mixtures of hydrogen-air can be sustained in the SSDA test vessel for the time period necessary to conduct the detonation experiments.

### 3.1.2 Slow Oxidation Experiments

After establishing the maximum operating temperature, experiments were carried out with the objective of quantifying the rate of hydrogen oxidation at a given temperature as a function of mixture composition and residence time. Since the reaction rate is so slow, we may adequately describe the reaction as a one-step process where hydrogen and oxygen combine to form water. Since there is a reduction in the number of moles going from reactants to products one would expect the pressure in the test vessel to decrease as the hydrogen oxidation reaction proceeds. The oxidation process can be considered to be constant temperature, because any heat produced from the reaction is quickly lost to the large heat capacity vessel walls. For an isothermal, constant volume process the final hydrogen mole fraction, $X^f_{H2}$, can be calculated from the following expression

$$X^f_{H_2} = \frac{x^o_{H_2} + 2\,\frac{\Delta P}{P_o}}{1 + \frac{\Delta P}{P_o}} \qquad (3\text{-}1)$$

where $P_o$ is the mixture initial pressure, $\Delta P$ is the drop in mixture pressure at time t, and $X^o_{H2}$ is the initial hydrogen mole fraction in the mixture. The derivation of Equation (3-1) can be found in Appendix C.

Since the mixture pressure is an experimentally measurable quantity, using Equation (3-1) one can infer the amount of hydrogen depletion from the measured drop in the test vessel pressure. A more direct approach to measure hydrogen depletion is to grab mixture samples at various times and, using a gas chromatograph, measure the hydrogen concentration. The pressure technique allows one to get a continuous (inferred) reading of hydrogen concentration, whereas, in the grab sample technique one is limited to the number of samples taken. Both these methods were used in the slow oxidation experiments.

Since the test vessel pressure is a global quantity, in order to get meaningful results the entire test vessel must be at a uniform temperature. To do this the driver endcover was replaced with a blind flange which was equipped with heaters and insulation. Additionally, to minimize the potential for steam condensation in the large diameter tubing connecting the pressure transducer to the test vessel, the pressure transducer was relocated. The transducer was connected to the test vessel through the second instrumentation port from the driver end using a short section of 6 mm diameter tubing.

In these experiments, the mixture is downloaded into the test vessel in 40 seconds and the mixture is allowed to stand while the test vessel pressure is recorded. Experiments carried out at 500K showed no measurable drop in the test vessel pressure over time. Figure 3.3 shows the test vessel pressure-time history for three mixtures, a rich and lean dry hydrogen-air mixture and a 30 percent steam inerted rich hydrogen mixture all measured at 650K. In all three mixtures the test vessel pressure decreases over time. This pressure drop cannot be attributed to a leak since in all cases the mixture pressure starts at atmospheric and proceeds to sub-atmospheric pressure. The maximum pressure drop was measured in the dry 50 percent hydrogen mixture and the other two mixtures had similar pressure drops.

Experimental Results

As mentioned above, besides inferring the hydrogen depletion rate from the test vessel pressure we measured the hydrogen concentration in the test vessel by taking grab samples and analyzing them using a gas chromatograph. In a typical experiment, a sample bottle is left open to the test vessel during the 40 second downloading of the test mixture from the mixing chamber. Two additional samples are taken at later times by opening the bottles to the test vessel for 5 seconds. Each experiment results in three samples which yields two data points corresponding to the change in hydrogen concentration. Since the sample bottles are outside the heating envelope (i.e., at room temperature) water vapor which is formed through the oxidation process in the test vessel condenses after being injected into the sample bottle. The gas chromatograph gives the percentage hydrogen in the gas mixture which, in this case, does not include the steam which condenses. Appendix D gives the details for calculating the hydrogen concentration taking into account the condensed steam.

Figure 3.4 shows the oxidation results for dry 15 percent and 50 percent hydrogen-air mixtures using both the pressure method and the grab sample method. For each of the two mixtures tested the four grab sample data points are from two separate tests. The data point shown at 40 seconds is taken to be a nominal initial condition for the mixture (i.e., 15 percent and 50 percent hydrogen). In one test the samples were taken at times 120 and 240 seconds, and in the other test the samples were taken at 180 and 300 seconds, after the start of mixture downloading. The vertical error bars on the grab sample data show the variation in the five measurements taken from each sample bottle. From Figure 3.4, we see that the oxidation rate for the two mixtures, as measured by the grab sample method, are not very different. The oxidation rates, as inferred from the drop in test vessel pressure, indicate that the 50 percent hydrogen mixture reacts at a rate substantially higher than the 15 percent hydrogen mixture. A comparison of the oxidation rate using the two methods is more favorable for the 15 percent hydrogen mixture. The major difference in the the results obtained using the two methods is that the oxidation rate inferred from the pressure history gives a high initial rate compared to that obtained from the grab sample data. At this time, the cause of the initial rapid drop in the test vessel pressure (i.e., high oxidation rate) is not known.

The grab sample data from Figure 3.4 is reproduced in Figure 3.5 along with the hydrogen depletion predicted by the following expression (DeSoete, 1975) for the overall reaction rate

$$\frac{dX_{H_2}}{dt} = -630\, X_{H_2}^{2.7}\, X_{O_2}^{0.2} \exp\left(\frac{-16}{RT}\right) \tag{3-2}$$

where X denotes the constituent mole fraction, T is temperature (K), and R is the universal gas constant (kcal/mol K).

The prediction from DeSoete's expression for the overall reaction rate correlates extremely well with the gas sample measurements for the 50 percent hydrogen mixture. However, for the 15 percent hydrogen mixture, DeSoete's expression predicts almost no oxidation as opposed to that measured experimentally using the grab sample method. This could be due to the fact that the temperature coefficient in the overall reaction rate expression, given in Equation (3-2), was obtained by fitting data from a 60 percent hydrogen in air mixture. It is possible that the temperature coefficient, at these temperatures, is a function of the mixture composition.

## 3.2 Detonation Experiments

In this section, experimentally measured detonation cell sizes are reported for a range of hydrogen-air-steam mixtures at various temperatures. The experimental results are compared with theoretical predictions using the one-dimensional ZND model. In order to compare the experimental results with the theoretical predictions, one must ensure that the detonation is stable, and, thus, the average cell size measured is unique to the test mixture. This entails that any initial overdrive by the acetylene-oxygen driver has diminished by the time the detonation arrives at the "smoked foil." Experimentally, only those experiments where a constant detonation velocity is observed in the last half of the vessel is considered. In several experiments, 1.5-meter long foils were used to verify that the average cell size was constant over the length of the foil. The computer program used in the present calculations was developed by Shepherd (1986). The program requires initial

mixture composition, pressure, and temperature and CJ detonation velocity. The CJ detonation velocity is obtained using the chemical equilibrium code STANJAN (Reynolds, 1986). The cell size is taken to be proportional to the calculated reaction zone length. The program has four options for selecting the reaction zone thickness; we have chosen the point where the temperature gradient is a maximum, which corresponds to the point in the reaction zone where the energy release is a maximum. The test conditions and the experimental results are tabulated in Appendix B. The results are presented in graphical form in the sections which follow.

### 3.2.1 Detonation Cell Size Measurement Technique

Detonation cell size is most commonly measured from the smoked foil technique. Figure 3.6 shows a typical smoked foil and a corresponding interpretation sketch taken from Moen et al. (1982). The structure consists of larger cells, which can be distinguished by sharper, higher contrast lines. These large cells are superimposed over smaller scale cells, often referred to as "substructure," whose lines are much fainter. The cellular structure observed on this foil is considered to be fairly "irregular," in the sense that there is a visible variation in cell size and shape over the foil. This irregularity in cellular structure is typical in hydrogen-air mixtures. As pointed out by Moen et al. (1984), it is not clear if the variation in cell width is the result of the perturbation of a dominant mode or simply the superposition of several modes.

Moen et al. (1982) outlined two methods for measuring the average cell size from a smoked foil. The first method is to identify and measure a large number of cells and then simply take the average. In this method there is a substantial amount of judgment required in choosing the appropriate cells, considering the existence of substructure and the general irregularity in the cells. The second method abstracts away the cell, and thus the subjectivity of identifying a cell, and bases the cell size on the distance between diagonal parallel lines. In general, the longest lines with the most contrast are chosen as prime candidates. There still remains some subjectivity in choosing the lines. However, the authors believe the amount of judgment required in this method is much less than with the first method. As a result, the second method, often referred to as the "dominant mode method" was used in this study to determine the average cell width.

For each experiment, after the smoked foil has been sprayed with the clear lacquer, the tracks on the smoked foils are traced onto a mylar sheet. Only those lines which are considered to be dominant, (i.e., not substructure) are traced. Lines are drawn in the transverse direction wherever the best tracks are located. For each line, a sample length is chosen and the total number of diagonal track lines in the same direction contained in the segment are counted. Taking the sample length and dividing by the number of diagonal lines counted, less one, gives the average line spacing (i.e., the average cell size). This is repeated for each transverse line drawn and then globally averaged. For foils with small cells on the scale of several centimeters, the total number of lines sampled could be up to one hundred. For foils with large cells on the order of several tens of centimeters, the total number of lines sampled could be as few as ten.

### 3.2.2 Baseline Experiment at 300K

Detonation experiments were initially performed at 300 K with several objectives in mind: (1) to compare with existing experimental data, (2) to check instrumentation, and (3) to develop and refine operating procedures. Cell size data obtained from the SSDA for hydrogen-air mixtures at 300 K and 0.1 MPa are plotted in Figure 3.7. The data, displayed as cell size versus hydrogen concentration, result in a typical "U"-shaped curve. The cell size data correspond to mixtures containing a minimum of 17.5 percent to a maximum of 58 percent hydrogen by volume. Steady-state detonations were initiated below this minimum, but it was felt that in order to be assured that the data are not influenced by boundary conditions; there should be at least three transverse cells on the smoked foil. Results for weaker mixtures where there are less than three cells across the foil will be discussed in Section 3.6, which deals with detonability limits of the SSDA. Experimental cell size data obtained at McGill University (Guirao et al., 1987) and from the Heated Detonation Tube (HDT) at Sandia National Laboratory (Tieszan et al., 1987) are also shown in Figure 3.7. The McGill data was obtained in 5 and 15 cm diameter tubes and the Sandia HDT is 43 cm in diameter. The McGill data covers the complete range of hydrogen mixtures tested in the SSDA. In general, the McGill data appears to give slightly larger cell size, as compared to the SSDA data, over the entire range of mixture composition. For example, the cell size obtained at stoichiometric conditions (i.e., 30 percent hydrogen) from the SSDA is about 1 cm as compared to 1.5 cm obtained from the McGill 5 cm diameter tube. There is much better agreement for the lean mixtures. Unfortunately, the HDT data does not cover the

entire range of hydrogen mixtures tested in the SSDA. The HDT data for lean hydrogen-air mixtures correlates very well with both the SSDA and McGill data. Cell size measurements from HDT reported at stoichiometric conditions agree with the data from the SSDA. The slightly larger cell sizes reported by the McGill researchers could possibly be attributed to water vapor in the test mixture resulting from the use of atmospheric air; dry bottled air was used in both the SSDA and HDT experiments.

Figure 3.7 also shows the ZND model prediction for cell size as a function of hydrogen concentration. Recall, the theoretical cell size is obtained by using the ZND model to calculate the reaction zone length, l, for a given mixture and initial conditions. This calculated reaction zone length is multiplied by a constant, A, to give the cell size. This value of the constant is obtained by anchoring the predicted cell size data to one of the experimentally measured cell size data points. The choice of which experimental point is arbitrary. For the present study, 30 percent hydrogen was chosen as the mixture to anchor the theoretical data. This yields a constant of proportionality, between the calculated reaction zone thickness and the cell size, of 51. The general trend in the experimental data is very well predicted by the ZND model. Quantitatively, the model predictions and the SSDA data for the cell width for hydrogen concentrations between 25 and 50 percent are very good. However, outside this range, the model predictions begin to deviate from the experimental data.

It is very difficult to assign uncertainty bounds for detonation cell width measurements. The overall uncertainty of the measured average cell size includes variations in the cell size inherent in the detonation phenomenon itself plus the uncertainty associated with the subjectivity of the person making the measurement. For example, one person might consider a particular line on a smoked foil to be a dominant line whereas another person reading the same foil might interpret the same line as substructure and not consider it in his estimate of the average cell size. In an attempt to quantify this uncertainty, Tieszen et al. (1987) had three people read several foils and compared their results. They found that for the most part all the readings could be bounded by a $\pm$ 25 percent spread of the most probable cell width, which was taken as the reading by R. Knystautas from McGill University, Montreal, Quebec, Canada, an experienced "foil reader."

In this study, image analysis, similar to that performed by Lee (1991), was performed on a limited number of the foils in order to quantify the variation in cell size about the mean. This is different from the uncertainty analysis performed by Tieszen et al. (1987), in that we are quantifying the variation in cell size within a single foil, whereas they determined the variation in the average cell size on a given foil as measured by three different people. The present approach more directly quantifies the variation in cell size due to the detonation phenomenon itself. However, human judgment still plays a role due to the initial interpretation of the foil (i.e., identification of the dominant lines).

The procedure taken in analyzing the foil for cell width variability is to digitize the smoked foil image. This is done by hand-tracing the lines on the smoked foil onto a sheet of mylar. This tracing is then digitized using a Hewlett Packard Scanjet IIP. After the line tracing is digitized, several gray-scale line profiles are taken in the tranverse direction of the foil. In such a profile, a series of spikes appear corresponding to the lines on the tracing. A program was written to measure the spacing between these lines and to process the data to output the average spacing and the standard deviation. This procedure was performed on four smoked foils for hydrogen-air mixtures at 300K.

The results of the analysis are given in Figure 3.8 in terms of the average cell size denoted by the open circles and the standard deviation denoted by the vertical error bars. A general observation is that the standard deviation, representing the variation in the cell size, increases with the average cell size. The variation in the cell size, as characterized by the standard deviation, varies from a low of about $\pm$ 2.8 percent of the average cell size for 30 percent hydrogen to a high of $\pm$ 55 percent for the 20 percent hydrogen mixture. This is comparable to the $\pm$ 25 percent spread in the measured average cell size reported by Tieszen (1987).

### 3.2.3 Effect of Temperature

The effect of temperature on cell size was investigated by performing two series of experiments covering a wide range of hydrogen concentration at nominal temperatures of 500K and 650K. Cell size data obtained for hydrogen-air mixtures at 500K and 650K are shown in Figures 3.9 and 3.10. Again, only the data where three or more transverse cells are

recorded on the smoked foil are presented. The hydrogen concentrations varied from a low of 13.8 percent to a high of 50 percent for the series performed at 500K and between 10 and 50 percent hydrogen at 650K. Also shown in these figures are the ZND model predictions using the same constant of proportionality used to anchor the prediction at 300K (i.e., A = 51). As in the 300K series shown in Figure 3.7, the ZND model does a good job in predicting the qualitative features of the data. Quantitatively, the model predictions at 500K are better than that at 650K where the model tends to overestimate the cell size over the entire range of mixtures tested.

The effect of temperature on cell size is best seen in Figures 3.11 and 3.12. The cell size data for hydrogen-air at 300K and 650K from Figures 3.7 and 3.10 is replotted in Figure 3.11. From this graph, it is clear that temperature has little effect on cell size for mixtures between 25 and 45 percent hydrogen. For mixtures outside this range, increasing the mixture temperature tends to decrease the measured detonation cell size. This effect is also predicted by the ZND model. Figure 3.12 shows the effect of temperature on cell size for lean, rich and stoichiometric hydrogen mixture conditions. The experimental data shows that in all cases increasing the mixture temperature decreases the mixture cell size. It also shows that the temperature effect is most pronounced at off-stoichiometry conditions as one approaches the limits. In the case of 50 percent hydrogen, and especially for the 17.5 percent hydrogen mixture, the temperature effect is most prominent at the lower temperatures. For the three mixtures shown, the cell size data tends to converge at 650K. The ZND model predictions also display the trends observed in the experimental data, except that for the 30 percent hydrogen mixture, the model predicts a slight increase in the cell size with temperature.

### 3.2.4 Effect of Steam

In most accident scenarios, there is a large amount of steam which is liberated into containment along with the hydrogen. For this reason, a series of tests were performed to look at the effect of steam on the detonation cell size of hydrogen air mixtures at different temperatures. The results from these experiments are shown in Figure 3.13. In all tests with steam, the hydrogen-to-air ratio was that for stoichiometric conditions. The steam fraction was varied from 10 to 30 percent, in steps of 5 percent, and the tests were done at temperatures of 400K, 500K and 650K. In all cases, the steam is under superheat conditions. Also plotted in Figure 3.13 is the calculated cell size using the ZND model.

The ZND model predictions reproduce the general trend of the data satisfactorily. As before, the model compares best with the experimental data for the most sensitive mixtures. Three data points obtained from the HDT at Sandia are also included for comparison purposes. These experiments were performed at a mixture temperature of roughly saturation conditions (i.e., 373K). The 15 and 20 percent steam fraction data can be compared directly with the SSDA data. The smallest steam fraction reported in the HDT data is 11.5 percent, which is also shown in Figure 3.13. This can be compared to the 10 percent data from the SSDA. In general, the agreement between the SSDA and HDT data is very good considering the difference in the scale of the respective experimental apparatus.

From Figure 3.13, one can deduce the relative effect of steam on the mixture sensitivity. As one would expect, at a given temperature, as the steam fraction is increased the cell size also increases. This is due to the reduced post-shock mixture temperature, due to the high heat capacity of steam. The steam thus desensitizes the mixture. As the mixture temperature increases, this desensitizing effect from the steam becomes less prominent. It appears that at very high temperatures, greater than 650K, the cell size for the various steam fraction converge and the desensitizing effect of the steam is lost. However, at these elevated temperatures mixture oxidation becomes significant and must be taken into account. This effect was discussed in Section 3.1 and will be considered further in Section 3.5.

## 3.3 Detonation Velocity

Figure 3.14 shows the variation in the detonation velocity down the length of the tube for a 20 percent hydrogen-air mixture for various driver slug lengths. Typically, a 20-cm long driver slug length is used, and as can be seen from Figure 3.14, the transmitted detonation quickly adjusts to the test mixture CJ velocity. For a very long driver slug, a substantial distance is required before the detonation adjusts to the test mixture conditions. The detonation is initially overdriven (i.e., detonation velocity is above the CJ steady-state velocity) as it is transmitted from the more sensitive acetylene-oxygen driver. The detonation velocity decays to the steady-state CJ value for the test mixture as it propagates

down the length of the tube. The measured spatial variation in the detonation velocity is used to ensure that the detonation has reached steady-state before the smoked foil. In general, the weaker the mixture, the longer it takes for the detonation wave to decay to steady-state conditions. Therefore, great care must be taken in interpreting lean mixture experiments where the tube is not long enough for the detonation to decay to steady-state conditions.

The average detonation velocity measured for hydrogen-air mixtures at 300K, 500K and 650K are given in Figures 3.15, 3.16, and 3.17, respectively. The average velocity plotted in these figures is based on the times-of-arrival at the last four probes, or the last 1.8 meters of the test vessel. The theoretical CJ velocity is calculated using the chemical equilibrium code STANJAN (Reynolds, 1986). As can be seen from Figures 3.15 and 3.16 for hydrogen-air mixtures at 300 and 500K, the measured detonation velocities are almost exactly equal to the calculated value. The only noticeable discrepancy is at 50 percent hydrogen where the experimental value is slightly below the predicted value. The detonation velocity measured for hydrogen-air at 650K, shown in Figure 3.17, is consistently below the theoretical prediction. Typically for large cell size mixtures, a velocity deficit is considered normal due to momentum and heat losses to the vessel walls (Dupre, et al., 1986; Fay, 1959). However, in this case the cells are very small and thus losses at the wall cannot account for the deficit. Since the same procedure was used to prepare the mixtures at 650K and 500K there is no reason to suspect that the mixture composition is incorrect. As discussed in Section 3.1.2 at a temperature of 650K, there is a significant amount of hydrogen depletion over time. Therefore, the only plausible explanation for this measured deficit is that at 650K some of the hydrogen oxidizes during the period of time between the start of the vessel fill and ignition (i.e., 60 seconds). At the elevated temperatures, some of the hydrogen oxidizes during this time, thereby changing the mixture composition. The sub-CJ detonation velocities observed at 650K, as shown in Figure 3.17, could occur as the result of a 1 to 2 percent reduction in the hydrogen mole fraction. This phenomenon of preignition hydrogen oxidation will be further discussed in more detail in Section 3.5.

## 3.4 Detonation Pressure

A typical signal from a flush mounted pressure transducer recorded during the passage of a detonation wave is shown in Figure 2.12, the sensitivity of the pressure transducer is nominally 5 mV/psi (735 mV/MPa). In order to understand the pressure-time signal, let us consider a gas particle moving through the detonation wave. To simplify matters, let us first consider a one-dimensional ZND structure for the detonation. Before the particle reaches the incident shock wave, it experiences a constant ambient pressure. The pressure then increases almost instantaneously as the particle crosses the leading shock wave. Following the shock wave, within the so called "induction zone," the pressure is constant at the shock pressure. The pressure then decreases through the active portion of the reaction zone where the temperature begins to rise due to the start of recombination reactions. The particle then reaches the CJ plane which is located at the end of the reaction zone and the head of the expansion fan which follows the detonation wave. Therefore, the pressure continuously decreases after the induction zone. The rate at which the pressure drops is dictated by the geometry of the mixture boundary conditions, i.e., planar, cylindrical, or spherical (Nettleton, 1987).

In reality, the detonation wave has a 3-dimensional cellular structure, and the pressure history that a particle would experience is very different and less deterministic than that just described. For example, the particle could potentially encounter two shock waves, the incident and the transverse wave. The shock strength and corresponding reaction zone length within a cell is not constant as in the case of a steady one-dimensional wave. In a cellular detonation wave, the shock strength of the incident wave varies within a given cell. For example, within a cell the incident shock wave velocity varies from 1.6 times the calculated CJ velocity at the start of the cell to 0.6 times the CJ velocity at the end of the cell (Lee, 1984). Therefore, the pressure that the particle experiences depends on the position within the cell where it meets the incident shock wave.

The size of the crystal head for most common pressure transducers is typically 6 mm in diameter. The pressure transducer measures an average pressure over its face. Due to the finite size of the transducer sensor one cannot resolve the detailed pressure fluctuations within a cell unless the cell is much larger than the transducer head. Therefore, the question is: what theoretical pressure can be used as a comparison for the experimentally measured detonation peak pressure? It is clear that one cannot compare with the instantaneous incident shock pressure, commonly referred to as the von Neumann pressure, since its characteristic length is very short compared to the transducer head. Typically, one compares the experimentally

measured detonation pressure with the CJ pressure. The reason for this is that the CJ pressure is roughly the average pressure over the cell length.

Unlike detonation velocity which one can compare directly with theoretical predictions, experimentally measured detonation pressure has been historically very difficult to interpret, for reasons described above. However, from a practical standpoint one need only consider the gross aspects of the pressure-time history when assessing damage potential. Therefore, the main concern is the ability to predict as best possible these gross features such as the peak pressure and impulse. As mentioned above, in the past the experimentally measured detonation pressure has been compared with the theoretical CJ pressure for the mixture. Typically, the measured peak pressure was found to be within 10 to 15 percent of the theoretical CJ pressure

The experimentally measured peak detonation pressure for the hydrogen-air mixtures tested at 300K, 500K and 650K are shown in Figure 3.18. Also, shown in Figure 3.18 is the corresponding CJ pressure calculated using the STANJAN chemical equilibrium code. Qualitatively, it is evident that the experimentally measured detonation pressure is closely related to the calculated CJ pressure. On the average, the measured pressure is in the range of 10 percent of the calculated mixture CJ pressure, which is in agreement with past findings. It is interesting to note that in these experiments, conducted with fixed initial pressure, the detonation pressure for a mixture at an initial temperature of 650K is less than half of that of a mixture at 300K.

## 3.5 Effect of Pre-Detonation Hydrogen Oxidation

In the detonation experiments, the mixture is downloaded from the mixing chamber into the test vessel. The shortest injection time possible without the mixture burning off at 650K is about 30 seconds. The mixture is allowed to sit for an additional 30 seconds so that a uniform mixture temperature is achieved throughout the test vessel. The effect of pre-ignition residence time was investigated using a 50 percent hydrogen-air mixture at 650K. Note, since the driver end flange is not heated one would expect there to be a variation in temperature, and thus mixture composition, near the driver. Also, over a long period of time, any water vapor produced via the hydrogen oxidation process diffuses to the cold driver end and condenses, thus reducing the effectiveness of the acetylene-oxygen driver. In the first test, the mixture was loaded into the test vessel in 30 seconds and then immediately detonated. The results indicated that there was no measurable difference in the cell size or final steady-state detonation velocity compared to when the mixture was allowed to stand the additional 30 seconds. In a second series of tests, the mixture was allowed to stand 4.5 minutes after the mixture was injected. In these experiments, a detonation could not be initiated using even the longest driver slug. Typically, a fast flame developed which pushed a shock wave down the tube. The reflection of the shock wave off of the end plate initiated a detonation which propagated back towards the driver end. It is postulated that the mixture had degraded to a level that was below the detonability limit for the tube.

## 3.6 Detonability Limits

For a given tube size, there exists a lean and rich hydrogen concentration limit outside of which a self-sustained, steady-state detonation cannot propagate. Detonations in limit mixture conditions typically propagate as a single-head spin, where a single triple point follows a helical trajectory over the inner tube surface (Moen, et al, 1981). The single-head spin is often referred to as the lowest mode of propagation. The next higher mode of propagation is often referred to as a "slapping wave" where two heads propagate in opposite directions colliding every 180 degrees rotation. One can exploit the existence of a single head spin as a criterion for identifying the detonability limits. Since the single head spin may persist over a range of mixture conditions a more precise criterion for the detonability limit is the onset of single head spin. Care must be taken in implementing this criteria. Only those detonations which have truly reached steady-state condition, where all initiation effects have decayed, must be considered.

There are two diagnostic tools which can be used to identify the structure of the detonation wave for near limit combustible mixtures--namely, the single and double head spin. These diagnostics include smoked foils and fast response pressure transducers. Both these diagnostics can be used to identify the unique structure of both the single and double head spin (Moen, et al., 1981).

## Experimental Results

The smoked foil technique can be considered as more reliable than the detonation pressure history. However, it is more time consuming since it involves having to open the vessel up before and after each experiment. As shown in Figure 3.19, a single-head and double-head spin detonation leave a distinct smoked foil signature. In the case of a single head spin repeated diagonal lines are etched onto the smoked foil. The diagonal lines are produced by the helical trajectory of the single triple point on the tube inner wall. The pitch, or distance between thes diagonal lines, is typically three times the tube inner diameter (Fay, 1952). The double-head spin mode of propagation is characterized by the repeated collision of two transverse waves propagating in opposite circumferential directions. This phenomenon manifests itself on the smoked foil as a single large cell, where the cell size is equal to the tube inner circumference. Finally, in the case where a detonation is not initiated in the test gas, the smoked foil is wiped clean.

In the present study, only the lean detonability limit was sought. Detonation experiments were carried out with smoked foils where the hydrogen mole fraction was lowered until a single head spin was observed, or the mixture failed to detonate. The criterion used to identify the detonability limit is: that mixture at which the detonation structure switches from a double head to a single head spin. Figure 3.20 shows the effect of temperature on the lean detonability limit for hydrogen-air mixtures in the SSDA. At each temperature and mixture composition near the detonability limit, the mode of propagation is indicated (e.g., single head, double head, or no detonation). At 300K, the onset of single head spin was observed at 15 percent hydrogen. At 500K a single head spin was not observed over the incremental change in hydrogen tested. Instead, a double head resulted at 11.5 percent hydrogen, and a detonation failed to be initiated at 11 percent hydrogen. It is possible that a single head spin could have been initiated at 11 percent had the driver length been increased. At 650K all three phenomena described above were observed in different experiments performed with 9 percent hydrogen. As a result, the lean detonability limit, where a stable single-head spin is initiated, is above 9 percent hydrogen but below 10 percent where a multi-head wave was always observed. Furthermore, at 650K and 9 percent hydrogen, the detonation velocity could not be accurately obtained due to the weak signals from the ionization probes.

If we consider that the detonability limit is characterized by the onset of a single-head spin, we could predict these limits with an appropriate criterion for the onset of single-head spin. It was first proposed by Kogarko and Zeldovich (1948) without derivation that at the onset of single-head spin, the mixture cell size equals the tube circumference (i.e., $\lambda = \pi d$). Shchelkin (1966) proposed the criterion $\lambda = d$ for the existence of a single-head spin in a circular tube. Experiments carried out at McGill University have demonstrated that both these criteria are applicable under specific conditions. An extensive study looking at the detonability limits in a circular tube was carried out by Dupre (1985). In these experiments, detonations were initiated using a strong energy source (i.e., high explosives), and it was found that the detonability limits corresponded to the criterion $\lambda < \pi D$. Experiments carried out by Knystautas et al. (1985) looking at the DDT phenomena in rough walled tubes found that a detonation could be successfully transmitted from a rough-walled tube section into a smooth-walled tube section if the mixture cell size was less than the inner diameter of the smooth-walled tube.

Considering the above two experiments, it is generally believed that detonability limits for a tube correspond to the mixture whose cell size lies between the tube inner diameter, d, and the tube inner circumference (i.e., $d \leq \lambda \leq \pi d$). Shown in Figure 3.21 is the ZND prediction for the lean detonability limits as a function of temperature using the above criterion along with the experimentally determined limit. The experimental data at 500K and 650K falls in the range predicted by the ZND model. The 300K data fall below the prediction.

Detonability limits for steam-diluted stoichiometric hydrogen-air mixtures were not investigated in as much detail as the dry hydrogen-air. The results for the steam diluted mixture detonability limit is given in Figure 3.22. As in the case of the dry hydrogen-air mixtures it was found that inreasing the mixture temperature tended to widen the detonability limits. For example, it was found that at 400K the detonability limit for stoichiometric hydroge-air was between 20 and 25 percent steam and at 650K the limit widened to between 30 and 35 percent steam.

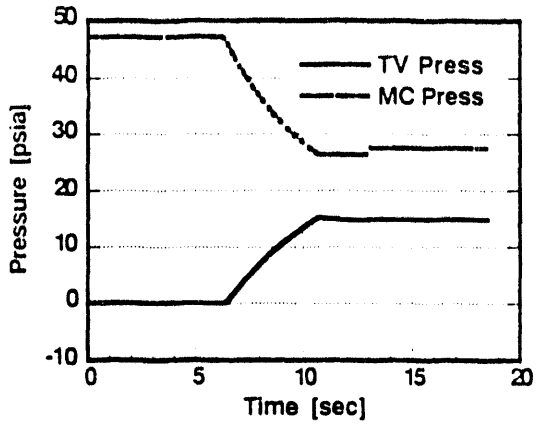


(a) Test vess (TV) and mixing chamber (MC) pressure-time history

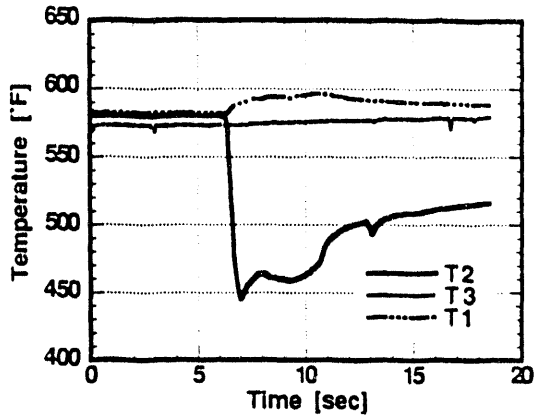


(b) Test mixture temperature-time history in the test vessel

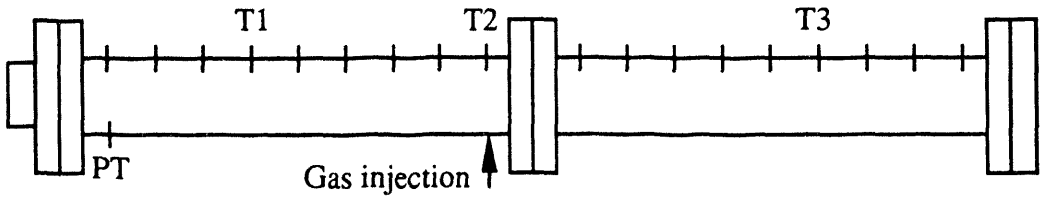


(c) Instrumentation layout

Figure 3.1: Volumetric oxidation test; injecting stoichiometric hydrogen-air into the test vessel heated to 588K

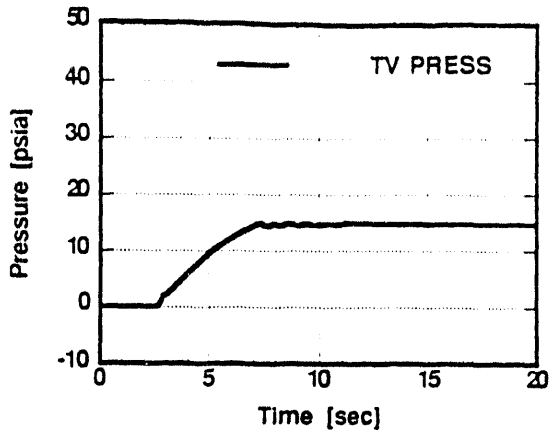


(a) Test vess (TV) pressure-time history

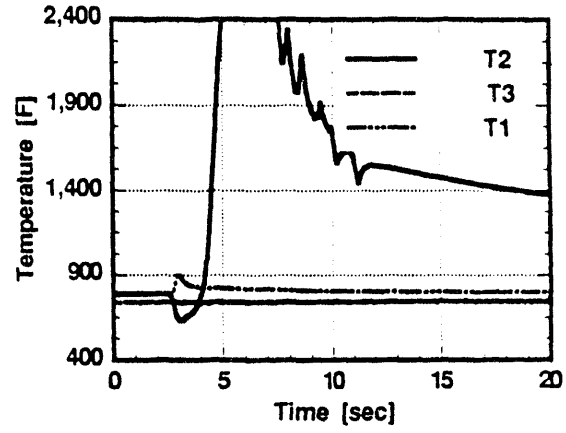


(b) Test mixture temperature-time history in the test vessel

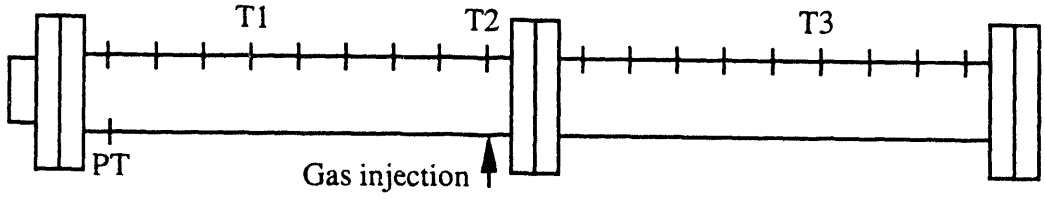


(c) Instrumentation layout

Figure 3.2: Volumetric oxidation test; injecting stoichiometric hydrogen-air into the test vessel heated to 700K

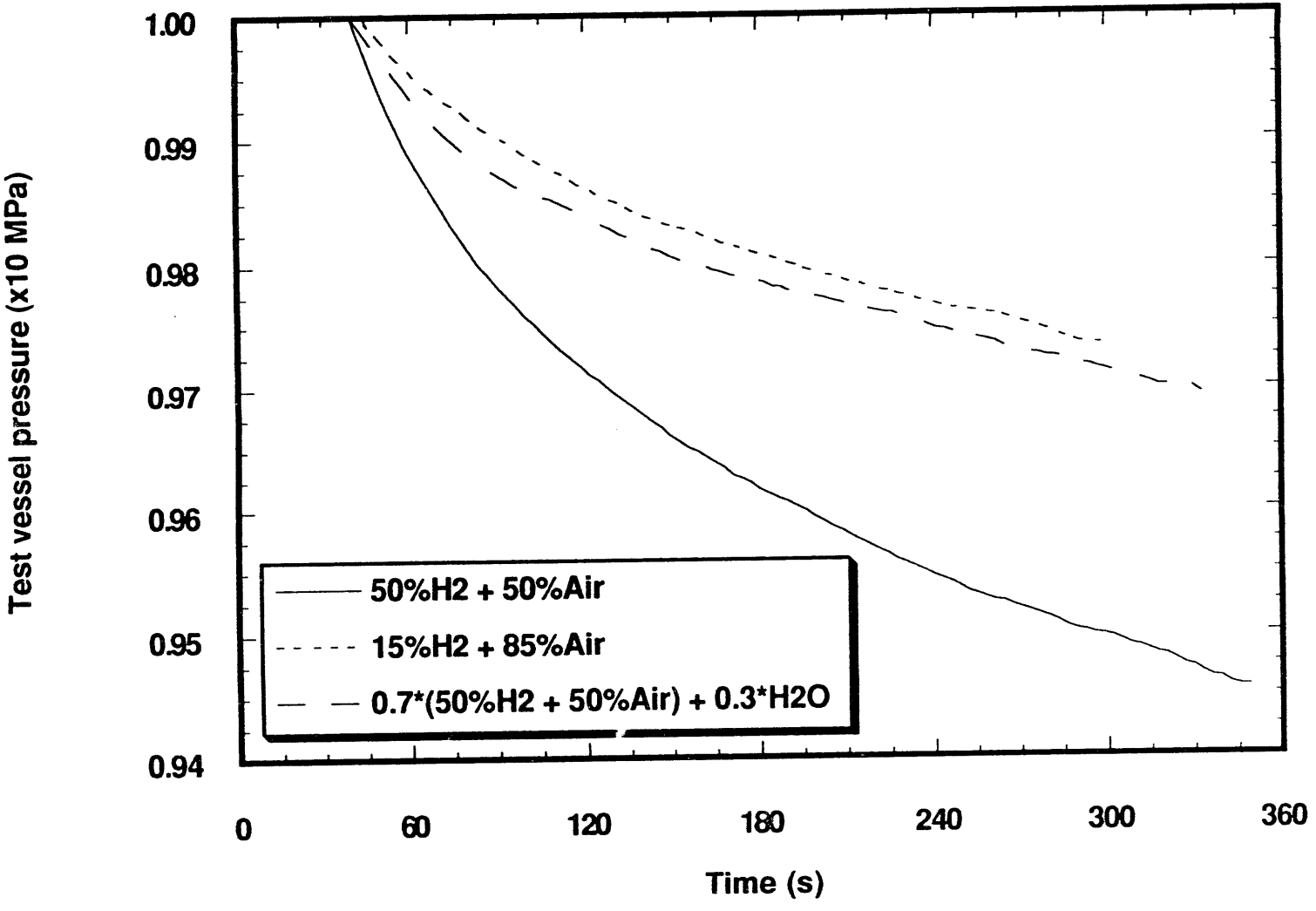


Figure 3.3: Test vessel pressure during slow oxidation of hydrogen-air-steam mixtures at 650K

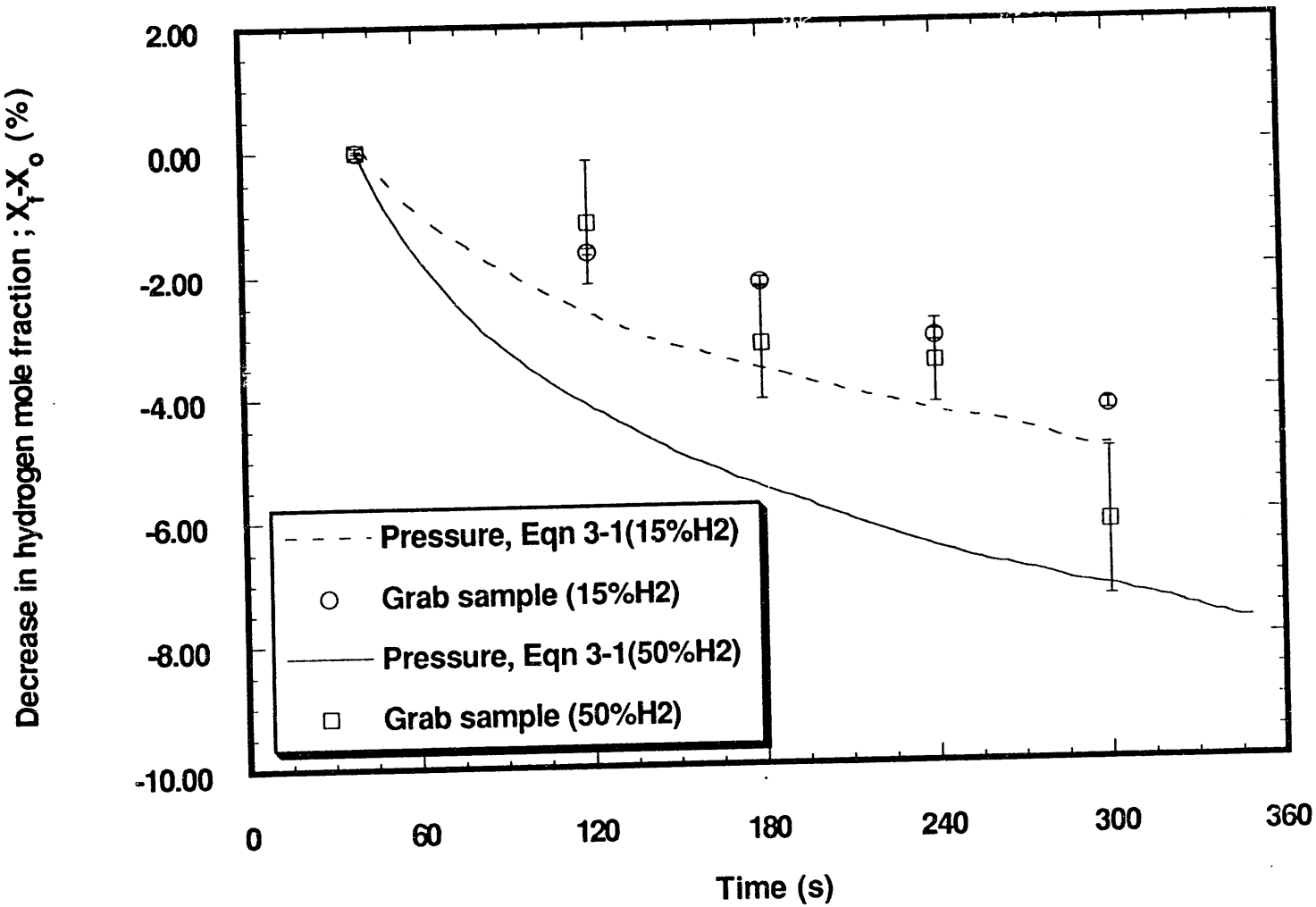


Figure 3.4: Comparison of hydrogen depletion results for slow oxidation of hydrogen-air at 650K using grab samples and inferring from test vessel pressure history using Equation (3-1)

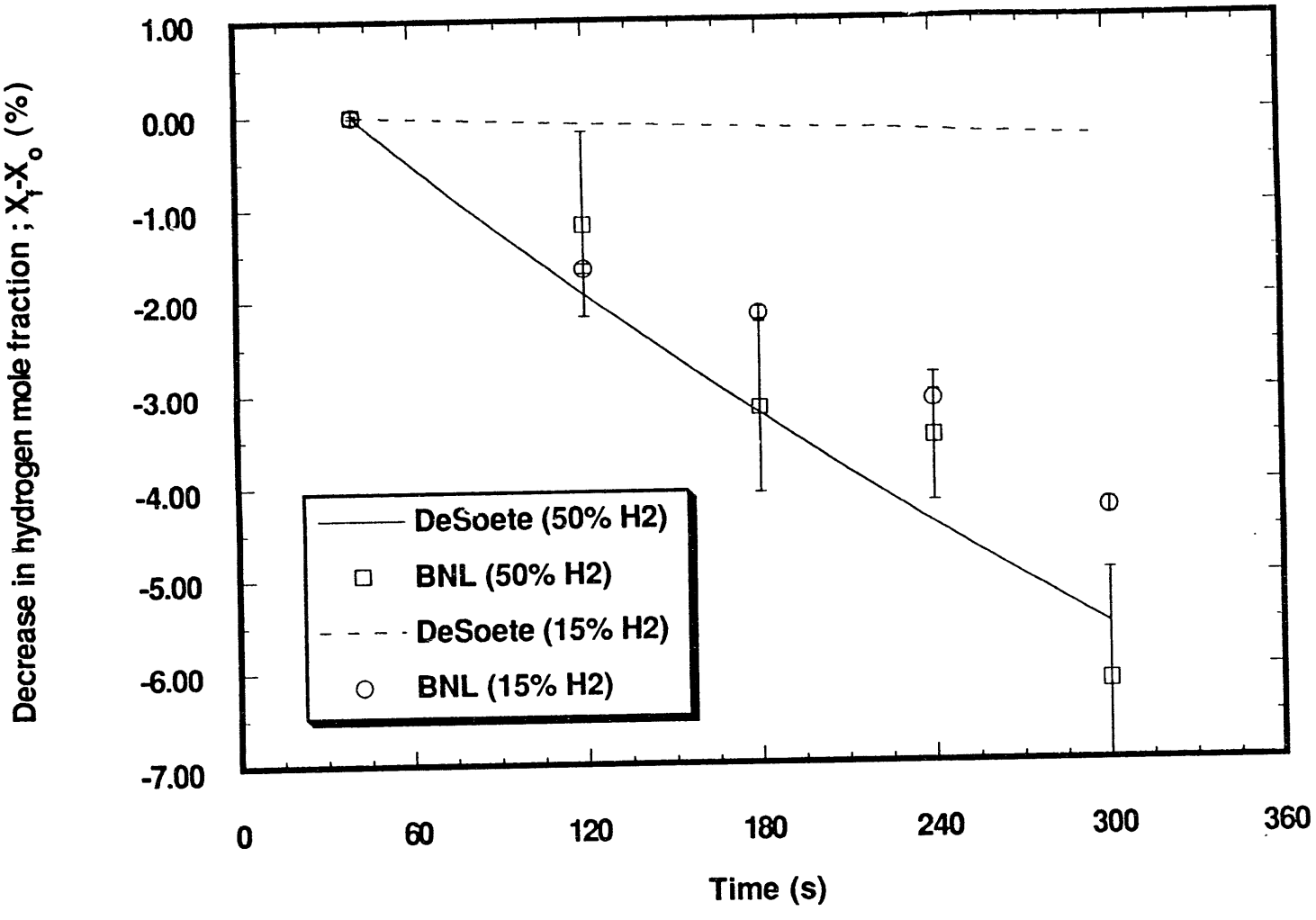


Figure 3.5: Comparison of slow oxidation SSDA grab sample results of Hydrogen-Air at 650K with prediction from Equation (3-2)

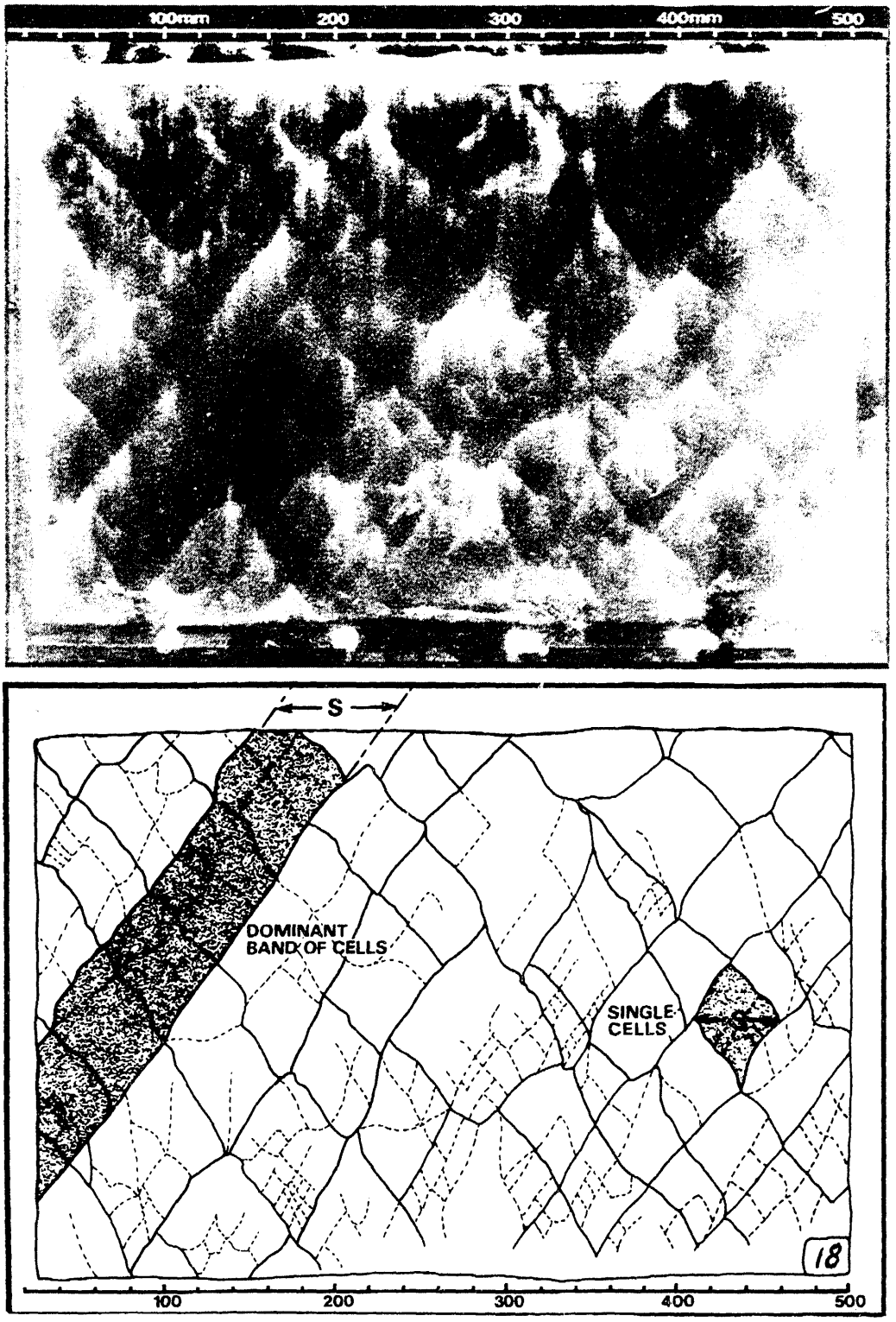


Figure 3.6: Typical smoked foil with interpretation sketch illustrating both single cell and dominant diagonal band of cells (Moen et al., 1982)

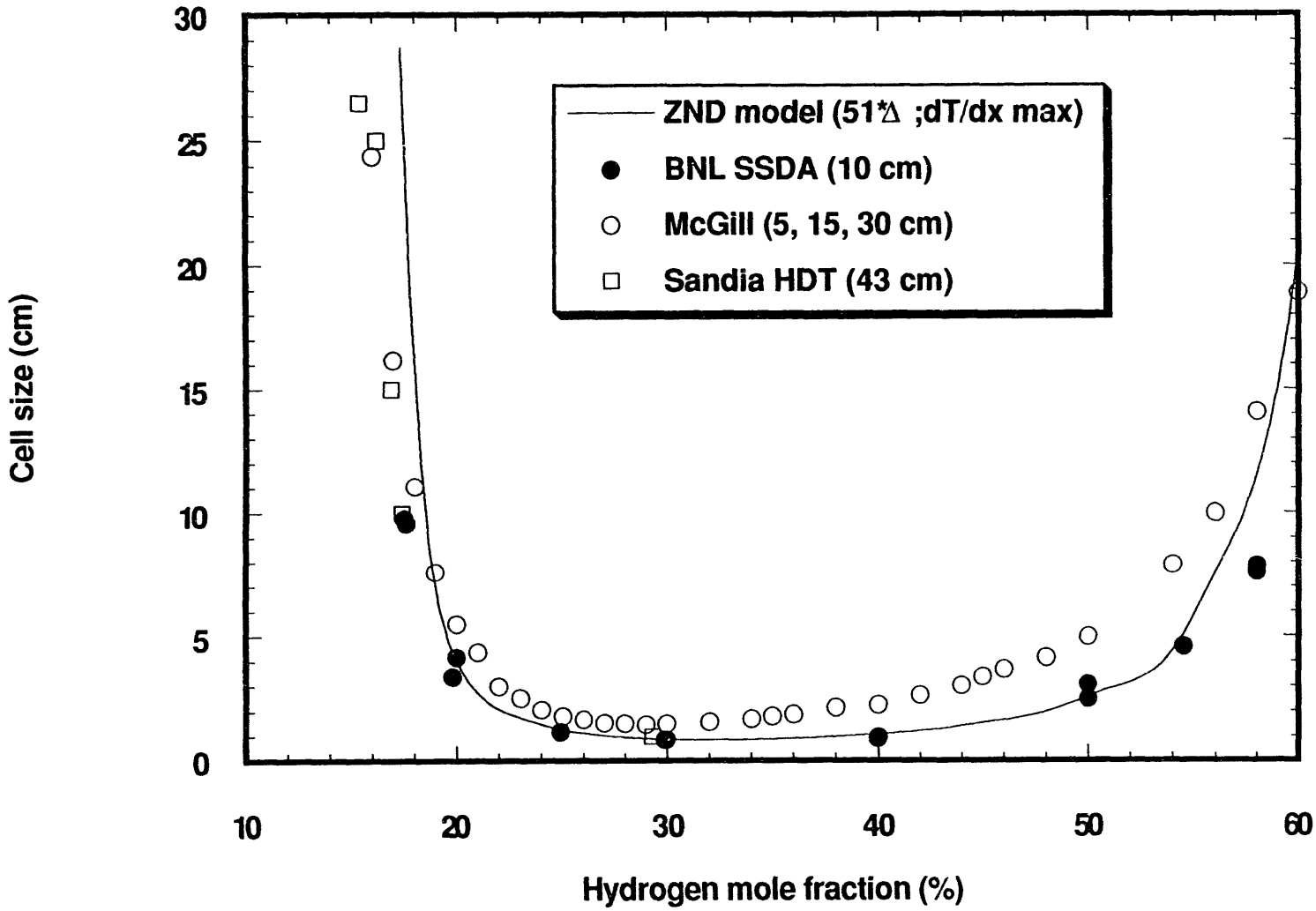


Figure 3.7: Comparison of the measured average detonation cell size and the ZND model prediction for hydrogen-air at 300K and 0.1 MPa

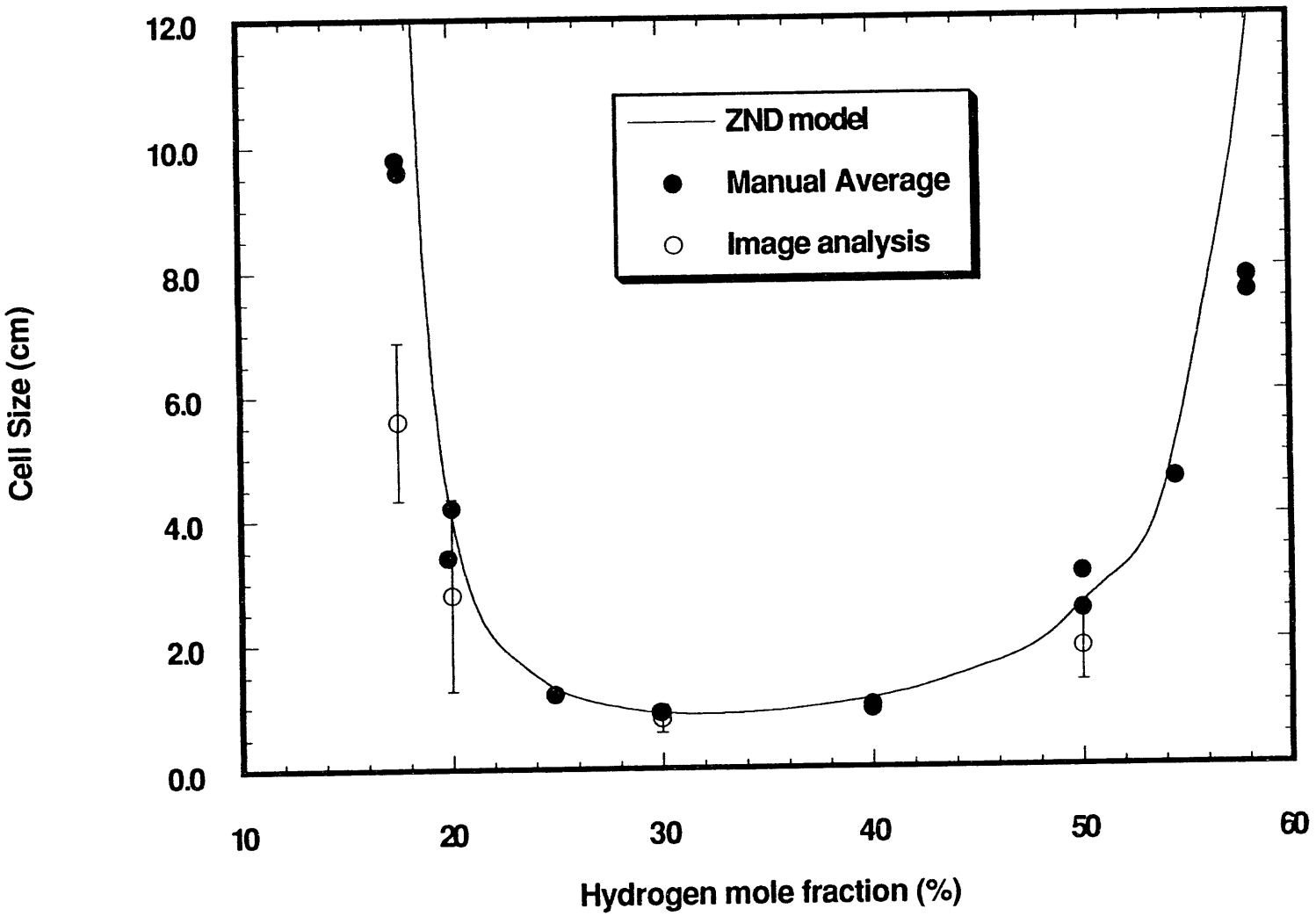


Figure 3.8: Cell size measurement using image analysis overlayed on the data from Figure 3.7

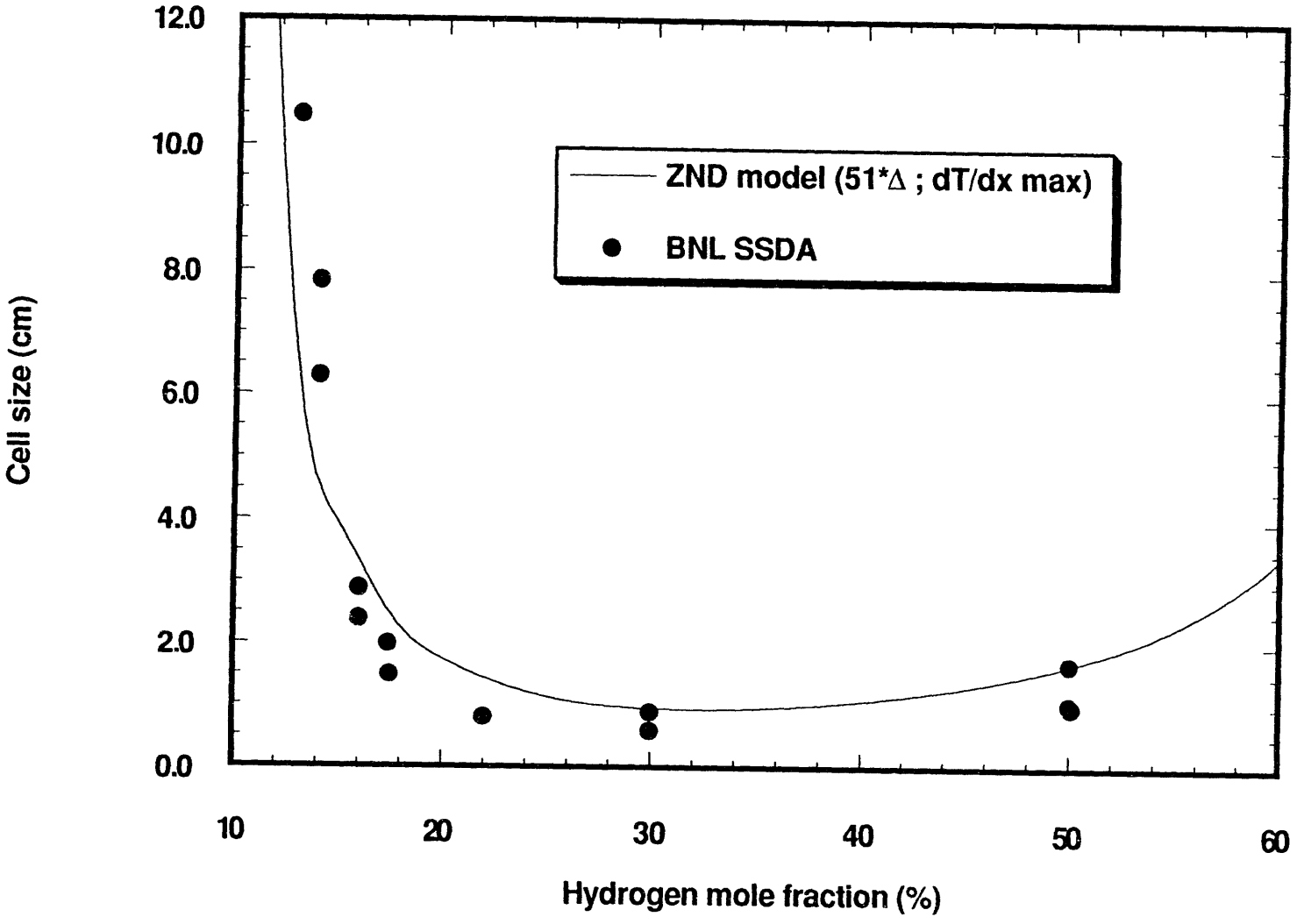


Figure 3.9: Comparison of the measured average detonation cell size and the ZND model prediction for hydrogen-air at 500K and 0.1 MPa

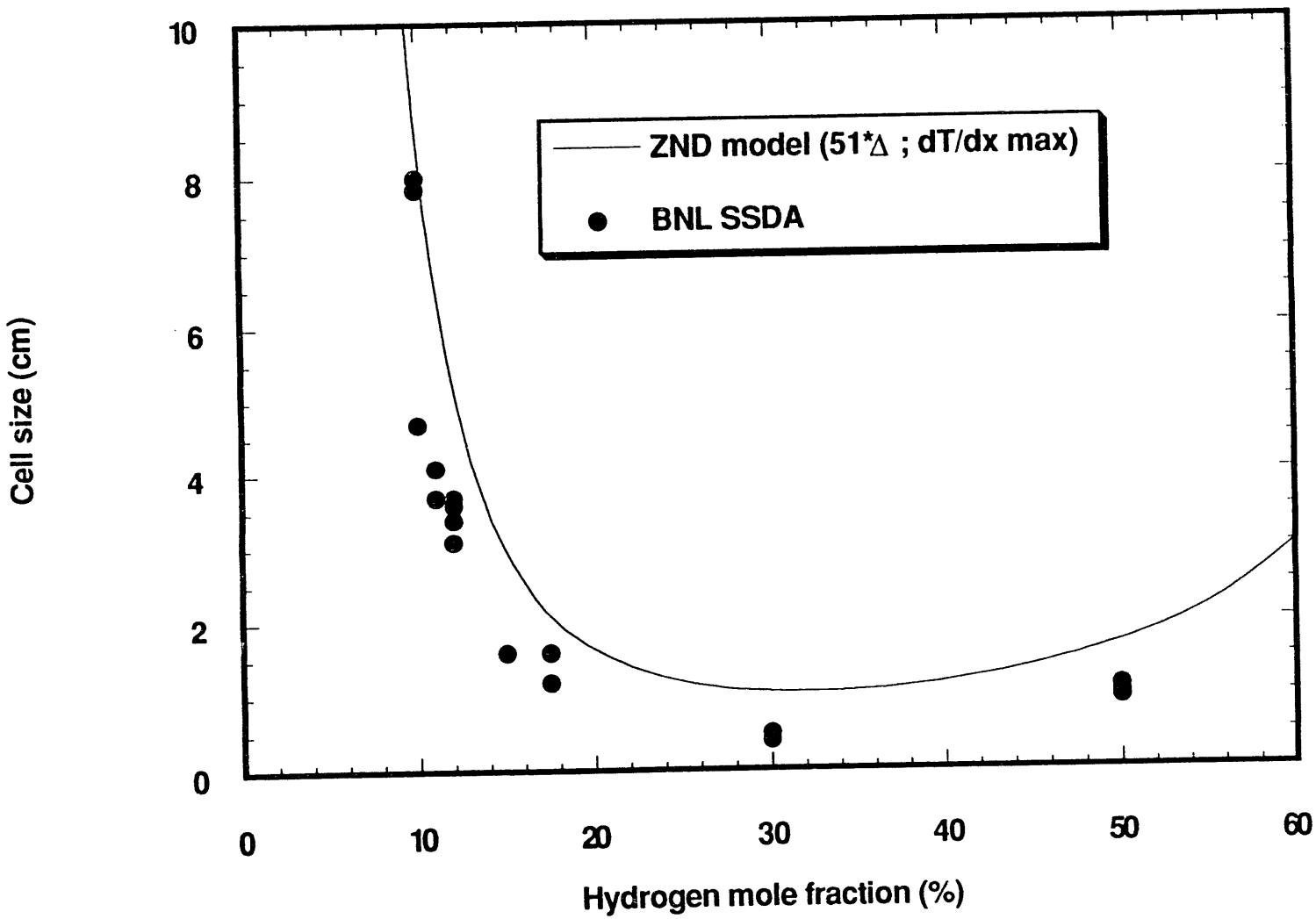


Figure 3.10: Comparison of the measured average detonation cell size and the ZND model prediction for hydrogen-air at 650K and 0.1 MPa

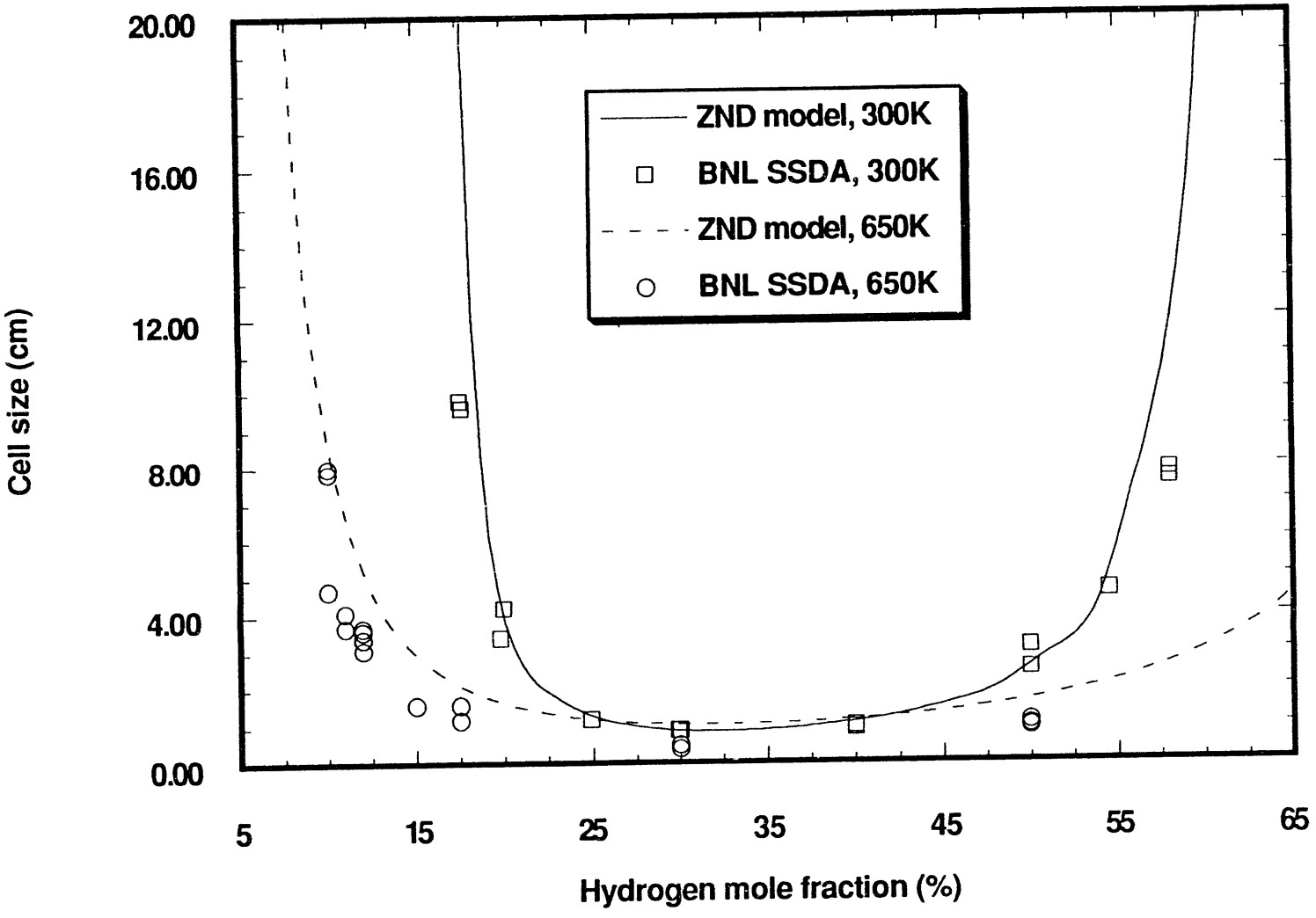


Figure 3.11: Effect of temperature on the average detonation cell size for hydrogen-air mixtures

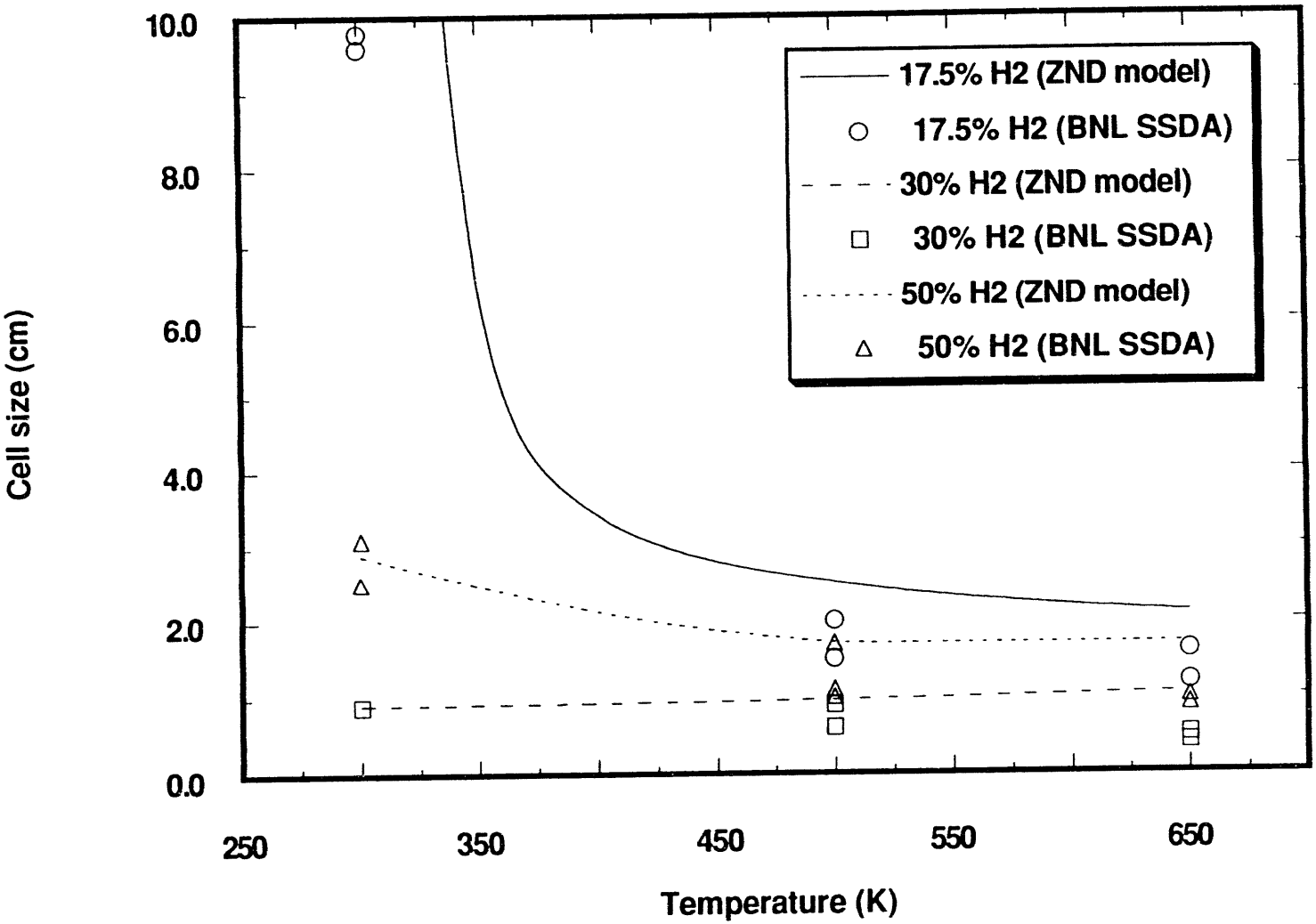


Figure 3.12: Effect of temperature on average detonation cell size for hydrogen-air mixtures containing 17.5%, 30%, and 50% hydrogen

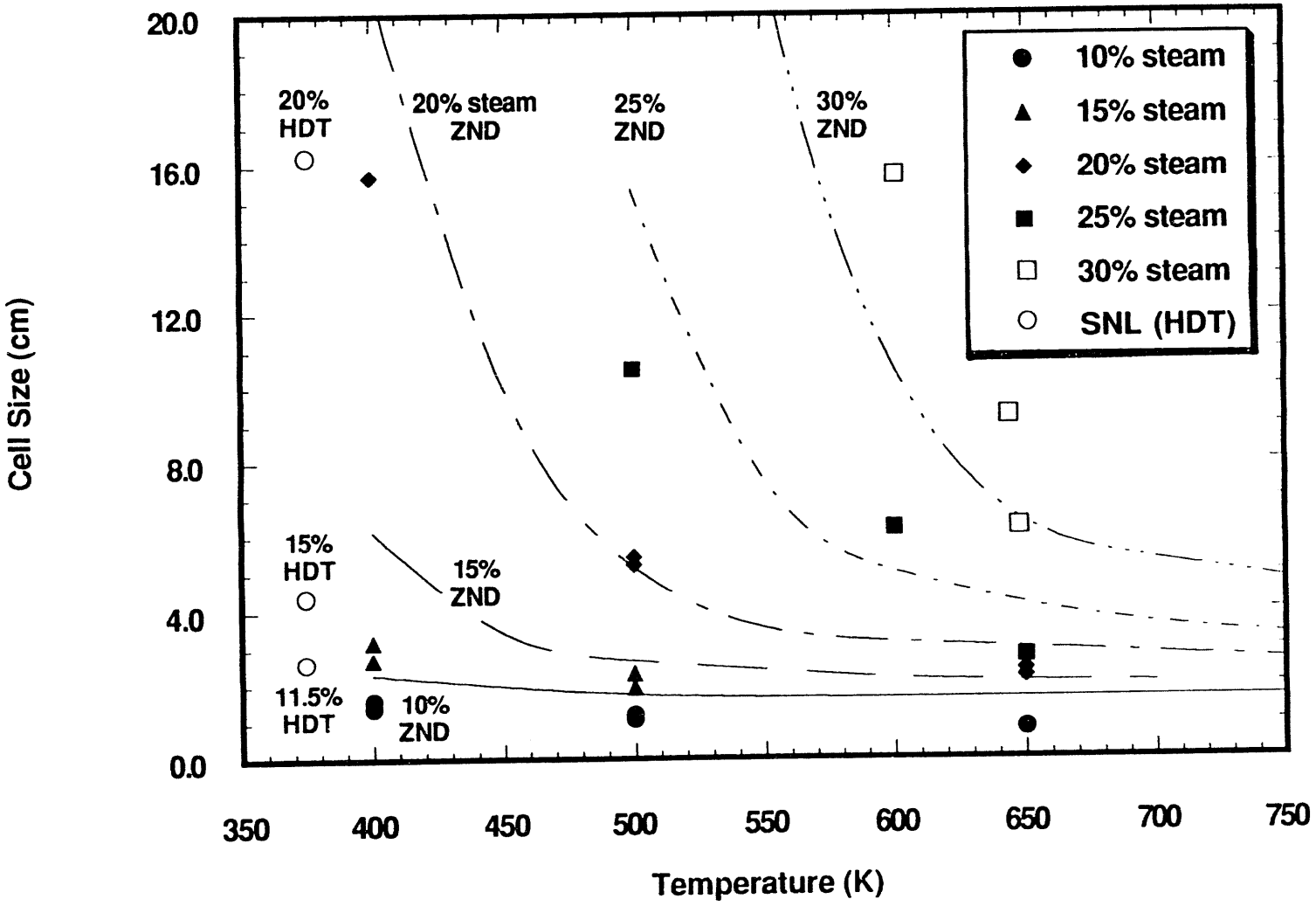


Figure 3.13: Comparison of the measured average detonation cell size and the ZND model prediction for stoichiometric hydrogen-air-steam diluted mixtures at 0.1 MPa as a function of temperature

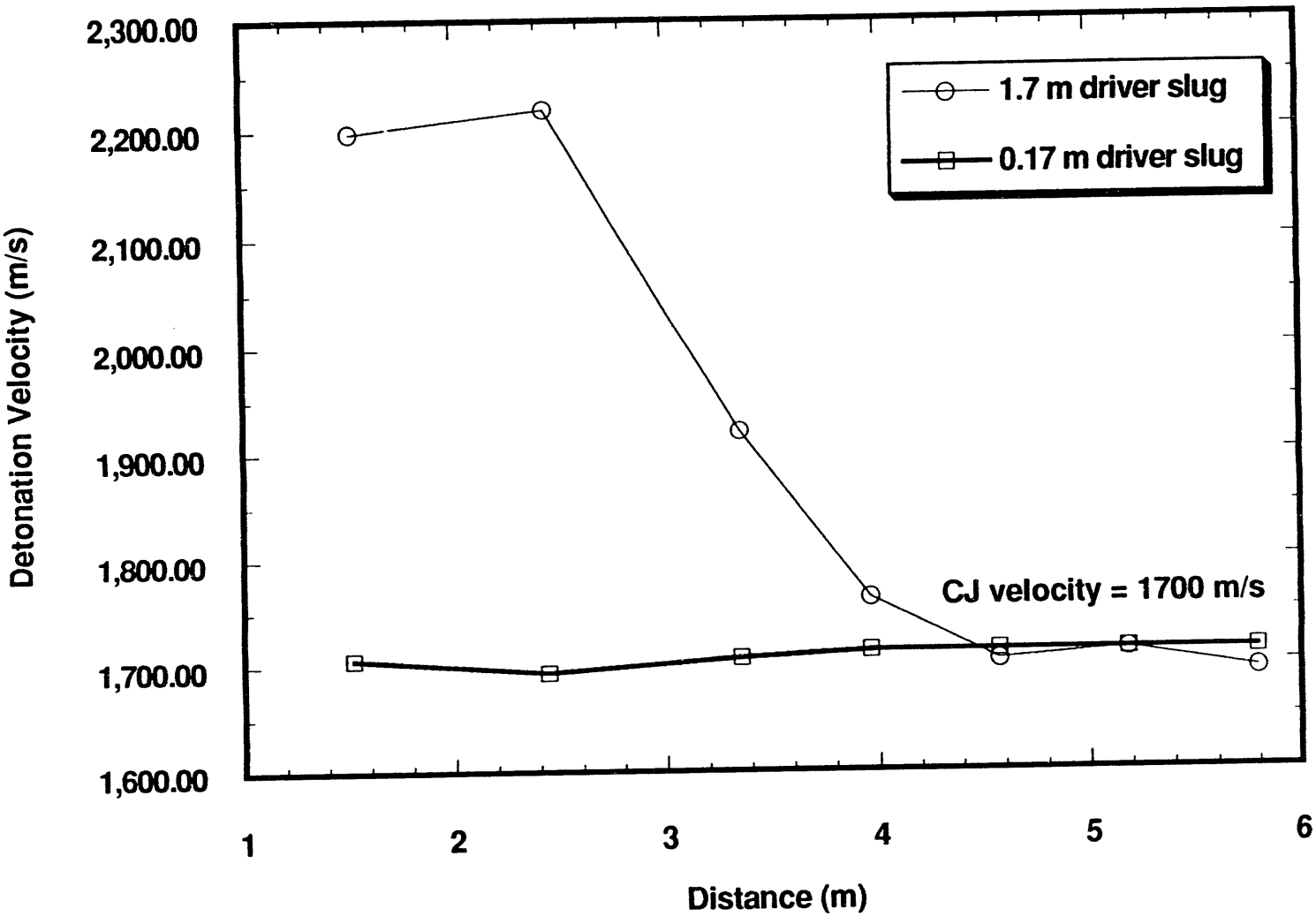


Figure 3.14: Effect of driver slug length on detonation velocity in a 20% hydrogen and 80% air mixture at 300K and 0.1 MPa

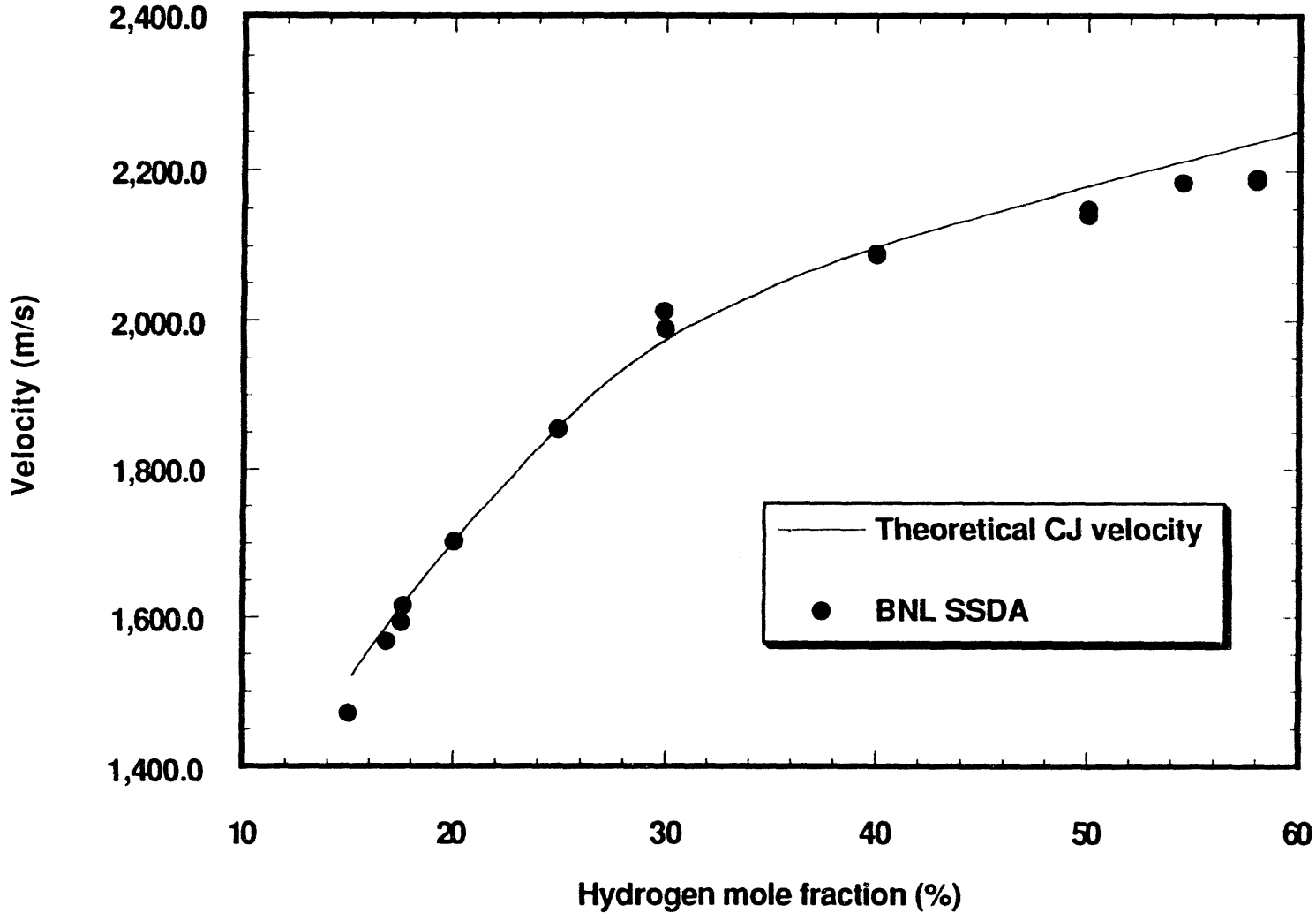


Figure 3.15: Comparison of experimentally measured detonation velocity for hydrogen-air mixtures at 300K with the theoretical CJ velocity

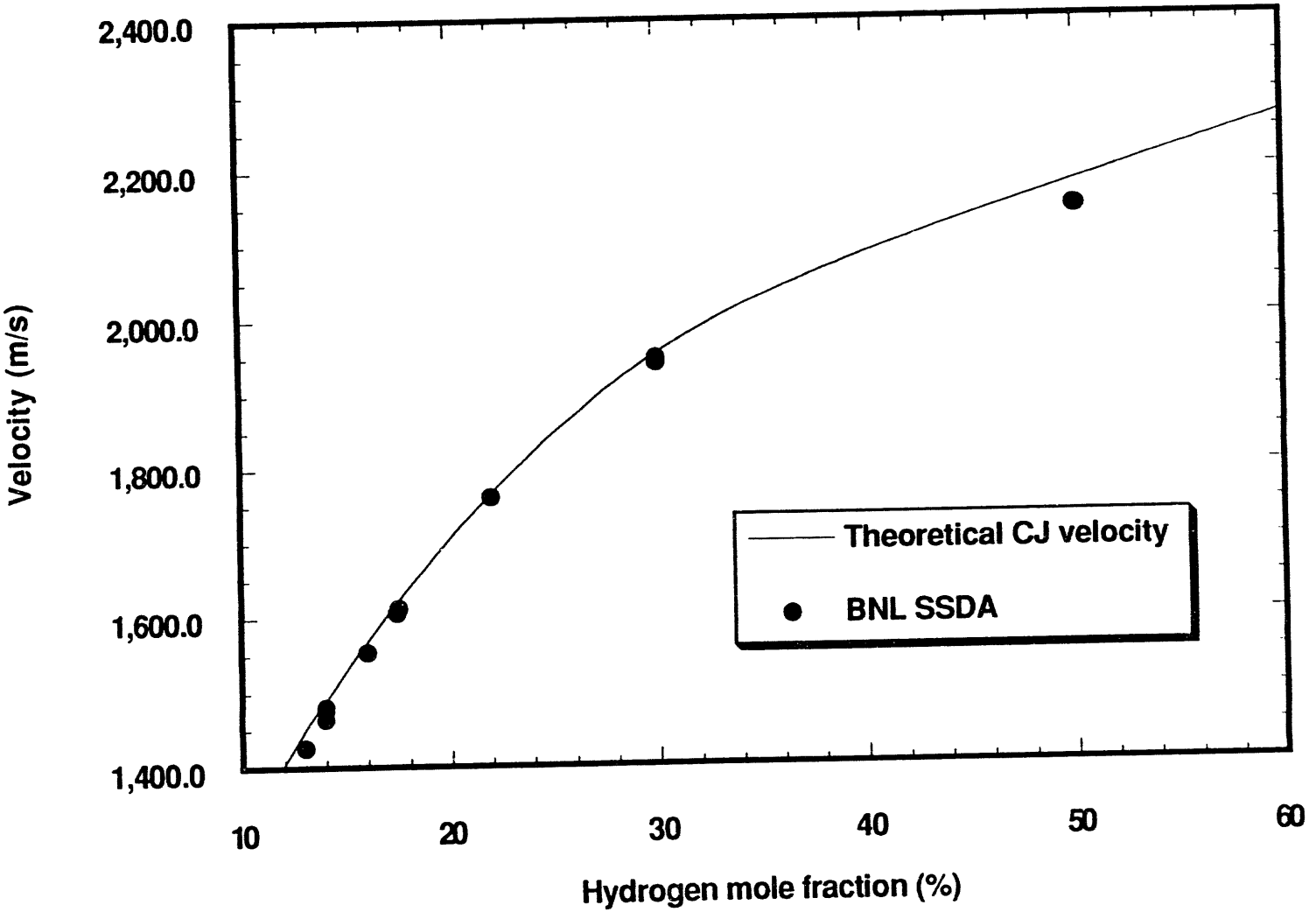


Figure 3.16: Comparison of experimentally measured detonation velocity for hydrogen-air mixtures at 500K with the theoretical CJ velocity

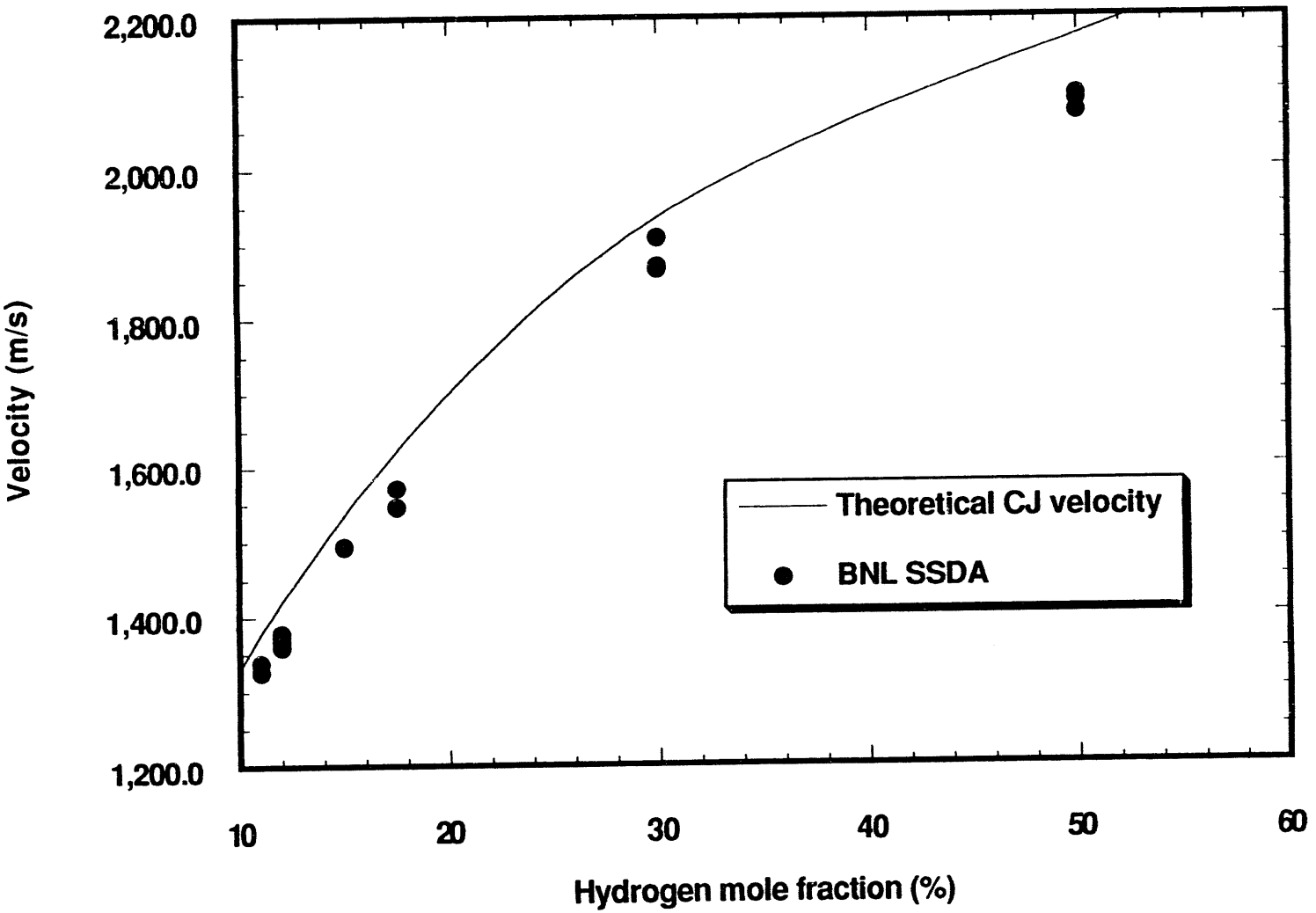


Figure 3.17: Comparison of experimentally measured detonation velocity for hydrogen-air mixtures at 650K with the theoretical CJ velocity

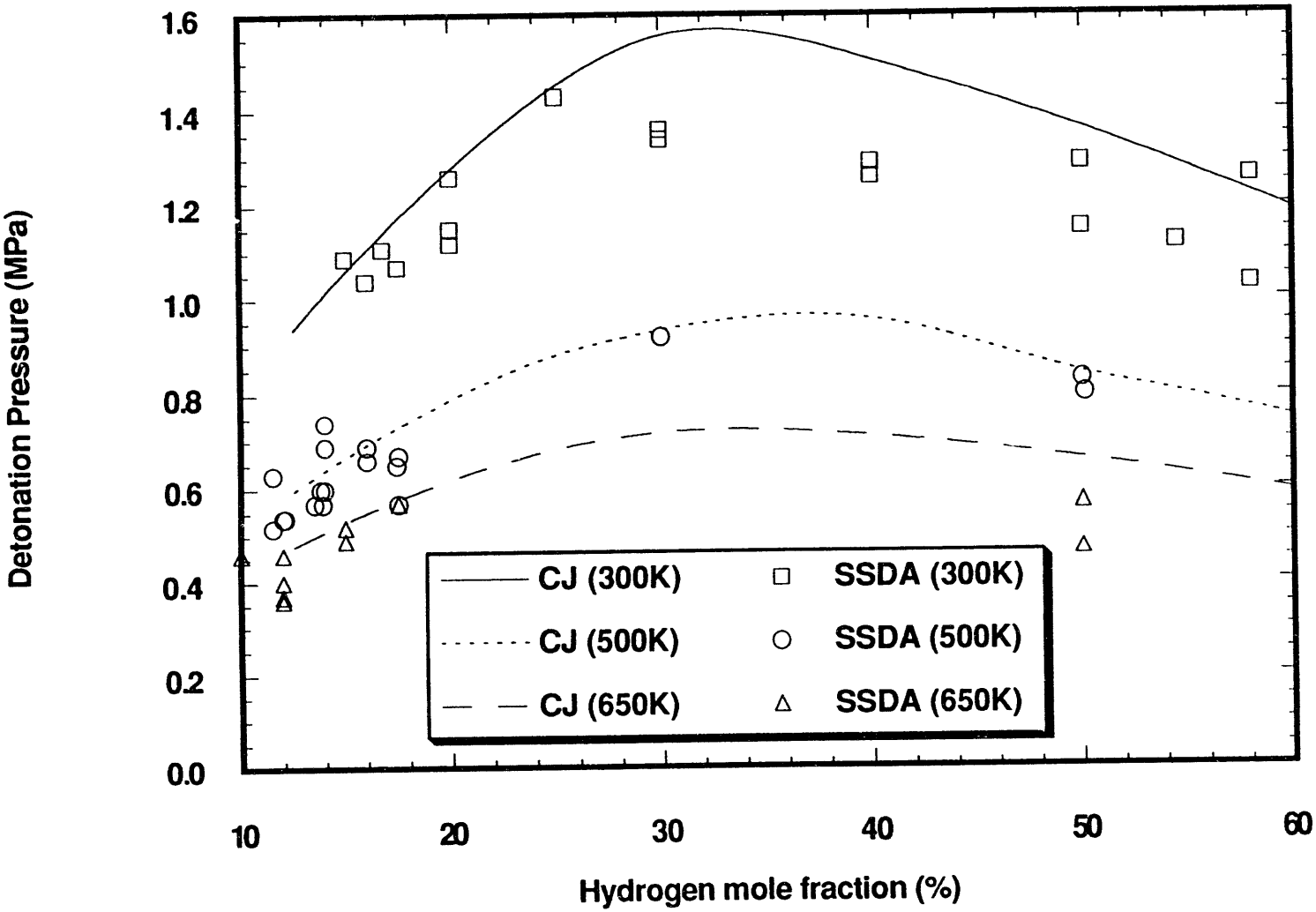


Figure 3.18: Comparison of measured detonation pressure with the theoretical CJ pressure for hydrogen-air mixtures


Figure 3.19: Smoked foil records obtained from the SSDA for near limit detonations in hydrogen-air mixtures at 0.1 MPa

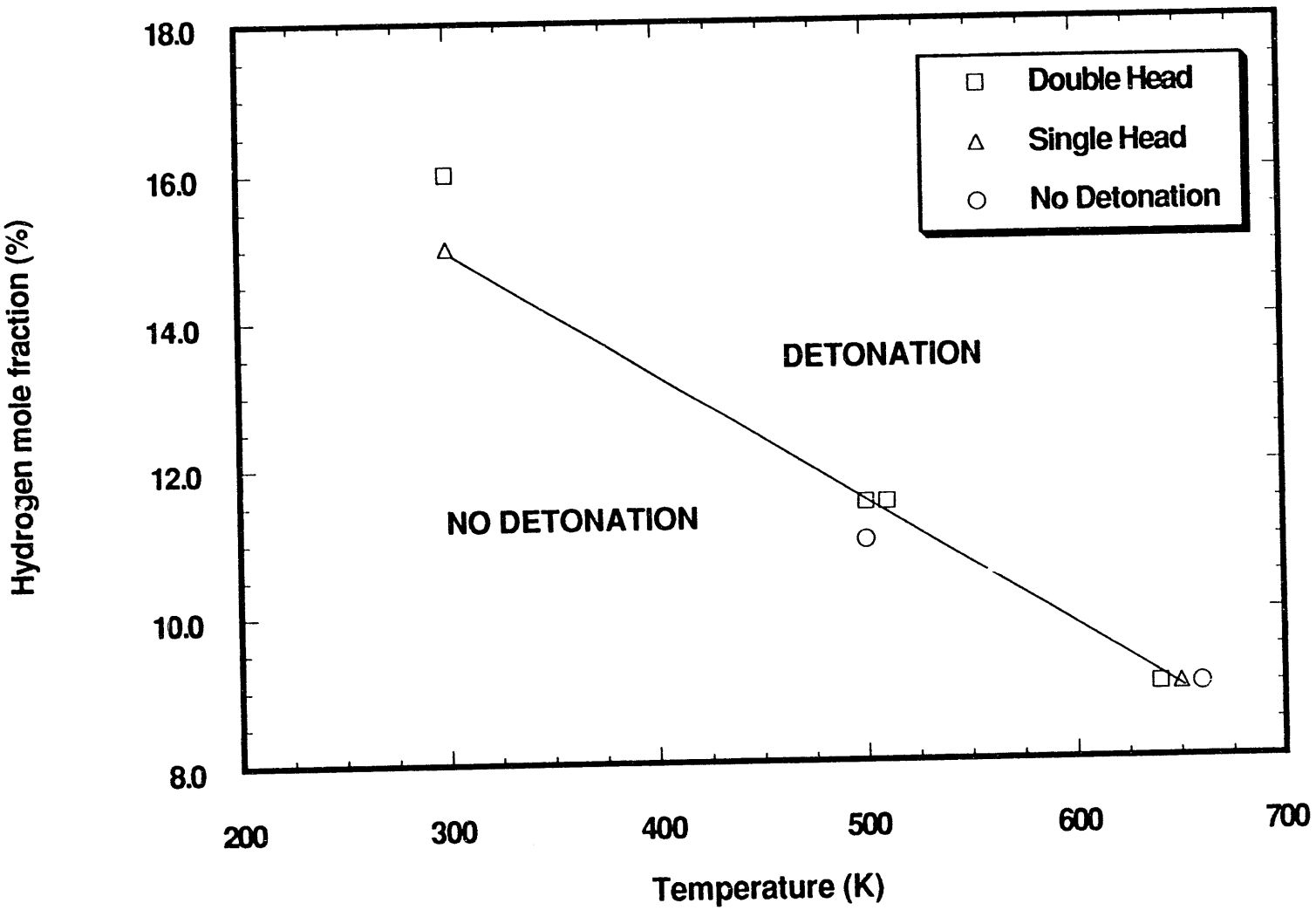


Figure 3.20: Detonability limit for hydrogen-air mixtures at 0.1 MPa in the SSDA

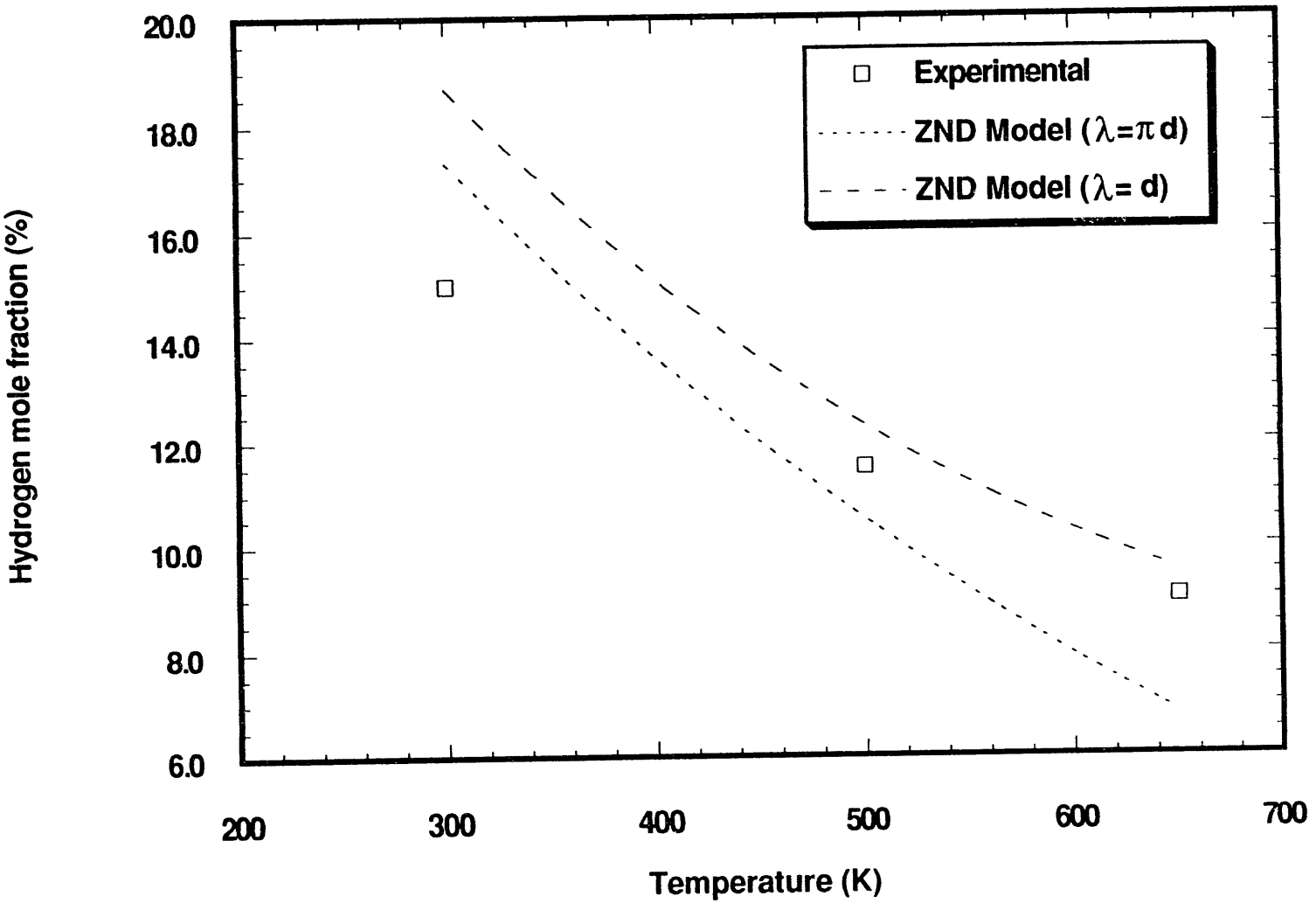


Figure 3.21: Comparison of SSDA experimentally determined detonability limit with ZND model predictions for hydrogen-air mixtures at 0.1 MPa

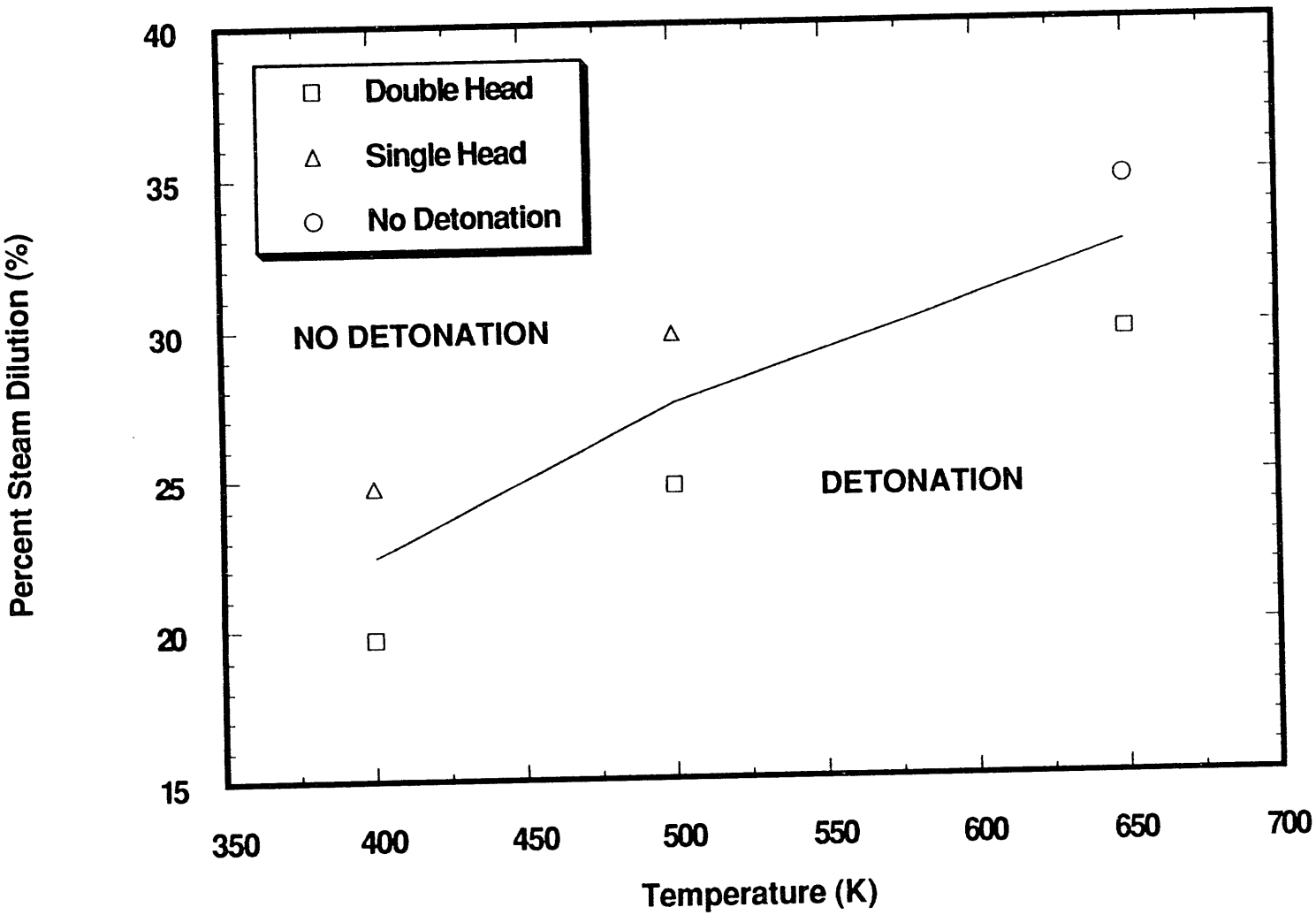


Figure 3.22: Detonability limit for stoichiometric hydrogen-air and steam at 0.1 MPa in the SSDA

# 4 DISCUSSION

A major objective of the Small-Scale Development Apparatus (SSDA) was to provide the basic experimental data required for assessing the potential for a self-sustained detonation in a reactor containment in a high-temperature environment containing hydrogen, air, and steam. The experimental data have provided clear evidence that:

(1) temperature increases the sensivity to detonation of hydrogen-air-steam mixtures,

(2) steam content decreases the sensitivity,

(3) in the presence of steam, increased temperature significantly reduces the desensitizing effect of steam, and

(4) the lean detonability limit of the SSDA test vessel decreases with temperature.

Importantly, however, the high-temperature experiments have also provided evidence that high-temperature mixtures of hydrogen, air, and steam cannot be sustained for very long times, since the mixture chemical reactivity at the temperatures of interest leads to significant hydrogen oxidation in the absence of ignition sources, which reduces the sensitivity of the mixtures as time progresses.

The major result of the experimental research reported here is that the sensitivity to detonation of gaseous mixtures of hydrogen, air and steam increases with temperature. The experimental results clearly demonstrate that cell size decreases with temperature, indicating that the mixture sensitivity to detonation increases with temperature for all mixtures tested. Figure 3.11 demonstrates that at 300K, the cell width of a 17 percent hydrogen-air mixture was measured as 10 cm, whereas at 650K, the same test mixture had a cell width of approximately 1 to 1.5 cm. A 10 percent hydrogen-air mixture at 650K was consistently detonated in the SSDA pipe geometry test vessel having an inside diameter of 10 cm. The lean limit of detonation, defined by the onset of single-head spin, in the 10-cm SSDA test vessel, as shown in Figure 3.20, is 9 percent hydrogen at 650K. At 300K, the leanest mixture in which a sustained, multicell detonation could be regularly achieved was 17 percent hydrogen-air and the detonation limit is 15 - 16 percent hydrogen, as shown in Figure 3.20.

The experimental results also demonstrate the strongly desensitizing influence of steam and the opposing, strongly sensitizing effect of temperature in steam-rich mixtures. Because of the size of the SSDA test vessel, only stoichiometric hydrogen-air-steam mixtures could be tested. At a temperature of 400K, Figure 3.13 demonstrates that a stable detonation in a mixture of 30 percent steam could not be achieved, whereas at 650K, a detonation cell size of about 8 cm was measured. The planned experiments in the HTCF will explore the likelihood of sustained detonations with hydrogen-air-steam mixtures which are more clearly representative of containment conditions than stoichiometric hydrogen-air.

Previous research (Moen, et al., 1981) has demonstrated that as the pipe diameter increases, detonations in leaner hydrogen mixtures can be sustained. The results of the current investigation indicate that the lean detonability limit for the SSDA test vessel decreases with increasing temperature. It can be argued that in a reactor containment, where the geometric length scale may be on the order of meters, self-sustained detonations of hydrogen-air mixtures of 10 percent hydrogen would be possible for gas mixtures of approximately 650K if detonation initiation occurred and if boundary constraints were similar to those of the experiments. The first phase of the planned experiments in the High-Temperature Combustion Facility (HTCF) will explore the likelihood of sustained detonations at 650K for hydrogen-air mixtures leaner than 10 percent hydrogen.

While the experimental results discussed above can be used to argue that the effect of temperature is to sensitize mixtures to detonations under severe accident containment conditions, the argument presupposes the stable existence of reactive mixtures at the elevated temperatures. If, however, the mixture at elevated temperature does not immediately ignite and some time passes, then there are several competing effects which arise. As time progresses, the results of the hydrogen oxidation experiments indicate that the hydrogen will oxidize, thereby desensitizing the mixture. The rate at which the hydrogen oxidizes is likely related to the temperature-dependent kinetics of reaction between hydrogen and oxygen, perhaps influenced by reactions at metal surfaces. The current data for the rate of reaction agrees with Equation (3-2) for rich mixtures, but does not agree very well for lean mixtures. The data, however, demonstrate that the extent of chemical

reaction is significant over a period of minutes at a temperature of 650K. No measurable reactions were observed at 500K. As time progresses, heat transfer to containment structures would decrease the mixture temperature and would condense steam. The cooling of the gas limits the oxidation process, limits the amount of hydrogen which is oxidized and thereby limits the desensitization of the gas due to chemical reaction. At the same time, cooling of the gas would tend to decrease the sensitivity of the mixture, while condensation of steam would tend to increase the sensitivity of the mixture to detonation.

The above discussion suggests that the outcome of any high-temperature accident scenario involving combustible gas depends on the competing rates of heat transfer, condensation and chemical reaction. If a high-temperature mixture does not detonate or deflagrate immediately, and if the temperatures above 650K are sustained for a period of at least minutes, then time will tend to decrease the sensitivity of the mixture through mixture oxidation. These observations are based upon the slow hydrogen oxidation data. The data are preliminary, may be influenced by boundary conditions, and further experiments on a larger scale are required in order to reach firm conclusions. However, if ignition sources are not present for some period of time, it appears that the conditions for a self-sustained detonation may be difficult to achieve at temperatures in excess of 650K. Further experiments are needed, in particular for leaner mixtures at larger scale than performed heretofore in the SSDA. The data and interpretation given above lead to the conclusion that in order to assess the sensitivity to detonation of a region of containment which could exist at temperatures in the range 500K-650K, a model is required which accounts for the rates of heat transfer, condensation and chemical reaction of the constituents. Such a model is not yet available.

The experimental data provide clear evidence that the effect of increased temperature is to sensitize hydrogen-air-steam mixtures to undergo self-sustained detonations. The impact of the effect of temperature on the potential for detonations during severe accidents in reactor containments has not yet been established with suitable experimental data. The effect of temperature on three sources of detonation initiation must be considered: direct initiation, deflagration-to-detonation transition (DDT) and hot-jet initiation of detonation (Ferrell, C.M., et al., 1989; Berman, et al., 1986). Since it is known that the critical energy, the energy required to directly initiate (using high-explosives or high-energy electrical sources) a spherical detonation in an unconfined medium is proportional to the cube of the detonation cell size (Lee, 1984) it follows, from the observations of the variation of cell size with temperature, that the effect of temperature is to decrease the energy required to directly initiate a detonation in a gas mixture. A quantitative assessment of the effect of temperature on initiation energy will be made following completion of the experimental program in the HTCF. Experimental data for the effect of temperature on conditions for DDT and hot-jet initiation in hydrogen-air-steam mixtures in the temperature range 400K-650K are not available. As a result, the effect of the increased sensitivity of the gas mixtures with increased temperature on the conditions for detonations in containments during severe accidents is not yet known. Experiments planned for the HTCF, discussed in Section 6, will address these detonation phenomena. A more complete assessment of the effect of temperature on the likelihood of detonations in containment will be possible following availability of this data from the HTCF test program.

# 5 SUMMARY AND CONCLUSIONS

The Small-Scale Development Apparatus (SSDA) was developed as the first phase of the BNL High-Temperature Hydrogen Combustion Research Program. The objective of the SSDA was to provide preliminary experimental data to characterize the sensitivity of hydrogen-air-steam mixtures to undergo detonations at elevated temperature and to resolve a number of high-temperature problems associated with the design and operation of the larger High Temperature Combustion Facility (HTCF). The HTCF is currently under construction.

The SSDA was designed to study self-sustained detonations in gaseous mixtures of hydrogen, air, and steam at temperatures up to 700K. The central element of the SSDA is a 10-cm inside diameter, 6.1-m long tubular test vessel, designed to comply with the ASME Boiler and Pressure Vessel Code to accomodate a maximum allowable working pressure of 12.2 MPa at 700K. The test vessel is heated by ceramic heating blankets which are fastened to the test vessel and constructed of ceramic beads through which nichrome resistance wire is threaded. Heating uniformity tests demonstrated that the tempertures along the vessel are uniform within $\pm$ 14K. The system is remotely operated behind secure boundaries in an adjacent control room and is controlled by a 486 personal computer equipped with commercially available data acquisition and control hardware and software. Instrumentation is provided to measure properties of the detonation wave, including detonation cell width, detonation propagation speed, and pressure.

A typical experiment is conducted by first evacuating the vessel and preheating the vessel to the desired temperature. The test gas mixture of hydrogen, air, and steam is premixed by partial pressures in a separate mixing chamber. The mixture is downloaded into the test vessel to a fill pressure of slightly less than 0.1 MPa. Detonations are initiated in the test vessel using a "gas driver" initiation system. Just prior to a run, a small quantity of acetylene-oxygen gas driver mixture is forced into the driver end of the test vessel, raising the vessel pressure to 0.1 MPa. A detonation is initiated in the acetylene-oxygen by discharge of a capacitor through a pair of electrodes connected by an exploding wire, which vaporizes when a large current is passed through it. The detonation is transmitted from the acetylene-oxygen slug to the test mixture within the test vessel. This method of detonation initiation obviates the need for high-energy sources needed to initiate a detonation directly in hydrogen-air-steam systems.

The detonation cell size, the experimental measure of the sensitivity of the mixture to undergo self-sustained detonations, was measured using the smoked-foil technique, adapted and modified for the high-temperature experiments. Ion probes were used to measure the time-of-arrival of the detonation front at various positions along the tube, from which the detonation wave speed was computed. Water-cooled piezoelectric pressure transducers were employed to measure the transient detonation pressure. The ion probe and pressure transducer signals were monitored on a digital oscilloscope with a sampling rate of 100 MHz.

Preliminary experiments were performed to determine the maximum temperature for which hydrogen oxidation occurs at a sufficiently low rate so as to allow introduction of the test gases to the heated test vessel and firing of the detonation initiation system. These experiments showed that while the test vessel design temperature was 700K, the maximum temperature for which experiments could be practially run was 650K. At higher temperatures, the mixtures would immediately burn off upon introduction into the test vessel. Additionally, experiments were conducted to measure the rate of hydrogen oxidation at temperatures of 500K and 650K, for hydrogen-air mixtures of 15 percent and 50 percent, and for a mixture of equimolar hydrogen-air and 30 percent steam at 650K.

Experimental data for detonation cell size, detonation pressure and velocity are presented for detonations in gaseous mixtures of hydrogen, air, and steam with hydrogen concentration in the range of 9 percent to 60 percent by volume, with steam fractions to 30 percent and temperature in the range 300K to 650K. Initial pressure in all experiments was 0.1 MPa. The detonation cell width data are compared with predictions based on the one-dimensional ZND detonation model . The pressure and velocity data are compared with Chapman-Jouguet theory. The detonation limits for the SSDA test vessel were determined experimentally and compared with a criteria based on low-temperature data.

All of the objectives of the SSDA program delineated in Section 1.4 were successfully accomplished. The following conclusions have been reached on the basis of the experimental data and analysis presented in this report:

Conclusions

**SSDA Detonation Experiments and Analysis**

(1) Detonation cell size measurements in the SSDA using hydrogen-air mixtures at 300K, and additional measurements using hydrogen-air-steam mixtures at 400K, demonstrate good agreement with previous cell size data reported in the literature. This agreement provides confidence that the experimental techniques used in the work reported here are reliable. Multiple measurements made under identical conditions indicate good reproducibility of cell size data.

(2) Detonation cell size measurements provide clear evidence that the effect of hydrogen-air gas mixture temperature, in the range 300K-650K, is to decrease cell size and, hence, to increase the sensitivity of the mixture to undergo detonations. Initial pressure was 0.1 MPa in all experiments.

(3) Increasing the steam content, in the range zero to 30 percent by volume, of a stoichiometric hydrogen-air mixture increases the cell size and thus decreases its sensitivity to detonate. However, at elevated temperature, this desensitizing effect becomes less pronounced.

(4) The hydrogen-air detonability limits for the 10-cm inside diameter SSDA test vessel, based upon the onset of single-head spin, decreased from 15 percent hydrogen at 300K down to about 9 percent hydrogen at 650K. At 300K, multicell detonations were observed for hydrogen-air mixtures with hydrogen concentration greater than 17.5 percent. At 650K, 10 percent hydrogen mixtures were regularly detonated and multicell detonations were observed.

(5) The detonability limit for mixtures of hydrogen, air, and steam with a stoichiometric ratio of hydrogen and air increases from between 20 to 25 percent steam at 400K to between 30 to 35 percent steam at 650K.

(6) The one-dimensional ZND model does a very good job at predicting the overall trends in the cell size data over the range of hydrogen-air-steam mixture compositions and temperature studied in the experiments. For the experiments run in the SSDA, the constant of proportionality between the average measured cell size and the calculated reaction zone thickness was found to be 51.

Despite the ability of the ZND model to predict the trends in the data, one must be extremely cautious in using the ZND model to predict average cell size. For example, the constant of proportionality used should be chosen by fitting the portion of the experimental data which includes the condition of interest. In the case of larger scales (i.e., leaner mixtures), the constant of proportionality should be obtained by fitting the leanest available experimental data.

(7) The experimentally measured detonation velocity generally agrees with predictions based upon the Chapman-Jouget theory. The data at 650K, however, are approximately 3 to 4 percent low compared with the CJ theory predictions. This velocity deficit is attributed to preinitiation hydrogen oxidation.

(8) The experimentally measured peak detonation pressure agrees reasonably well with the calculated CJ pressure. In the worst case, the data are found to be about 10 percent below the calculated CJ pressure. For the fixed initial pressure experiments reported here, the CJ pressure is found, both experimentally and according to CJ theory, to decrease with increasing mixture temperature.

**SSDA Hydrogen Oxidation Phenomena**

(1) The maximum temperature which it was found possible to load combustible gases into the test vessel without an immediate burn was 650K. At 700K, the mixtures immediately reacted and detonation

experiments could not be carried out. This is significantly below the often-quoted minimum autoignition temperature for hydrogen-air mixtures of 793K (Zabetakis, 1956).

(2) The rate of hydrogen oxidation was found to be significant at the highest temperature tested. A hydrogen-air mixture of 50 percent hydrogen was reduced to 44 percent, and a hydrogen-air mixture of 15 percent hydrogen was reduced to 11 percent, in five minutes at 650K. The hydrogen oxidation rate for the 50 percent mixtures agreed quite well with the rate equation proposed by DeSoete (1975). The measured rate of reaction was considerably greater than predicted by the DeSoete expresssion for the 15 percent mixtures.

**SSDA Design and Operational Issues**

(1) The maximum temperature above which the injected test mixture immediately burned is 650K, as described above.

(2) The gas driver detonation initiation system was successfully implemented. Tests demonstrated that the gas driver system initiates constant-velocity detonations at Chapman-Jouget wave speeds. This system will be used in the HTCF.

(3) All instrumentation concepts were tested and evaluated in the SSDA. The smoked-foil technique for measurement of detonation cell width was successfully adapted to the high-temperature conditions of the SSDA experiments. The water-cooled pressure transducers operated successfully in the high-temperature environment of the SSDA. After some initial experimentation, ion probes were implemented to measure time-of-arrival and, hence, velocity of the detonation wave. These probes, and their associated circuitry, provided good quality signals for analysis under high-temperature conditions. All these techniques will be adopted for use in the HTCF.

# 6 FUTURE WORK

The objectives of the experimental program using the Small-Scale Development Apparatus (SSDA) have been successfully accomplished. All design and operational issues related to the implementation of the High-Temperature Combustion Facility (HTCF) have been resolved, and the HTCF is scheduled for completion in October 1993. The central feature of the HTCF is a 30-cm diameter, 21.3-m long, high-temperature detonation test vessel.

The first phase of the experimental program in the HTCF will focus on the characterization of the effect of temperature on the experimentally measured average cell size for gaseous mixtures of hydrogen, air, and steam. Due to the size of the SSDA (10-cm diameter), the range of mixture conditions (i.e., hydrogen composition, steam fraction) was limited to more sensitive mixtures. Experiments will be carried out in the HTCF which will expand on the data obtained from the SSDA to include less sensitive, more prototypic mixtures. Detonation cell sizes will be measured as a function of temperature for these less sensitive mixtures.

The SSDA experiment were all performed using mixtures at initial pressure of 0.1 MPa. In a reactor accident scenario, the containment atmosphere is composed of steam, air, and hydrogen, where the initial pressure is above 0.1 MPa. The effect of mixture pressure on the sensitivity of hydrogen-air-steam mixtures to undergo self-sustaining detonations will be investigated in the experimental program planned for the HTCF. Detonation cell sizes will be measured as a function of pressure.

The limited number of slow hydrogen oxidation experiments performed in the SSDA indicated that at high-temperature the mixture composition is continuously changing as a result of chemical reaction of the constituents. Clearly, it is very important to account for this chemical reaction phenomenon in order to assess the likelihood of deflagration or detonation of a mixture which exists for any period of time prior to ignition. Additional experiments will be carried out in the HTCF in order to determine whether the phenomena are influenced by the surface-to-volume ratio of the experimental apparatus.

The experiments performed in the SSDA were directed at extending the database on cell size for hydrogen-air-steam mixtures to high temperatures. This data can be used in conjunction with several existing criteria to provide a judgment about whether or not a detonation can propagate wihtin a room of a given size. However, it is generally accepted that an ignition source large enough to directly initiate a detonation does not exist in a reactor containment building. Deflagration-to-detonation transition (DDT) is thought to be a more likely mechanism for initiation of a detonation in a containment building (Ferrell, et al., 1989). Available evidence, based upon low-temperature data, suggests that the conditions favorable for the occurrence of DDT can be related to the mixture detonation cell size and one or more geometric scales of the confining medium (Lee, 1984; Berman, 1986). The effect of gas mixture temperature on the sensitivity of hydrogen-air-steam mixtures to undergo DDT has not been investigated at elevated temperatures. A preliminary series of DDT experiments will be performed in the SSDA using an array of rings, to be installed inside the test vessel, to produce the turbulence in the gas mixture ahead of the flame. These experiments will be followed later in the program with DDT experiments in the larger scale HTCF, performed in a similar manner. The objective of these experiments is to provide data to assess the effect of gas mixture temperature on the sensitivity of mixtures to undergo DDT. The effects of geometric scale and of steam content will also be investigated.

# 7 REFERENCES


Berman, M., et al., "A Critical Review of Recent Large-Scale Experiments on Hydrogen-Air Detonations," Nuclear Science and Engineering, 93, 321-347, 1986.

Camp, A. L., et al., "Light Water Reactor Hydrogen Manual," NUREG/CR-2726, SAND82-1137, 1983.

Chapman, D. L., Phil. Mag., Vol. 47:Series 5, No. 284, pp. 90-104, 1899.

Denisov, Yu. H., and Ya. K. Troshin, Phys. Chem. Sect., Vol. 125, p. 217, 1960.

Doring, W., "On the Detonation Process in Gases," Ann. Phys. Lpz., Vol. 43, pp. 421-436, 1943.

DeSoete, G.G., "The Flammability of Hydrogen-Oxygen-Nitrogen Mixtures at High Temperature," presented at the Italian Flame Days, Sanremo, Italy, April 10-11, 1975.

Dupre, G., R. Knystautas, J. Lee, Prog. in Astro. and Aero., Vol. 106, p. 244, 1985.

Fay, J., "A Mechanical Theory of Spinning Detonation," Journal of Chemical Physics, Vol. 20, No. 6, 1952.

Ferrell, C.M., et al., "Resolution of Unresolved Safety Issue A-48, Hydrogen Control Measures and Effects of Hydrogen Burn on Safety Equipment," NUREG-1370, September 1989.

Guirao, C.M., Knystautas, R, Lee, J.H., "A Summary of Hydrogen-Air Detonation Experiments," NUREG/CR-4961, SAND87-7128, 1989.

Hustad, J.E. et al., "Experimental Studies of Lower Flammability Limits of Gases and Mixtures of Gases at Elevated Temperatures," Combustion and Flame, Vol. 71, pp. 283-294, 1988.

Jouget, E., Encyclopedic Scientifique, Doin et Fils, Paris, pp. 516, 1917.

Kee, R. J., et al., "CHEMKIN-II: A Fortran Chemical Kinetics Package for Analysis of Gas-Phase Chemical Kinetics," Sandia National Laboratories, SAND89-8001, September 1989.

Knystautas, R., Lee, J.H, Peraldi, O., and Chan, C., "Transmission of a Flame from a Rough to a Smooth -Walled Tube," presented at the 10th International Colloquium on Dynamics of Explosions and Reactive Systems, Berkeley, CA, 1985.

Kogarko, S.M., and Zeldovich, Y.B., Doklady Akad.Nauk SSSR NS 63, p. 553, 1948.

Lee, J, presented at the 13th International Colloquium on Dynamicsof Explosions and Reactive Systems, Nagoya, Japan, 1991.

Lee, J.H.S, "Dynamic Parameters of Gaseous Detonations," Ann. Rev. Fluid Mech., 311-336, 1984.

Lewis, B. and von Elbe,G., Combustion, Flames, and Explosions of Gases, 2nd Edition, Acedemic Press, New York, 1961.

Moen, I.O., Murray, S.B, Bjerketvedt, D., Rinnan, A., Knystautas, R., Lee, J., "Diffraction of Detonation From Tubes Into a Large Fuel-Air Explosive Cloud," 19th Int'l Symposium on Combustion, p. 635, 1982.

Nettleton, M.A., Gaseous Detonations Their Nature, Effects and Control, Chapman and Hall, NY, 1987.

## References


Reynolds, W.C., "The Element Potential Method for Chemical Equilibrium Analysis: Implementation in the Interactive Program STANJAN Version 3," Dept. of Mechanical Engineering, Stanford University, Palo Alto, California, January 1986.

Shchelkin, K. I., and Troshin, Y. K., Gas Dynamics of Detonations, Mono Book Corp., Baltimore, Maryland, 1965.

Sheldon, M., "Understanding Autoignition," Fire Engineers Journal, pp. 27-32, June 1984.

Shepherd, J. E., "Chemical Kinetics of Hydrogen-Air-Diluent Detonations," Progress in Astronautics and Aeronautics," 106, Dynamics of Explosions, J.R. Bowen, et al., eds., 1986.

Stamps, D. W., et al., "Hydrogen-Air-Diluent Detonation Study for Nuclear Reactor Safety Analyses," Sandia National Laboratories, NUREG/CR-5525, SAND89-2398, January 1991.

Stamps, D. W. and M. Berman, "A Critical Review of High-Temperature Hydrogen Combustion in Reactor Safety Applications," Paper presented at the International Conference on Thermal Reactor Safety, Avignon, France, October 1988.

Tieszen, S.R, Martin, P.S., Bennedick, W.B., Berman, M., "Detonability of H2-Air-Diluent Mixtures," NUREG/CR-4905, SAND85-1263, 1987.

Toth, L.M., et al., Ed., "The Three-Mile Island Accident, Diagnosis and Prognosis," American Chemical Society Symposium Series, No. 293, 1985.

Westbrook, C.K and Urtiew, P.A., "Chemical Kinetics Prediction of Critical Parameters in Gaseous Detonations," 19th Symposium on Combustion, 615-623, 1982.

White, D. R., "Turbulent Structure of Gaseous Detonations," Physics of Fluids, Vol. 4, No. 4, pp. 465, 1961.

von Neumann, J., "Theory of Detonation Waves," Proj. Report No. 238, April 1942; OSRD Report No. 549, 1942.

Yang, J. W., "High-Temperature Combustion in LWR Containments Under Severe Accident Conditions," Brookhaven National Laboratory, Technical Report L-1924 1/17/92, January 1992.

Zabetakis, M.G., "Research on the Combustion and Explosion Hazards of Hydrogen-Water Vapor-Air Mixtures," US Atomic Energy Commission, AECU-3327, September, 1956.

Zel'Dovich, Y. B., "The Theory of Propagation of Detonation in Gaseous Systems," Expt. Theor. Phys. S.S.S.R., Vol. 10, p. 542, 1940; Translation, NACA TM 1261, 1950.

# APPENDIX A

# MECHANICAL DRAWINGS OF TEST VESSEL

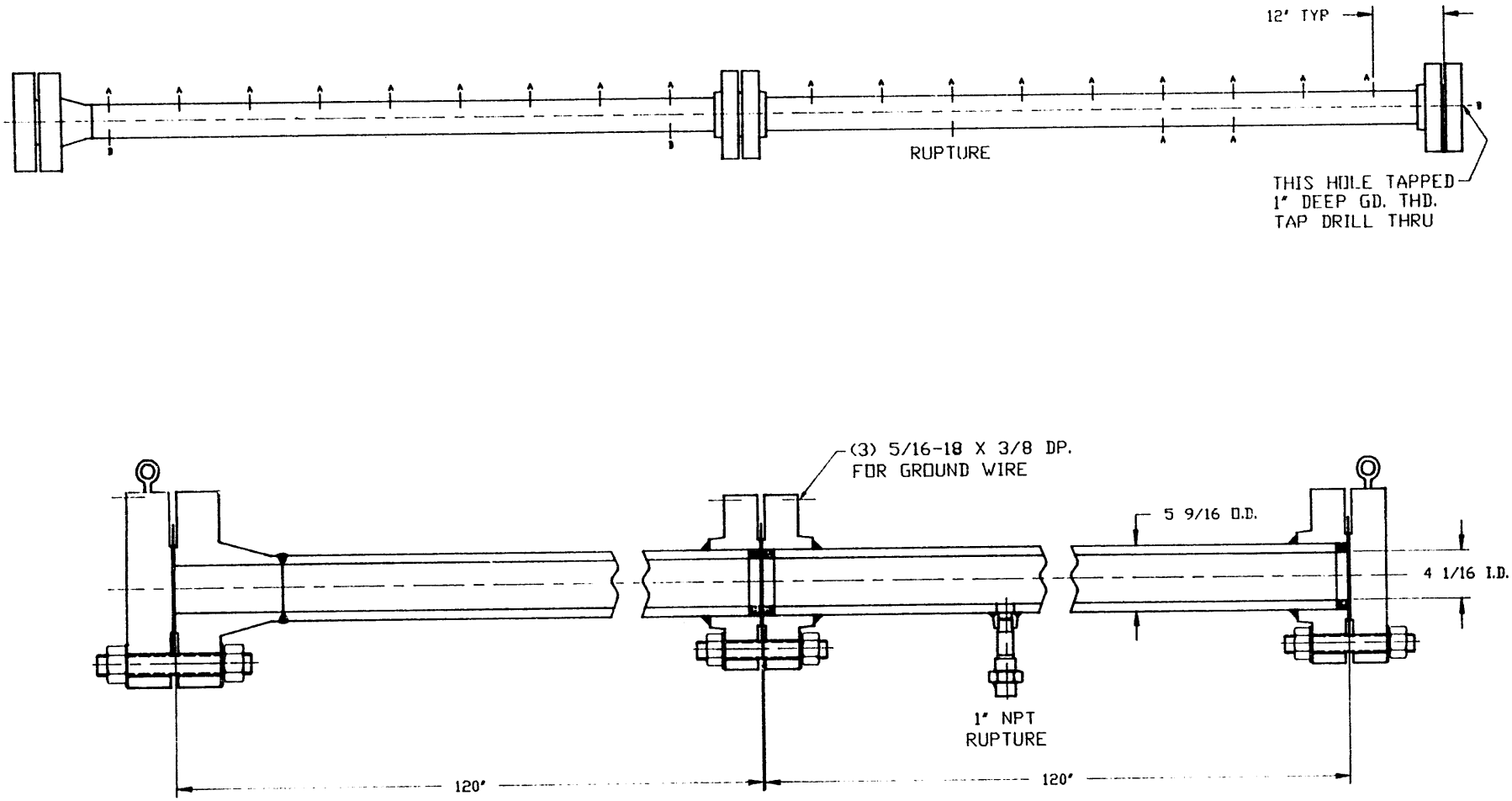


DESIGN FULL VACUUM TO 2000 PSI @ 800° F
MDMT -20° F
HYDROTEST 3550 PSI @ ROOM TEMP.

ASME CODE
SECTION 8 DIVISION 1

**Figure A.1 Mechanical Drawing of Test Vessel**



fluitron
Ivyland PA 18974

COLUNM ASM

| DATE | SCALE | BY | S. O. NO. | REV. |
|---|---|---|---|---|
| REF. | ASS'Y | | DWG. NO. | |

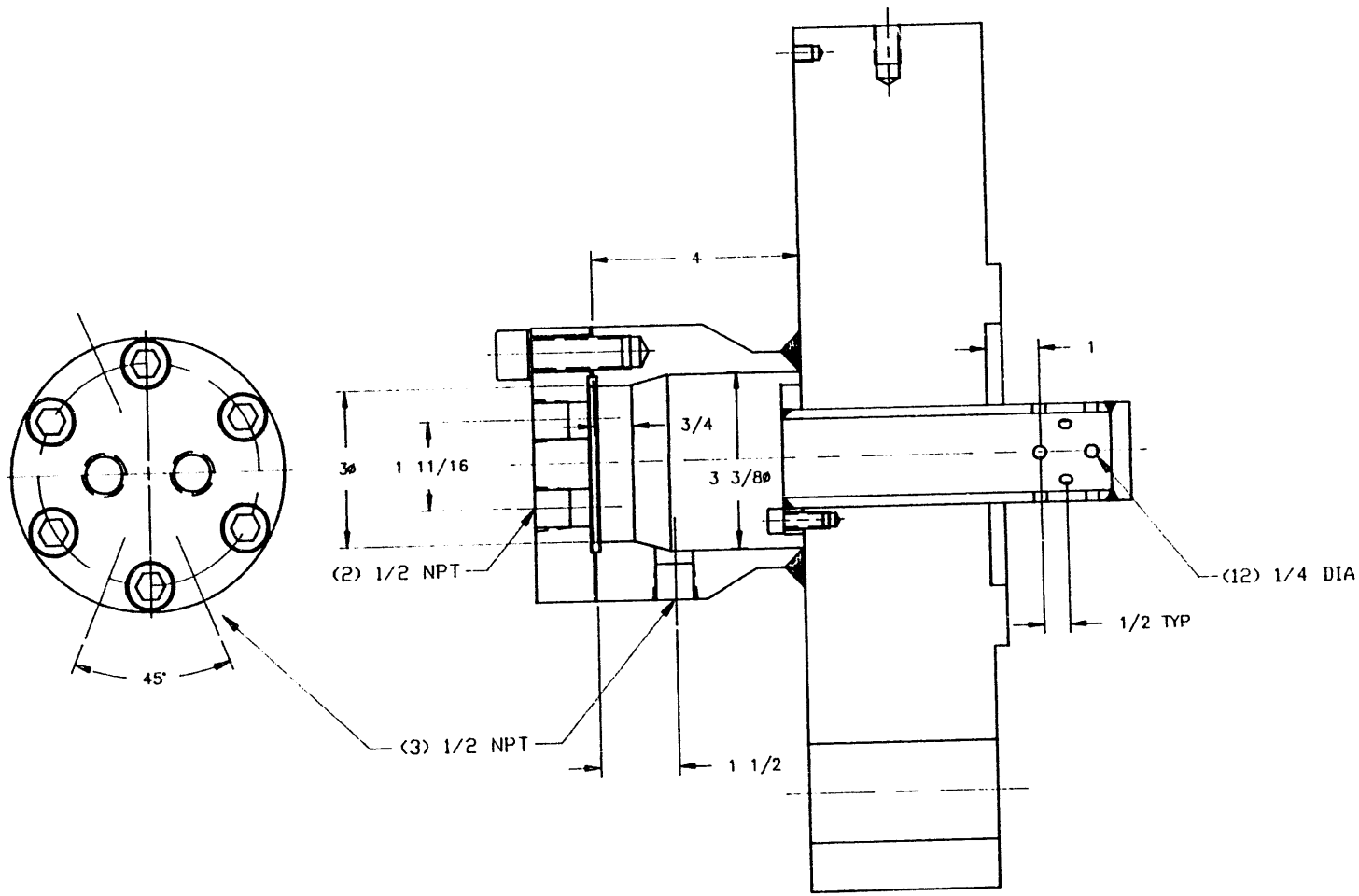


Figure A.2 Mechanical Drawing of Gas Driver Endcover Including Initiation Chamber



fluitron
Ivyland PA 18974

| DATE | SCALE | BY | S. O. NO. | REV. |
|---|---|---|---|---|
| REF. | ASS'Y | | DWG. NO. | |

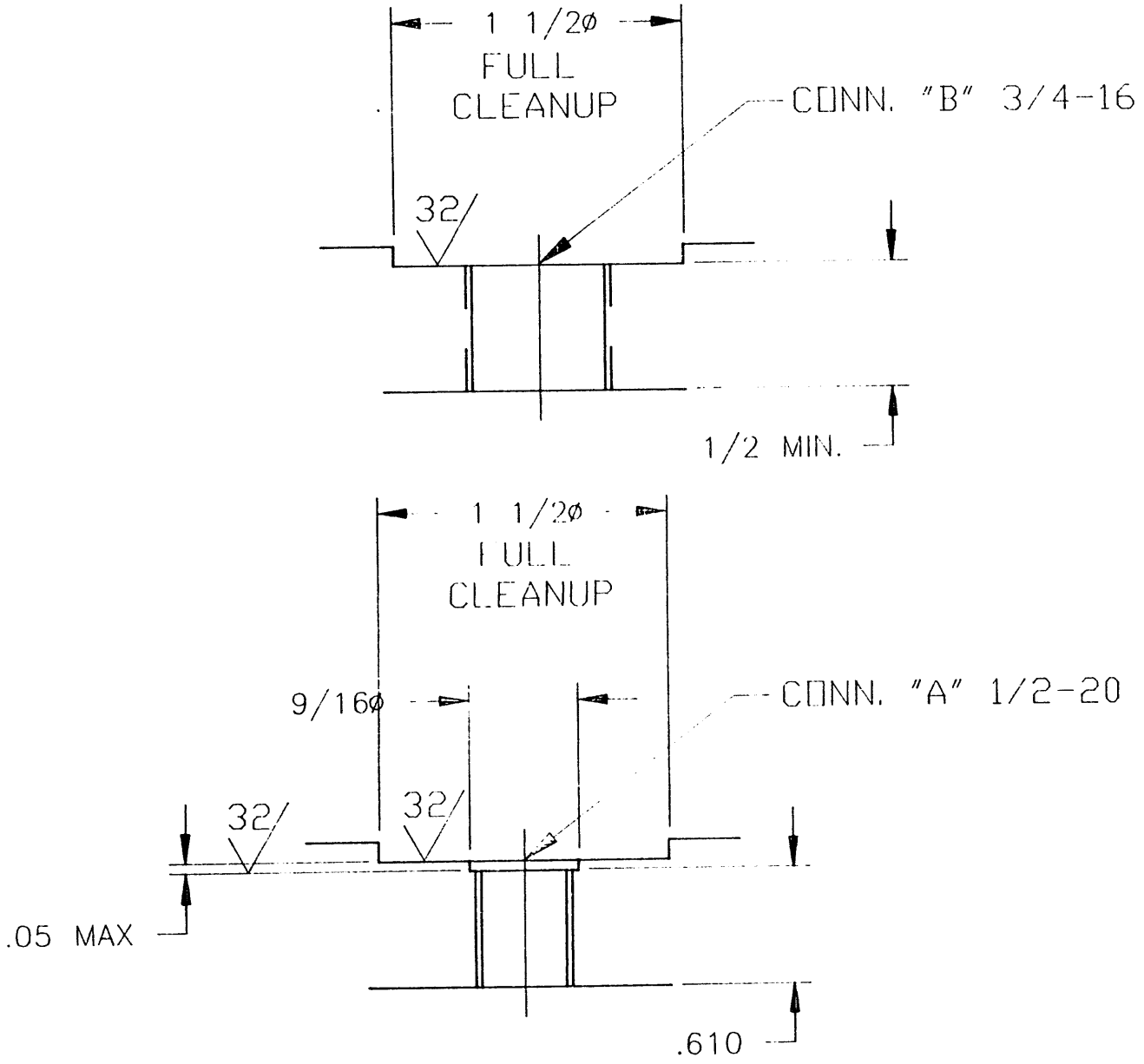


Figure A.3 Mechanical Drawing Showing Instrumentation Port Design



fluitron
Ivyland PA 18974

| DATE | SCALE | BY | S. O. NO. | REV. |
|---|---|---|---|---|
| REF. | ASS'Y | | DWG. NO. | |

# APPENDIX B

# SUMMARY OF EXPERIMENTS PERFORMED AND RESULTS

The initial thermodynamic conditions and the experimental results for each experiment performed is given in tabular form. All experiments were performed at a nominal initial pressure of one atmosphere. The reported hydrogen and steam mole fraction are calculated from the partial pressures obtained in loading the mixture constituents into the mixing chamber. For parameters, such as the initial mixture temperature and detonation velocity, where multiple measurements are taken, a minimum, maximum, and average valve are given. In all cases, the average is taken of the measurements made in the driven half of the test vessel. Typically, the average temperature is derived from three different measurements and the average detonation velocity is derived from four velocity measurements taken at 91.4 cm intervals. The following is a list of abbreviations and definitions used in the following tables.

N/A = Not Available
N/D = No Detonation
N/R = Not Readable
D.H. = Double-Head Spin
S.H. = Single-Head Spin

## TABLE B-1: EXPERIMENTAL RESULTS FOR HYDROGEN-AIR AT 650K

| RUN NO. | H2 MOLE FRACTION (%) | INITIAL PRESSURE (kPa) | INITIAL TEMPERATURE (K) | | | DRIVER LENGTH (cm) | DETONATION PRESSURE (x $10^5$ Pa) | DETONATION VELOCITY (m/s) | | | CELL SIZE (cm) |
|---|---|---|---|---|---|---|---|---|---|---|---|
| | | | Min | Avg | Max | | | Min | Avg | Max | |
| 205 | 50.03 | 102.2 | 636 | 643 | 648 | 20.3 | 4.7 | 1890 | 1960 | 2018 | 0.9 |
| 287 | 50.01 | 102.2 | 638 | 658 | 668 | 20.3 | 5.7 | 2025 | 2073 | 2073 | 1 |
| 200 | 30.06 | 102.2 | 645 | 646 | 647 | 20.3 | N/A | 1870 | 1870 | 1870 | 0.5 |
| 199 | 30 | 102.2 | 647 | 648 | 649 | 20.3 | N/A | 1858 | 1866 | 1876 | 0.5 |
| 184 | 30 | 101 | 647 | 647 | 647 | 20.3 | N/A | 1905 | 1908 | 1911 | 0.4 |
| 201 | 17.47 | 102.2 | 646 | 649 | 652 | 20.3 | N/A | 1524 | 1547 | 1567 | 1.2 |
| 286 | 17.43 | 102.1 | 636 | 657 | 669 | 20.3 | 5.7 | 1555 | 1573 | 1588 | 1.55 |
| 282 | 14.92 | 102.1 | 638 | 650 | 659 | 20.3 | 5.2 | 1480 | 1495 | 1505 | 1.6 |
| 285 | 15.04 | 102 | 637 | 655 | 666 | 20.3 | 4.9 | 1480 | 1495 | 1505 | 1.6 |
| 265 | 11.99 | 102.7 | 640 | 647 | 653 | 40.6 | 3.7 | 1349 | 1352 | 1358 | N/R |
| 267 | 12 | 102.7 | 638 | 643 | 647 | 40.6 | 4.6 | 1352 | 1360 | 1373 | 3.7 |
| 333 | 12 | 102.7 | 634 | 652 | 663 | 30.5 | 4 | 1361 | 1374 | 1411 | 3.1 |
| 337 | 12.02 | 102.7 | 634 | 641 | 647 | 30.5 | N/A | 1362 | 1379 | 1392 | 3.6 |
| 269 | 12.12 | 102.7 | 639 | 646 | 654 | 40.6 | N/A | 1349 | 1368 | 1382 | 3.4 |
| 228 | 11.95 | 102.2 | 635 | 650 | 659 | 20.3 | 3.6 | 1337 | 1341 | 1340 | N/R |
| 338 | 10.99 | 102.7 | 634 | 640 | 640 | 30.5 | N/A | 1319 | 1339 | 1343 | 4.1 |
| 290 | 11.04 | 102.1 | 640 | 652 | 661 | 20.3 | N/A | 1305 | 1327 | 1340 | 3.7 |
| 339 | 10 | 102.6 | 637 | 642 | 649 | 30.5 | N/A | 1286 | 1299 | 1319 | Unstable |
| 347 | 10.02 | 102.7 | 640 | 644 | 649 | 30.5 | N/A | 1281 | 1295 | 1302 | 4.7 |
| 376 | 10.01 | 102.7 | 642 | 644 | 646 | 26.4 | N/A | 1270 | 1292 | 1305 | 7.85 |
| 293 | 9.96 | 102.5 | 645 | 647 | 651 | 30.5 | N/A | 1262 | 1297 | 1297 | 7.85 |
| 224 | 10.07 | 102.2 | 630 | 641 | 651 | 20.3 | 4.6 | 1236 | 1277 | 1349 | -- |
| 348 | 9 | 102.7 | 639 | 642 | 646 | 30.5 | N/A | 1238 | 1261 | 1290 | D.H. |
| 225 | 8.97 | 102.1 | 626 | 636 | 644 | 20.3 | N/A | | N/D | | -- |
| 375 | 9 | 101.7 | 641 | 642 | 642 | 26.4 | N/A | N/A | N/A | N/A | S.H. |

## TABLE B-2: EXPERIMENTAL RESULTS FOR HYDROGEN-AIR AT 500K

| RUN NO. | H2 MOLE FRACTION (%) | INITIAL PRESSURE (kPa) | INITIAL TEMPERATURE (K) | | | DRIVER LENGTH (cm) | DETONATION PRESSURE (x $10^5$ Pa) | DETONATION VELOCITY (m/s) | | | CELL SIZE (cm) |
|---|---|---|---|---|---|---|---|---|---|---|---|
| | | | Min | Avg | Max | | | Min | Avg | Max | |
| 343 | 49.99 | 102.1 | 494 | 497 | 502 | 20.3 | N/A | 2139 | 2147 | 2154 | 1.05 |
| 204 | 50.08 | 102 | 496 | 500 | 504 | 20.3 | 8 | 2146 | 2146 | 2146 | 1 |
| 273 | 50.03 | 102 | 492 | 504 | 510 | 20.3 | 8.3 | 2146 | 2146 | 2146 | 1.7 |
| 208 | 29.98 | 102 | 494 | 498 | 503 | 20.3 | 9.2 | 1929 | 1942 | 1954 | 0.6 |
| 274 | 30 | 101.9 | 494 | 508 | 516 | 20.3 | 4.6 | 1929 | 1948 | 1954 | 0.9 |
| 341 | 21.9 | 101.8 | 493 | 497 | 501 | 20.3 | N/A | 1752 | 1762 | 1772 | 0.815 |
| 271 | 17.49 | 102 | 491 | 510 | 523 | 20.3 | 5.7 | 1600 | 1613 | 1626 | 1.5 |
| 272 | 17.43 | 102 | 497 | 506 | 510 | 20.3 | 6.7 | 1600 | 1613 | 1626 | 1.5 |
| 203 | 17.42 | 101.9 | 496 | 498 | 499 | 20.3 | 6.5 | 1606 | 1607 | 1608 | 2 |
| 280 | 16.01 | 101.9 | 494 | 506 | 512 | 20.3 | 6.6 | 1551 | 1559 | 1571 | N/R |
| 350 | 16.01 | 102 | 496 | 500 | 505 | 20.3 | N/A | 1539 | 1551 | 1555 | 2.4 |
| 281 | 15.93 | 101.9 | 494 | 505 | 511 | 20.3 | 6.9 | 1540 | 1555 | 1571 | 2.86 |
| 355 | 13.98 | 102 | 482 | 495 | 504 | 20.3 | N/A | 1465 | 1465 | 1465 | 7.85 |
| 351 | 14 | 102 | 496 | 500 | 504 | 20.3 | N/A | 1451 | 1476 | 1505 | 7.85 |
| 342 | 14.02 | 102 | 493 | 497 | 501 | 30.5 | N/A | 1445 | 1482 | 1509 | 6.3 |
| 266 | 13.51 | 102.3 | 497 | 504 | 512 | 40.6 | 5.7 | 1438 | 1454 | 1475 | N/R |
| 279 | 13.93 | 101.8 | 495 | 500 | 505 | 20.3 | 6 | 1465 | 1473 | 1485 | 9.8 |
| 264 | 13.91 | 102.3 | 487 | 492 | 497 | 40.6 | 5.7 | 1472 | 1479 | 1494 | N/R |
| 268 | 13.9 | 102.1 | 497 | 501 | 505 | 40.6 | 7.4 | 1437 | 1466 | 1480 | N/R |
| 270 | 13.96 | 102.1 | 491 | 514 | 530 | 40.6 | 6.9 | 1438 | 1464 | 1487 | N/R |
| 278 | 14 | 102 | 496 | 500 | 504 | 20.3 | 6 | 1451 | 1470 | 1483 | N/R |
| 344 | 13 | 102.2 | 495 | 497 | 500 | 30.5 | N/A | 1424 | 1432 | 1441 | 10.5 |
| 356 | 13 | 102.1 | 485 | 497 | 505 | 30.5 | N/A | 1398 | 1428 | 1451 | 10.5 |
| 218 | 12.09 | 102 | 492 | 497 | 504 | 20.3 | 5.4 | 1343 | 1365 | 1385 | N/A |
| 229 | 12.04 | 102 | 492 | 511 | 526 | 20.3 | -- | | N/D | | -- |
| 276 | 11.97 | 102.3 | 494 | 505 | 512 | 40.6 | 5.4 | 1309 | 1370 | 1405 | N/A |
| 283 | 11.96 | 102 | 491 | 513 | 529 | 20.3 | -- | | N/D | | -- |
| 284 | 12.04 | 102.2 | 492 | 512 | 525 | 40.6 | N/A | 1302 | 1362 | 1428 | D.H. |
| 275 | 11.49 | 102 | 493 | 506 | 512 | 40.6 | 5.2 | 1326 | 1327 | 1328 | N/A |
| 288 | 11.58 | 102.2 | 493 | 511 | 525 | 30.5 | 6.3 | 1317 | 1318 | 1319 | D.H. |
| 231 | 10.97 | 102.1 | 491 | 507 | 517 | 40.6 | -- | | N/D | | -- |
| 219 | 9.96 | 102 | 494 | 499 | 504 | 20.3 | -- | | N/D | | -- |

## TABLE B-3: EXPERIMENTAL RESULTS FOR HYDROGEN-AIR AT 300K

| RUN NO. | H2 MOLE FRACTION (%) | INITIAL PRESSURE (kPa) | INITIAL TEMPERATURE (K) | | | DRIVER LENGTH (cm) | DETONATION PRESSURE (x $10^5$ Pa) | DETONATION VELOCITY (m/s) | | | CELL SIZE (cm) |
|---|---|---|---|---|---|---|---|---|---|---|---|
| | | | Min | Avg | Max | | | Min | Avg | Max | |
| 334 | 57.96 | 14.73 | 68 | 82 | 97 | 30.5 | 10.3 | 2185 | 2187 | 2192 | 7.85 |
| 318 | 58.02 | 14.74 | 71 | 76 | 81 | 30.5 | 12.6 | 2177 | 2192 | 2209 | 7.6 |
| 258 | 54.54 | 14.76 | 67 | 68 | 68 | 40.6 | 11.2 | 2177 | 2185 | 2209 | 4.6 |
| 206 | 50.02 | 14.52 | 74 | 77 | 82 | 20.3 | 11.5 | 2131 | 2150 | 2165 | 2.5 |
| 151 | 49.99 | N/A | N/A | N/A | N/A | 40.6 | 12.9 | 2133 | 2142 | 2149 | 3.1 |
| 317 | 40.04 | 14.76 | 72 | 76 | 81 | 20.3 | 12.6 | 2073 | 2089 | 2102 | 0.94 |
| 207 | 40.09 | 14.76 | 74 | 77 | 81 | 20.3 | 12.9 | 2088 | 2091 | 2098 | 1.0 |
| 164 | 29.92 | N/A | N/A | N/A | N/A | 40.6 | 13.6 | 1966 | 2014 | 2088 | 0.9 |
| 175 | 29.98 | N/A | N/A | N/A | N/A | 40.6 | 11.8 | 1954 | 2047 | 2032 | 0.9 |
| 146 | 30.12 | N/A | N/A | N/A | N/A | 40.6 | 13.4 | 1887 | 1990 | 2052 | 0.9 |
| 156 | 24.94 | N/A | N/A | N/A | N/A | 40.6 | 14.3 | 1853 | 1855 | 1858 | 1.2 |
| 35 | 19.78 | N/A | N/A | N/A | N/A | N/A | 11.2 | N/A | N/A | N/A | 3.4 |
| 144 | 20.00 | N/A | N/A | N/A | N/A | 40.6 | 11.5 | 1647 | 1678 | 1693 | N/R |
| 254 | 19.93 | 14.78 | 65 | 66 | 67 | 20.3 | 11.5 | 1698 | 1703 | 1708 | 4.2 |
| 256 | 20.02 | 14.74 | 69 | 70 | 70 | 162.6 | 12.6 | 1693 | 1703 | 1703 | 4.7 |
| 147 | 17.49 | N/A | N/A | N/A | N/A | 40.6 | 11.5 | 1596 | 1600 | 1604 | 5.9 |
| 187 | 17.58 | N/A | N/A | N/A | N/A | 40.6 | N/A | 1563 | 1616 | 1648 | 9.6 |
| 177 | 17.51 | N/A | N/A | N/A | N/A | 40.6 | 10.7 | 1563 | 1594 | 1604 | 9.8 |
| 150 | 16.81 | N/A | N/A | N/A | N/A | 40.6 | 11.1 | 1539 | 1569 | 1600 | 14.0 |
| 148 | 16.00 | N/A | N/A | N/A | N/A | 40.6 | 10.4 | 1524 | 1524 | 1524 | D.H. |
| 255 | 15.00 | 14.74 | 67 | 68 | 69 | 40.6 | 10.9 | 1451 | 1472 | 1501 | S.H. |

## TABLE B-4: EXPERIMENTAL RESULTS FOR STOICHIOMETRIC HYDROGEN-AIR AND STEAM AT 650K

| RUN NO. | PERCENT (%) STEAM | PERCENT (%) H2/AIR | INITIAL PRESSURE (kPa) | INITIAL TEMPERATURE (K) | | | DRIVER LENGTH (cm) | DETONATION VELOCITY (m/s) | | | CELL SIZE (cm) |
|---|---|---|---|---|---|---|---|---|---|---|---|
| | | | | Min | Avg | Max | | Min | Avg | Max | |
| 327 | 9.97 | 30.14 | 102.2 | 637 | 650 | 661 | 20.3 | 1836 | 1846 | 1856 | 0.82 |
| 326 | 19.98 | 29.97 | 102.2 | 635 | 650 | 660 | 20.3 | 1772 | 1793 | 1814 | 2.2 |
| 328 | 20 | 29.94 | 102.2 | 635 | 651 | 662 | 20.3 | 1772 | 1788 | 1793 | 2.4 |
| 349 | 25 | 29.91 | 102.7 | 642 | 647 | 654 | 30.5 | 1747 | 1759 | 1772 | 2.45 |
| 325 | 29.99 | 29.33 | 102.7 | 637 | 651 | 660 | 30.5 | 1675 | 1694 | 1712 | Unstable |
| 340 | 29.86 | 29.94 | 102.6 | 637 | 642 | 649 | 30.5 | 1712 | 1728 | 1737 | 9.2 |
| 373 | 29.74 | 30.27 | 102.9 | 644 | 645 | 646 | 30.5 | 1679 | 1712 | 1732 | 6.28 |
| 227 | 35.48 | 30.01 | 102.9 | 625 | 635 | 643 | 40.6 | | N/D | | -- |

## TABLE B-5: EXPERIMENTAL RESULTS FOR STOICHIOMETRIC HYDROGEN-AIR AND STEAM AT 600K

| RUN NO. | PERCENT (%) STEAM | PERCENT (%) H2/AIR | INITIAL PRESSURE (kPa) | INITIAL TEMPERATURE (K) | | | DRIVER LENGTH (cm) | DETONATION VELOCITY (m/s) | | | CELL SIZE (cm) |
|---|---|---|---|---|---|---|---|---|---|---|---|
| | | | | Min | Avg | Max | | Min | Avg | Max | |
| 379 | 25.00 | 30.10 | 102.0 | 597 | 599 | 599 | 20.3 | 1752 | 1767 | 1772 | 6.2 |
| 380 | 29.91 | 29.94 | 102.0 | 590 | 594 | 597 | 20.3 | 1693 | 1717 | 1752 | 15.7 |

TABLE B-6: EXPERIMENTAL RESULTS FOR STOICHIOMETRIC HYDROGEN-AIR AND STEAM AT 500K

| RUN NO. | PERCENT (%) STEAM | PERCENT (%) H2/AIR | INITIAL PRESSURE (kPa) | INITIAL TEMPERATURE (K) | | | DRIVER LENGTH (cm) | DETONATION VELOCITY (m/s) | | | CELL SIZE (cm) |
|---|---|---|---|---|---|---|---|---|---|---|---|
| | | | | Min | Avg | Max | | Min | Avg | Max | |
| 320 | 9.98 | 29.94 | 102 | 496 | 500 | 505 | 20.3 | 1881 | 1881 | 1881 | 1.11 |
| 309 | 9.89 | 30.1 | 102 | 494 | 509 | 520 | 20.3 | 1881 | 1889 | 1893 | 1.22 |
| 323 | 14.99 | 29.99 | 102 | 497 | 509 | 516 | 20.3 | 1859 | 1859 | 1859 | 2.32 |
| 311 | 15 | 30.08 | 101.8 | 494 | 505 | 512 | 20.3 | 1842 | 1859 | 1876 | 1.94 |
| 324 | 19.92 | 30.07 | 102.1 | 494 | 504 | 510 | 30.5 | 1814 | 1814 | 1814 | 5.24 |
| 310 | 19.98 | 30.16 | 101.9 | 494 | 506 | 513 | 40.6 | 1809 | 1814 | 1820 | 5.44 |
| 319 | 24.98 | 29.98 | 102.2 | 495 | 499 | 505 | 30.5 | 1772 | 1774 | 1777 | 10.5 |
| 312 | 24.77 | 30.27 | 102.2 | 494 | 506 | 513 | 40.6 | 1712 | 1747 | 1777 | D.H. |
| 223 | 30.01 | 30.01 | 102.1 | 499 | 507 | 512 | 40.6 | 1551 | 1559 | 1567 | S.H. |

TABLE B-7: EXPERIMENTAL RESULTS FOR STOICHIOMETRIC HYDROGEN-AIR AND STEAM AT 300K

| RUN NO. | PERCENT (%) STEAM | PERCENT (%) H2/AIR | INITIAL PRESSURE (kPa) | INITIAL TEMPERATURE (K) | | | DRIVER LENGTH (cm) | DETONATION VELOCITY (m/s) | | | CELL SIZE (cm) |
|---|---|---|---|---|---|---|---|---|---|---|---|
| | | | | Min | Avg | Max | | Min | Avg | Max | |
| 322 | 10.00 | 30.00 | 102.0 | 399 | 410 | 417 | 20.3 | 1905 | 1905 | 1905 | 1.62 |
| 313 | 10.00 | 29.88 | 101.8 | 397 | 409 | 417 | 20.3 | 1905 | 1905 | 1905 | 1.41 |
| 315 | 14.80 | 30.03 | 102.0 | 399 | 409 | 414 | 20.3 | 1858 | 1858 | 1858 | 2.7 |
| 321 | 15.00 | 30.13 | 101.9 | 396 | 408 | 416 | 20.3 | 1858 | 1858 | 1858 | 3.22 |
| 314 | 19.96 | 29.92 | 101.8 | 397 | 408 | 415 | 30.5 | 1752 | 1804 | 1814 | D.H. |
| 316 | 24.95 | 29.92 | 101.9 | 399 | 409 | 414 | 30.5 | 1712 | 1732 | 1772 | S.H. |

# APPENDIX C

# RELATIONSHIP BETWEEN HYDROGEN BURNED AND CHANGE IN PRESSURE

Let us consider a combustible mixture in a closed volume at high temperature. Assuming ideal gas behavior and assume a constant temperature, constant volume process.

$$\frac{\Delta P}{P_o} = \frac{\Delta n}{n_o} \tag{C-1}$$

where P is the mixture pressure and $n_o$ is the initial number of moles in the mixture.

The overall reaction proceeds as

$$H_2 + \frac{1}{2} O_2 \rightarrow H_2O \tag{C-2}$$

where for every mole of hydrogen burned, $n^bH_2$, there is half a mole of oxygen consumed and one mole of water produced. As a result, there is a net decrease of half a mole of mixture, such that after the burn:

$$n = n_o - \frac{1}{2} n^b_{H_2} \tag{C-3}$$

$$\Delta n = -\frac{1}{2} n^b_{H_2} \tag{C-4}$$

dividing both sides of the equation by $n_o$ and using (C-1) yields

$$\frac{\Delta P}{P_o} = -\frac{1}{2} \frac{n^b_{H_2}}{n_o} \tag{C-5}$$

$$\frac{n^b_{H_2}}{n_o} = -2 \frac{\Delta P}{P_o} \tag{C-6}$$

The initial hydrogen mole fraction, $x^\circ_{H2}$, is given by:

$$x^o_{H_2} = \frac{n^o_{H_2}}{n_o} \tag{C-7}$$

where $n^\circ_{H2}$ is the initial number of hydrogen moles.

The hydrogen mole fraction at the end of the burn, $X^f_{H2}$, is:

$$x^f_{H_2} = \frac{n^o_{H_2} - n^b_{H_2}}{n_o - \frac{1}{2} n^b_{H_2}} = \frac{\frac{n^o_{H_2}}{n_o} - \frac{n^b_{H_2}}{n_o}}{1 - \frac{1}{2}\frac{n^b_{H_2}}{n_o}} \qquad \text{(C-8)}$$

Substituting expression (C-6) into (C-9) yields the final hydrogen mole fraction as a function of the pressure drop:

$$x^f_{H_2} = \frac{x^o_{H_2} + 2\frac{\Delta P}{P_o}}{1 + \frac{\Delta P}{P_o}} \qquad \text{(C-9)}$$

# APPENDIX D

# CORRECTION FOR GAS CHROMATOGRAPH MEASUREMENT

Let us consider the slow oxidation of the following hydrogen-air mixture

$$xH_2 + (1 - x)\,(.290_2 + .71N_2) \tag{D-1}$$

where x is the mole fraction of hydrogen. After a period of time at elevated temperature $\Delta x$ hydrogen reacts to form the following mixture

$$(x - \Delta x)H_2 + (1 - x)\left(.29 - \frac{\left(\frac{\Delta X}{2}\right)}{(1 - x)}\right) O_2 + .71N_2 + \Delta x H_2O \tag{D-2}$$

where one mole of hydrogen reacts with half a mole of oxygen to yield one mole of water. The total number of moles after reaction, excluding water, is $1 - 1.5\Delta x$. Since the sample bottle is at room temperature, for saturation conditions, $0.023(1 - 1.5\Delta x)$ moles of water exist in the vapor phase. Therefore, the total number of moles of mixture after reaction in the gas phase is $1.023(1 - 1.5\Delta x)$. The gas chromatograph gives a measure of the fraction of mixture in the gas phase consisting of hydrogen. So the gas chromatograph reading for the hydrogen concentration, $X_{GC}$, is actually

$$X_{GC} = \frac{(x - \Delta x)}{1.023}\,(1 - 1.5x) \tag{D-3}$$

and the decrease in the mole fraction is given by

$$\Delta x = \frac{(1.535X_{GC} - x)}{(1.023X_{GC} - 1)} \tag{D-4}$$

Therefore, the actual hydrogen mole fraction after reaction is

$$X_{H_2} = \frac{(x - \Delta x)}{\left(\frac{1 - \Delta x}{2}\right)} \tag{D-5}$$

DATE
FILMED
10/18/94
END